Adsorption of Charged Macromolecules on a Gold Electrode

Promotor: Prof. dr. M.A. Cohen Stuart
                   hoogleraar in de fysische chemie en kolloïdkunde

Copromotor: Dr. ir. J.M. Kleijn
                   universitair docent
                   bij de leerstoelgroep fysische chemie en kolloïdkunde

Promotiecommissie: Prof. P.M. Claesson, Royal Institute of Technology,
                   Stockholm

                   Prof. dr. ir. J.G.E.M. Fraaije, Universiteit Leiden

                   Dr. E.A. Meulenkamp, Philips Research, Eindhoven

                   Prof. dr. G.J. Fleer, Wageningen Universiteit

Adsorption of Charged Macromolecules on a Gold Electrode

D. Barten

Contents

1   General Introduction

1.1   Aim and background

The study presented here is a systematic investigation into the adsorption of different types of charged macromolecules from aqueous electrolyte solution onto a solid surface as a function of the electric potential of the solid/solution interface. Our aim is to elucidate the role of electrostatics in the adsorption process of macromolecules, and to be able to discriminate between effects of the potential of the sorbent surface and the effects of intrinsic changes in the adsorbing molecules. Our motivation is twofold: fundamental interest in the role of electrostatic interactions on adsorption phenomena, but also survey of the practical possibilities to control the adsorption of charged molecules - including proteins and small particles - by applying a potential across the solid/liquid interface.

Adsorption processes are rather complicated. For small molecules, adsorption from aqueous solution is generally governed by electrostatic and hydrophobic interactions between (i) the molecule in solution and the solid/liquid interface and (ii) between the adsorbed molecules. Furthermore, more specific interactions, i.e., chemical affinity may play a role (see, e.g., Refs. 1-3). For larger molecules, adsorption usually also involves conformational changes and rearrangement of charges within the adsorbing molecules[4-7].

There are various ways to systematically examine the role of electrostatic forces in the process of adsorption. Methods used to vary the electrostatic interactions are, for example, the use of sorbent surfaces with a pH-dependent charge and potential, like oxidic surfaces (see, e.g., Refs. 8-10), or functionalised surfaces with controllable acid to base ratio[11]. The electric properties of such surfaces as a function of pH and other solution conditions (type and concentration of electrolyte) can be assessed, e.g., by acid-base titrations[1], which give the surface density, and streaming potential measurements[12,13], which give the zeta-potential.

Another option to elucidate the role of electrostatics is to compare the adsorption behaviour of chemically more or less similar molecules with different charges, for example, small globular proteins with different i.e.p.[4,7,9,14], charged and uncharged surfactants[8], polyelectrolytes with various charge densities[6,15,16] etc.

A disadvantage of varying the charge and potential of the sorbent surface by changing the solution conditions, is that the properties of the adsorbing molecules in solution may also change. In particular, macromolecules with weak ionisable groups, like weak polyelectrolytes and proteins adjust their charge distribution and often also their conformation. Therefore, it is not always straightforward to explain observed trends in terms of changes in electrostatic interactions between sorbent and adsorbate. When the charge and potential of the surface are varied through an external electric circuit, this problem is avoided.

However, adsorption studies performed using a externally controlled surface potential are very limited in number and the results are far from unambiguous[14,17-23]. This is

probably due to a number of complications met in adsorption measurements with a potential applied at the substrate/electrolyte interface, for example, the occurrence of redox reactions limiting the potential range for the adsorption studies, interference of electro-optical effects (in case an optical detection method is used), and the problem that the potential applied across the solid/liquid interface is not the potential felt by the adsorbing molecules.

A number of studies on the adsorption of proteins onto a solid surface suggest that the effect of an externally applied potential at the interface is relatively small[14,17,20]. This is a rather surprising finding, since electrostatic forces are generally thought to play a major role in protein adsorption[4,9,13]. However, it is difficult to properly evaluate published results. For example, the study of Bos et al[14] has been performed using a semi-conductor as the substrate. Therefore, the potential at the solid/liquid interface was probably much lower than the potential applied to the solid phase with respect to the solution. Another factor that may have been of importance, is that the (de)protonation of oxidic surface groups has buffered the surface potential[24]. Beaglehole et al[20], who used gold as well as stainless steel as the substrate, observed a weak dependency of the adsorption of the polyelectrolyte polyethylene imine (PEI) on the externally applied potential. Morrissey et al[17] reported enhanced adsorption of various proteins on platinum, but only above a certain onset potential. However, in their study the potential was varied *after* adsorption had taken place, and it is not clear to which extent redox reactions or an electro-optical effect may have played a role.

1.2   Approach

Throughout this study gold was used as the substrate and we investigated the adsorption of three very different types of charged macromolecules. Adsorption measurements were performed *in situ*, using a reflectometer with impinging-jet system. In this set-up the hydrodynamic conditions are well-defined, making it possible to decide whether mass transport from the bulk solution or interfacial processes are determining the adsorption rate[25].

Gold was chosen as the sorbent, because it is a metallic conductor and because it is fairly inert, i.e., over a relatively large range of applied potentials no redox reactions occur when in contact with aqueous solutions. The gold surface is hydrophilic as it has a zero contact angle with water[26]. It should be said that, somewhat unexpectedly, the surface charge and potential of gold are dependent on pH[26,27]. This gives the opportunity to control the electric properties of the surface through the solution pH as well as by an external electric circuit. As said before, varying the potential of the solid/liquid interface by means of an external source as opposed to changing the pH of the solution, has the advantage that the properties of the adsorbing molecules in the bulk of the solution remain the same.

It is clear that for the interpretation of adsorption in terms of electrostatic interactions information on the surface potential or the electric double layer of the sorbent surface is crucial. A method to determine the surface potential is by measuring the double layer interactions of the gold surface with a colloidal silica probe, using an atomic force microscope[28-31]. How this surface potential depends on the externally applied potential and on the solution pH can then be assessed.

In this thesis the surface potential of the gold substrate is controlled by either the solution properties (pH and electrolyte concentration) or by applying an external potential across the gold/solution interface. For all experimental conditions, the corresponding double layer potential, i.e., the potential difference between the outer Helmholtz plane and the bulk solution[1], has been determined using colloidal probe atomic force microscopy. From the interaction curves between the gold surface and a colloidal silica probe of which the double layer potential is known, the double layer potential at the gold surface has been derived using DLVO theory (Derjaguin, Landau, Verweij and Overbeek[32a-d]). With the data obtained, the adsorption of various charged macromolecules onto the gold substrate as a function of the solution properties and as a function of external potential can be compared by plotting the adsorbed amounts and initial adsorption rates as a function of double layer potential. This offers the possibility to discriminate between the effect of electrostatic interactions between surface and adsorbing molecules and other factors, such as the effect of pH and electrolyte concentration on the structure and structure stability of the molecules, and specific hydrophobic interactions. Thus, the role of electrostatic interactions in the adsorption process can be evaluated.

We have chosen to first investigate the adsorption of a relatively simple macromolecule, namely a linear polyelectrolyte with a fixed charge (i.e., a strong polyelectrolyte). We then studied the adsorption of a dendrimer with weak basic groups and a rather fixed conformation. Finally, we investigated the adsorption behaviour of a more complex molecule: a protein with a high structure stability, which has a pH-dependent charge and a more flexible structure than the dendrimer. The various molecules in solution and at a solid surface are schematically drawn in Figure 1.1.
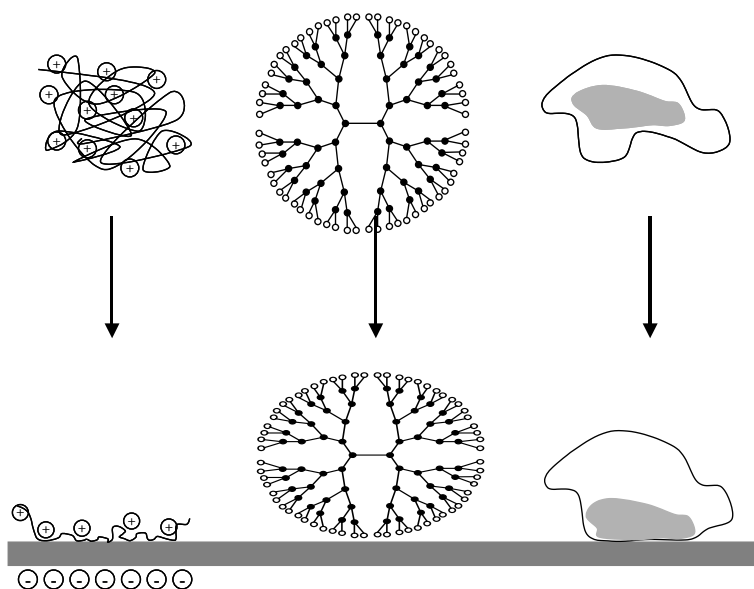

Figure 1.1: Schematic representation of the adsorption process of, respectively, a polyelectrolyte, a dendrimer and a protein.

1.2.1 Linear polyelectrolytes

Polyelectrolytes are polymers with a large number of charged or chargeable groups. The adsorption of polyelectrolytes onto a charged surface is controlled by electrostatic and non-electrostatic interactions between the surface and the polyelectrolyte and the mutual interaction between the charged segments[5,6,33]. In addition, adsorption of linear chain polyelectrolytes, which have in solution usually a swollen coil conformation, involves a loss in conformational entropy and this contribution (a given amount per segment) always opposes adsorption. However, this effect is already compensated by even a small binding energy per adsorbed segment to the reduction of the Gibbs energy. Since the molecule is very large, all the net contributions per segment add up to a considerable amount. Hydrophobic interactions and/or the chemical affinity of the segments for the surface, can make the polyelectrolyte chain adsorb onto a like-charged surface. Adsorption of linear polyelectrolytes is often found to compensate or even slightly overcompensate the bare surface charge[15,16]. The ionic strength of the solution is very important[5,34]. The presence of background electrolyte has different effects: on the one hand, it reduces the electrostatic repulsion between the segments as well as the electrostatic interactions between the segments and the surface. On the other hand, the small ions compete with the polyelectrolyte for adsorption sites. Depending on the relative contribution of non-electrostatic interactions, adsorbed amounts may either increase or decrease with increasing electrolyte concentration. In the case of pure electrosorption, adsorption of polyelectrolyte is predominantly lowered by adding salt.

1.2.2 Dendrimers

Dendrimers are synthetic polyelectrolytes with a highly branched structure. They are synthesized in a stepwise manner, resulting in successive generations[35,36]. Starting from a core and adding branches to it by an iterative procedure, a highly symmetric, monodisperse, tree-like macromolecule with a regular structure is formed (see Figure 1.2). At the branching points in the core ionisable groups are formed. At the outer shell of the dendrimer, ionisable end groups are situated which differ slightly from the groups at the branching points. When the groups are basic or acidic, the dendrimer is a polyelectrolyte of which the charge is pH-dependent. For the dendrimer used in this work, the branching points are tertiary amine groups and the end groups are primary amine groups. Upon adsorption its shape may change from a sphere to a more flattened shape, but the increase in width has been estimated to be 30% at most[35].

1.2.3 Proteins

Proteins are biological macromolecules consisting of amino acid residues, connected by peptide bonds. Their structure is often compact and highly ordered, with a large number of internal hydrogen bonds. In contrast to the adsorption of a linear polyelectrolyte, adsorption of a protein onto a surface sometimes implies an *entropy gain*, because in this process internal bonds may be broken and parts of the secondary and tertiary structure are lost[4,7,9]. The amphoteric character of proteins ensures that the molecule can easily adjust its charge distribution. The binding to a surface is often so strong that protein adsorption is usually irreversible.
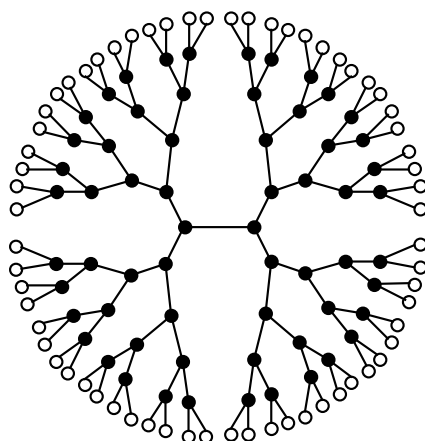
Figure 1.2: Schematic representation of the fifth generation poly(propylene imine) dendrimer DAB-64. Closed symbols are tertiary amines, open symbols represent primary amines. The connecting lines represent the carbon backbone of the dendrimer.

Protein adsorption studies often show results that are difficult to interpret. The charge of the protein is not always the dominant - and never the only - driving force for adsorption. Sometimes it is found that a protein adsorbs in higher amounts on a like-charged surface than on an oppositely charged surface, which is attributed to hydrophobic interactions or structural rearrangements within the protein[11,14]. Proteins can be classified according to their structural stability; the stability scale ranges from the so-called 'soft proteins', which can easily adjust their conformation and charge distribution, to the so-called 'hard proteins', which have a large internal stability[4,9,13]. Soft proteins tend to adsorb on all kinds of surfaces, irrespective of electrostatic repulsion, while for hard proteins on hydrophilic surfaces electrostatic interactions seem to be determining for the adsorbed amount. The effect of the ionic strength is dependent on the type of protein. High ionic strengths lead to screening of the charges of the surface and the protein and adsorbed amounts may increase or decrease, depending on the relative importance of other interactions, just like in the adsorption of linear polyelectrolytes. Although protein adsorption has been studied extensively (for reviews on protein adsorption see, e.g., Refs. 4, 7 and 38), there is still a lot of confusion about the mechanism of protein adsorption and about the interpretation of measured data in terms of electrostatic interactions versus other contributions.

1.3   Outline of this thesis

In this thesis we examine the role of electrostatic interactions in the adsorption of charged macromolecules from aqueous solution to a solid surface and the possibilities for manipulating this process through the electric potential of the interface. Gold has been used as the adsorbing surface. Before studying the adsorption of several types of macromolecules onto this substrate we have first examined the dependence of the double layer potential of gold on the pH and on the externally applied potential across the gold/electrolyte solution interface. The thesis is therefore organized as follows.

Chapter 2 describes a colloidal probe AFM study of the double layer of a gold electrode in aqueous solutions, as a function of the solution properties and as a

function of an externally applied potential. The double layer potentials of the gold surface were obtained by fitting the recorded force-distance curves to the DLVO theory. The data are interpreted in terms of an amphifunctional model for the electric double layer. This model describes the behaviour of the double layer charge and potential as a function of the solution pH *and* as a function of an externally applied potential. The results form the basis of the interpretation of the adsorption studies on gold, described in chapters 4, 5 and 6.

Chapter 3 addresses the sensitivity of the reflectometer set-up for our adsorption studies as well as the electro-optic effect. The sensitivity is calculated and the effect of several system parameters is evaluated. This provides a measure for the reproducibility of the adsorption data obtained with reflectometry. The electro-optic effect, i.e., the variation in the reflectometer signal due to changes in the optical properties of the gold/solution interface when an external potential is applied across this interface, is measured and its effect on the sensitivity is evaluated.

In **chapters 4, 5 and 6** the adsorption of charged macromolecules onto gold as measured using reflectometry, is described. Generally, the adsorption kinetics and adsorbed amounts are determined as a function of variables like the concentration of the macromolecule, the electrolyte concentration and the double layer potential of the gold. The double layer potential of the gold is varied through the pH as well as by applying an external potential. By comparing the results of adsorption measurements performed under pH control and under external potential control, effects of conformational changes and changes in the charge of the molecule in solution can be separated from effects of the electrostatic interaction between the molecule and the adsorbing surface.

In **chapter 4**, the adsorbing compound is quaternized polyvinyl pyridine (PVP^+) of various molecular masses. The charge of this molecule is fixed and independent on the solution pH. It was found that the two methods of variation of the double layer potential of the gold (pH and external electric source) have the same effect on the adsorption behaviour of this linear, strong polyelectrolyte. The adsorbed amount decreases more or less linearly with the double layer potential of the gold, but approaches zero only at a relatively high value of this potential, which we ascribe to non-electrostatic interactions between surface and segments. Surprisingly, the electrostatic barrier for adsorption is always low, even near the threshold potential for adsorption. This points to a relatively low effective charge of the polyelectrolyte coils in solution, presumably as a result of the presence of counterions in these structures.

Chapter 5 describes the adsorption of a fifth generation dendrimer, 1,4-diaminobutane poly(propylene imine). The charge of this molecule is determined by the solution pH. It is a spherical molecule and conformational changes are limited. The effect of changes in the electrostatic interactions are examined. The electrolyte concentration and the pH of the solution do not seem to have any effect on the total adsorbed amount. Neither do the initial adsorption rates as a function of pH and as a function of applied potential follow the electrostatic interactions, on the contrary. From this, it was concluded that electrostatics is not the dominant factor in the adsorption process. The total adsorbed amount as a function of the applied potential shows a linear decrease with increasing applied potential, similar to what was found

for the adsorption of PVP$^+$ onto gold. It was concluded that the effect of the applied potential on the adsorbed amounts must be an indirect one, e.g., stemming from an increase in binding strength between dendrimer and metallic surface sites with decreasing applied potential.

Protein adsorption was examined in **chapter 6**. Lysozyme was used in the adsorption experiments because the structure of this protein is relatively stable. The charge and structure stability of the protein is determined by the solution pH. It was concluded that for this system the adsorption process is - again - dominated by non-electrostatic interactions. Adsorption occurred even when electrostatics counteract the process. Much to our surprise we found that at constant pH adsorbed amounts increased both at increasing *and* decreasing potential. This points to the importance of the gold/water interfacial tension in the adsorption process.

In **chapter 7** the results of the previous chapters (4, 5 and 6) are compared and some general conclusions are drawn concerning the role of electrostatics in the adsorption process of charged molecules onto charged interfaces. The possibilities for controlling this process through the potential of the adsorbent surface are evaluated and an outlook for further research is given.

1.4 References

1) Lyklema, J., *Fundamentals of Interface and Colloid Science, Volume II: Solid-Liquid Interfaces*, **1995**, Academic Press Limited., London.
2) Somasundaran, P., Shrotri, S., Huang, L., *Pure & Appl. Chem.*, **1998**, 70, 621.
3) Koopal, L.K., Lee, E.M., Böhmer, M.R., *J. Colloid Interface Sci.*, **1995**, 170, 85.
4) Kleijn, J.M., Norde, W., *Heterogen. Chem. Rev.*, **1995**, 2, 157.
5) Fleer, G.J., Cohen Stuart, M.A., Scheutjens, J.M.H.M., Cosgrove, T., Vincent, B., *Polymers at Interfaces*, **1993**, Chapman & Hall, London.
6) Bajpai, A.K., *Prog. Polym. Sci.*, **1997**, 22, 523.
7) Bajpai, A.K., Dengre, R., *Indian J. Chem*, **1999**, 38A, 101.
8) Koopal, L.K., Lee, E.M., Böhmer, M.R., *J. Colloid Interface Sci.*, **1995**, 170, 85-97.
9) Norde, W., Arai, T., Shirahama, H., *Biofouling 4*, **1991**, 37-51.
10) Li, B., Ruckenstein, E., *Langmuir*, **1996**, 12, 5052-5063.
11) Burns, N.L., *J. Coll. Int. Sci.*, **1996**, 178.
12) Van der Linde, A.J., Bijsterbosch, B.H., *Colloids Surfaces*, **1989**, 41, 345.
13) Norde, W., Rouwendal, E., *J. Colloid Interface Sci.*, **1990**, 139, 169.
14) Bos, M.A., Shervani, Z., Anusiem, A.C.I., Giesbers, M., Norde, W., Kleijn, J.M., *Colloids Surf. B*, **1994**, 3, 91.
15) Hoogeveen, N.G., Cohen Stuart, M.A., Fleer, G.J., *J. Colloid Interface Sci.*, **1996**, 182, 133.
16) Hoogeveen, N.G., Cohen Stuart, M.A., Fleer, G.J., *J. Colloid Interface Sci.*, **1996**, 182, 146.
17) Morrissey, B.W., Smith, L.E., Strömberg, R.R., Fenstermaker, C.A., *J. Colloid Interface Sci.*, **1976**, 56, 557.

18) Kawaguchi, M., Hayashi, K., Takahashi, A., *Macromolecules*, **1988**, 21, 1016.
19) Khan, G.F., Wernet, W., *Thin Solid Films*, **1997**, 300, 265.
20) Beaglehole, D., Webster, B., Werner, S., *J. Colloid Interface Sci.*, **1998**, 202, 541.
21) Holmström, N., Askendal, A., Tengvall, P., *Colloids Surf. B*, **1998**, 11, 265.
22) Zhou, A., Xie, N., *J. Colloid Interface Sci.*, **1999**, 220, 281.
23) Zhou, A., Xie, Q., Wu, Y., Cai, Y., Nie, L., Yao, S., *J. Colloid Interface Sci.*, **2000**, 229, 12.
24) Duval, J., Lyklema, J., Kleijn, J.M., van Leeuwen, H.P., *Langmuir*, **2001**, 17, 7573.
25) Dijt, J.C., Cohen Stuart, M.A., Hofman, J.E., Fleer, G.J., *Colloids Surf.*, **1990**, 51, 141.
26) Giesbers, M., Kleijn, J.M., Cohen Stuart, M.A., *J. Colloid Interface Sci.*, **2002**, 248, 88.
27) Thompson, D.W., Collins, I.R., *J. Colloid Interface Sci.*, **1992**, *152*, 197.
28) Hu, K., Fan, F.F., Bard, A.J., Hillier, A.C., *J. Phys. Chem. B*, **1997**, *101*, 8298.
29) Hillier, A.C., Kim, S., Bard, A.J., *J. Phys. Chem.*, **1996**, *100*, 18808.
30) Wang, J., Bard, A.J., *J. Phys. Chem.*, **2001**, *105*, 5217.
31) Ducker, W.A., Senden, T.J., *Langmuir*, **1992**, 8, 1831.
32) (a) Derjaguin, B. *Trans. Faraday Soc.* **1940**, *36*, 203. (b) Derjaguin, B. V., Landau, L. D. *Acta Phys. Iochim.,* **1941**, *14*, 633. (c) Derjaguin, B. V., Landau, L. D., *J. Exp. Theor. Phys.* **1941**, *11*, 802. (d) Verwey, E. J. W., Overbeek, J. T. G., *Theory of the Stability of Lyophobic Colloids*, Elsevier: New York, **1948**.
33) Steeg, van de, H.G.M., Cohen Stuart, M.A., Keizer, de, A., Bijsterbosch, B.H., *Langmuir*, **1992**, 8, 2538.
34) Zhang, Y., Tirrell, M., Mays, J.W., *Macromolecules*, **1996**, 29, 7299.
35) Brabander, de, E.M.M., Meijer, E.W., *Angew. Chem., Int. Ed.*, **1993**, 32, 1308.
36) Brabander, de, E.M.M., Brackman, J., Mure-Mak, M., Man, de, H., Hogeweg, M., Keulen, J., Scherrenberg, R., Coussens, B., Mengerink, Y., Wal, van der, S., *Macromol. Symp.*, **1996**, 102, 9
37) Ramzi, A., Scherrenberg, R., Joosten, J., Lemstra, P., Mortensen, K., *Macromolecules*, **2002**, 35, 827.
38) Haynes, C.A., Norde, W., *Colloids Surf. B*, **1994**, *2*, 517.

2 The Double Layer of a Gold Electrode Probed by AFM Force Measurements[*]

Abstract

Colloidal probe atomic force microscopy was used to determine the electric double layer interactions between a gold electrode and a spherical silica probe. The double layer properties of the gold/solution interface were varied through the pH and salt concentration of the electrolyte, as well as by externally applying an electric potential. The double layer potentials ψ^d of the gold surface were obtained by fitting the force-distance curves according to the DLVO (Derjaguin – Landau – Verwey – Overbeek) theory, using earlier obtained values for the double layer potential of the silica probe as input parameter. It was found that the gold electrode combines the features of reversible and polarizable interfaces, i.e., its charge and potential are determined by both the solution pH and the external potential. The pH dependence is attributed to proton adsorption and desorption from oxidic groups on the gold surface. In the potential range studied, ψ^d varies linearly with the applied potential; the variation in ψ^d is roughly 10% of that in the applied potential. The potential of zero force (the external potential at which $\psi^d = 0$) varies with pH. The various features of the gold/electrolyte interface are described well by an amphifunctional double layer model. The results of this study form the basis of the interpretation of adsorption studies on gold as a function of pH and externally applied potential.

2.1 Introduction

The adsorption from aqueous solution of charged molecules like ionic surfactants, polyelectrolytes and proteins is commonly found to be influenced by the solution pH and background electrolyte concentration[1-4]. This is generally explained by the effect of the solution properties on the potential of the sorbent surface on the one hand, and, for (weak) polyelectrolytes and proteins, by changes in the charge, structure and structure stability of the adsorbing molecules on the other hand. In order to discriminate between these effects, Bos et al[5] have studied the adsorption of several proteins on indium tin oxide (ITO) as a function of an *externally* applied potential at the adsorbing interface, while keeping the solution properties constant. It was found that variation of the external potential has little or no effect on protein adsorption at ITO, in contrast to the pronounced influence of the pH.

This observation can be explained in two different ways: 1) the large effect of the solution pH on the adsorption behaviour of the studied proteins stems mainly from conformational changes within the protein or changes in the protein charge as a result of the solution pH and not so much from changes in the potential of the sorbent surface, or 2) the major part of the externally applied potential difference over the

electrode/solution interface is not felt by molecules in solution. Indeed, Hu et al[6] showed that for TiO_2, like ITO a semiconducting oxide, the influence of an applied potential on the diffuse double layer potential is very limited, typically less than 10% of the applied potential. It is clear that for interpretation of the adsorption as a function of externally applied potential additional information on the double layer in solution as a function of applied potential is required.

For further adsorption studies we have chosen gold as the sorbent because it is a metallic conductor and over a relatively large potential range no electrochemical surface reactions occur in contact with an aqueous solution. Earlier studies[7,8] have shown that the double layer potential of gold is dependent on the pH of the electrolyte solution. For a pristine metal surface, one would not expect this. In the case of gold it is probably due to adsorption and partial discharge of hydroxyl ions upon contact with aqueous solution, resulting in oxidic surface sites on the gold[8,9]. The protolytic activity of these sites is responsible for the pH-dependency of the double layer potential.

In this paper we present results concerning the double layer properties of the gold/electrolyte interface as a function of both solution properties and externally applied potentials. Our goal is to elucidate the mechanism that determines the double layer charge and potential when a potential is externally imposed as compared to the situation in which the double layer is reversibly built up by spontaneous exchange of ions with the solution. This allows a better understanding of the role of electrostatics in adsorption phenomena and the possibilities for manipulating the adsorption of charged macromolecules by applying an external potential to the interface.

A way of studying the effect of externally applied potentials on the solution part of the double layer is to perform force measurements between the electrode and a reference surface in aqueous solution. Hieda et al[10] used an atomic force microscope (AFM) to measure the interactions between a gold-coated microsphere tip and an oxidized silicon sample with their interfacial potentials independently controlled using a bipotentiostat. Bard and coworkers[6,11,12] characterized the double layer properties of gold and TiO_2 electrodes in aqueous electrolyte by using a spherical silica particle attached to an AFM cantilever to probe the electric double layer interactions. Recently, Fréchette and Vanderlick[13] designed a gold electrode for use in the surface force apparatus (SFA) and studied the forces between mica and gold under potentiostatic control. Here, we have applied the same method as Bard and co-workers: the interaction between a gold substrate and a silica probe has been measured using an AFM and from the force-distance curves the double layer potential of the gold surface was obtained by fitting these according to DLVO theory (Derjaguin and Landau[14a-c] and Verwey and Overbeek[14d]). The double layer potential of the silica probe was used as an input parameter, for which we used values determined by Giesbers et al[7,15] from silica-silica interactions as a function of pH. For practical reasons in the present study the gold substrate is a gold wire. In our adsorption studies, measurements are performed on a reflectometer in which gold-coated silicon wafers are used as the substrate.

As an extension to the work of Hillier et al[11], which focussed on specific adsorption of halide ions on gold as a function of applied potential, we have measured the

interactions as a function of both the applied potential and the pH of the solution. As background electrolyte we used KNO_3, which is considered to be indifferent in this system. The double layer potentials determined from fitting the force curves are quantitatively interpreted in terms of an amphifunctional double layer model developed in our group[16]. This model considers the simultaneous effects of the electronic charge and the protolytic charge, and has recently been extended to also account for specific adsorption[17]. Earlier, Hu et al[6] have measured the pH-dependence of double layer interactions between a TiO_2 electrode and a silica probe, but this was only done at the open circuit potential. Here we provide a 2D data set, i.e., plots of the double layer potential as a function of applied potential over a wide range of pH values. Finally, it is shown that roughness of the gold surface (on the dimensional scale of the diffuse double layer thickness) is an important factor in the experimental determination of the double layer potential.

In a forthcoming paper we will report on the adsorption of a cationic polyelectrolyte (polyvinylpyridinium, PVP^+) on gold as a function of pH and applied potential, using the results obtained here concerning the variations in double layer potential to interpret the changes in adsorption kinetics and adsorbed amounts.

2.2 Experimental

2.2.1 Materials and Methods

The force-distance measurements in this study were performed using a DI (Digital Instruments Inc., Santa Barbara CA, USA) Nanoscope III atomic force microscope equipped with a standard fluid cell and a piezo scanner "E" (x, y range 12.5 μm x 12.5 μm).

Silica spheres of 6 μm diameter, which were a gift from Philips Research Laboratories (Eindhoven, The Netherlands), were glued to the "wide-legged" 200 μm long standard contact mode cantilevers with integrated tip (Digital Instruments Inc., Santa Barbara CA, USA). The glue used for this purpose was an epoxy resin, Epikote 1004 (Shell Amsterdam, The Netherlands) which has a melting point of about 100ºC and is highly insoluble in water. The method used to glue the particles to the cantilever tips has been described by Hillier[11] and Giesbers[15]. Just prior to the experiments the cantilevers with attached silica spheres were cleaned in a plasma cleaner (model pdc 32G, Harrick Scientific, New York, USA) for 30 seconds.

After each series of measurements the cantilever spring constant was determined. Calibration of the cantilevers was performed following the Cleveland method[18]. According to this procedure, particles of known size and density are attached to the free end of the cantilever and the spring constant k is determined from the resulting shift of the cantilever's resonance frequency.

Flat gold electrode surfaces were obtained by polishing one end of a gold wire with a cross section of 2 mm², held in a Teflon sample holder, with a slurry of 40 nm silica particles in water (OP-U suspension, Struers bv, Denmark). After polishing, the surface was ultrasonically cleaned in ultrapure water (EASYpure UV, (Richard van Seenus Technologies bv, Almere, The Netherlands), specific resistance 18.3 MΩ cm)

to remove the silica particles left by the polishing treatment. This resulted in relatively flat gold surfaces, containing areas with a peak-to-valley distance less than 5 nm over an area of 0.1 μm^2, as determined by AFM imaging in the contact mode with a standard nitride tip. Force measurements were performed at selected positions where the gold surface was relatively flat. In order to select such positions, the gold surface was scanned with the silica probe.

The other end of the gold wire was connected to a potentiostat (model 2059, AMEL s.r.l., Milan, Italy). A platinum counter electrode and a Ag/AgCl (in 3 M KCl) reference microelectrode were put into the in- and outlet of the AFM fluid cell and connected to the potentiostat. A schematic representation of the experimental set-up is shown in Figure 2.1.
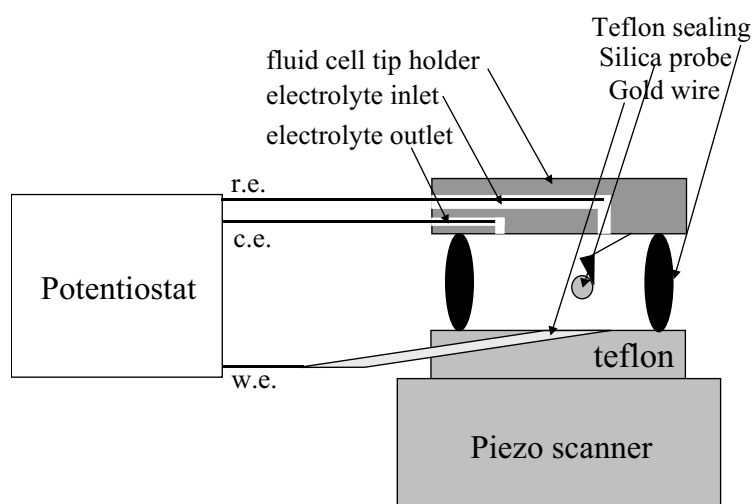
Figure 2.1: *Schematic representation of the experimental set-up. C.e. = counter electrode, r.e. = reference electrode, w.e. = working electrode.*

Aqueous electrolyte solutions were prepared from analytical grade KNO_3 in ultrapure water. Prior to each experiment nitrogen was bubbled through the solution for at least 30 minutes to deaerate the solution and to remove dissolved CO_2 which would decrease the pH. Approximately 10 ml of the solution was rinsed through the AFM cell after which the in- and outlet of the cell were closed. Three types of measurements were performed: double layer interactions between the silica probe and the gold substrate 1) as a function of salt concentration, 2) as a function of the solution pH; 1 and 2 under open circuit conditions, and 3) as a function of the applied potential, for several fixed pH values.

In the first series of measurements, the potential of the gold surface is determined by its equilibrium with the solution (open circuit potential). The pH was not adjusted; after deaeration for at least 30 minutes with nitrogen it was between 6.1 and 6.4. The series were started at the lowest salt concentration. After percolating the KNO_3 solution through the AFM cell and equilibration for 15 minutes, continuous force measurements with a measuring frequency of 1 Hz were started.

In the second series of measurements the sample and electrodes were connected to a voltmeter to measure the open circuit potential (OCP) as a function of the pH. In these measurements the pH was adjusted by adding aliquots of aqueous solutions of KOH or HNO_3. The experiments were performed as described above. At low pH, the system did not reach equilibrium until after about one hour; the OCP of the gold slowly changed from +100 mV to a value of +220 mV (vs. Ag/AgCl reference electrode). We waited until it shifted by less than 1 mV in 15 minutes.

Several series of measurements of the double layer interaction as a function of the applied potential were performed in 1 mM KNO_3 solution, each at a fixed pH. After rinsing the cell with the solution, and closing it, the sample, reference- and counter electrode were connected to the potentiostat. A voltammogram of the system was recorded to check the electric circuit and the functionality of the gold electrode. Subsequently an external potential was applied and after 10 to 15 minutes continuous force curves were measured with a measuring frequency of 1 Hz.

2.2.2 Determination of the double layer potential of the gold surface from the force curves

During the acquisition of a force curve, the measured experimental parameters are: the output signal of the photodiode (in V) which is directly related to the tip deflection. This can be calibrated by comparing the detector signal to the piezo displacement in the constant compliance region, and the substrate displacement in nm. These data are converted into a normalized force (F/R) vs. separation curve by use of the cantilever spring constant and the probe radius R. The onset of the constant compliance region is taken as the point of first contact and the point of zero separation ($r = 0$) in the DLVO fits.

According to DLVO theory the Gibbs interaction energy between two surfaces is given by the sum of the van der Waals and electrostatic interaction Gibbs energies. In the present work the electrostatic interaction between two parallel dissimilar surfaces is calculated using the non-linear Poisson-Boltzmann equation for the diffuse double layer in a symmetrical (z:z) electrolyte solution (see, e.g., Ref. 11, 19 and 20). Since this equation is one-dimensional, it applies to flat surfaces or relatively large colloidal particles only ($\kappa R \gg 1$, κ^{-1} being the Debye length and R the radius of the particle). In our system κR varies from about 100 to 1000 for electrolyte concentrations between $1 \cdot 10^{-4}$ M to $1 \cdot 10^{-2}$ M, so this condition is satisfied. The nonretarded equation according to Hamaker has been used to calculate the van der Waals interaction. For a detailed treatment of van der Waals forces between two macrobodies, see e.g., Ref. 21.

Interaction curves were solved numerically for the boundary conditions of both surfaces at constant potential as well as for both surfaces at constant charge, using a computing program of Hillier[11]. From the total Gibbs energy G_{tot} as a function of the separation distance r between two flat plates, the normalized interaction force $F(r)/R$ was obtained for a sphere of radius R and a flat plate using Derjaguin's approximation[22]:

$$\frac{F(r)}{R} = 2\pi G_{tot}(r) \qquad (2.1)$$

The calculated force curves were fitted to the experimental ones choosing the double layer potential (ψ^d) of the gold substrate and the Debye length (κ^{-1}) as the fit parameters. Generally, the resulting Debye-length agreed with the value calculated from the bulk electrolyte concentration. The double layer potential of the silica probe at various salt concentrations and pH values was taken from Giesbers et al[7,15] and used as an input parameter in the fitting of the double layer potential of the gold.

From previous measurements in our laboratory on symmetric systems (silica-silica and gold-gold) it is known that both the silica and the gold surface exhibit a certain degree of charge regulation, i.e., interaction curves are in between the two limiting cases of constant diffuse charge and constant diffuse potential surfaces. Here, the *measured double layer potential* $\psi^d_{measured}$ was taken as an average value of the two double layer potentials calculated for these two limiting cases, which never differ more than 5 mV.

Generally, fits were performed using a Hamaker constant for the gold-water-silica system of $5.7\cdot10^{-20}$ J[21]. However, van der Waals forces may be obscured by hydration forces and surface roughness as discussed by Giesbers et al[7]. It should be noted that the surface roughness was not necessarily constant, because the gold sample was polished anew before every series of measurements. Van der Waals forces are most pronounced at a distance of a few nanometers from the surface. At a salt concentration of 10^{-3} M, the fitting of the force curve on the basis of DLVO theory mostly refers to the region at 10 – 40 nm from the surface, where the contribution of van der Waals forces is very small. At the higher salt concentrations however, the Debye-length is so small that a large part of the potential drop takes place in the first 10 nm where the van der Waals forces do count. Especially here it is evident that van der Waals forces are considerably less than expected on the basis of the Hamaker constant for the ideally planar gold/water/silica system. Therefore, those force curves were fitted without the van der Waals contribution to the total Gibbs energy. At the lower salt concentrations, fitting with or without van der Waals forces was found not to be crucial for the resulting value of the double layer potential, the differences being in the order of a few millivolts.

2.3   Results and Discussion

Double layer interactions of the gold electrode with the silica probe were measured at various salt concentrations. Figure 2.2 gives representative examples of the force/distance curves obtained at two KNO_3 concentrations, at neutral pH and without external potential. Only the approach curves are shown, since upon retraction the double layer interactions are somewhat obscured due to adhesion, which makes the corresponding force curves less suitable for fitting with double layer theory. The double layer potential at zero separation ($\psi^d_{measured}$) calculated from these fits is -16 mV at 10^{-3} M KNO_3 and -12 mV at 10^{-2} M KNO_3. The decrease in double layer potential with increasing salt concentration is due to screening effects. The fitted values for the Debye-length (κ^{-1}) were 9.2 nm and 3.6 nm, respectively. The Debye-lengths calculated from the electrolyte concentrations are 9.6 nm and 3.0 nm, respectively.
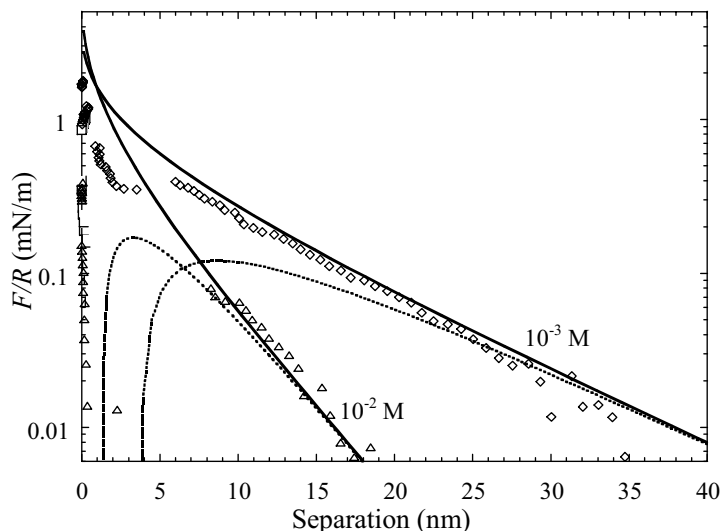
Figure 2.2: *Force – distance curves for a silica sphere ($\varnothing$ 6 μm) interacting with a gold electrode in KNO_3 solutions of concentrations as indicated at room temperature and pH ~ 6.4, at the open circuit potential. Data points correspond to the measurements. The dotted lines denote the numerical solutions of the non-linear Poisson-Boltzmann equation under the condition of both surfaces at constant surface potential. The solid lines are the fits for both surfaces at constant surface charge.*

2.3.1 Double layer potential of gold as a function of pH

For pH values in the range of 3.5 – 10.5 gold/silica interaction curves and the OCP values of the gold electrode (with respect to a Ag/AgCl reference electrode) were measured simultaneously. The higher salt concentration of the solution due to the adding of HNO_3 or KOH was accounted for in the DLVO fits. The results of the fits are plotted as a function of pH in Figure 2.3A. This diagram illustrates that ψ^d shows a steep change (30 mV/pH) in the range of pH 3 - 5. The iso-electric point of the gold surface, i.e., the pH for which $\psi^d = 0$, is at pH 4.95 ± 0.15. At higher pH, ψ^d levels off to a value of -17 mV.

We used solutions of KNO_3 - which is generally considered to be an indifferent electrolyte on gold – as supporting electrolyte. Giesbers et al[7] used solutions of potassium chloride – chloride ions are known to form complexes on the gold surface - to perform similar measurements. The ψ^d values obtained by Giesbers are slightly more negative than those presented in this work. However, the differences between the two data sets (Figure 2.3A) are so small as to be nearly within experimental error.

The OCP, measured simultaneously with the double layer potential, is given in Figure 2.3B. Going from high to low pH the OCP values were approximately the same as those obtained when measurements were started with a fresh surface for every pH. In one case hysteresis was observed, in that upon going from low to high pH OCP values were found to be different from those given in Figure 2.3B. This observation could not be reproduced in measurements outside the AFM cell and was not considered any further. The trends of figures 2.3A and 2.3B are similar, but quantitatively the

variation in the measured ψ^d is much lower than in the OCP. This is because by AFM measurements only a (diffuse) part of the double layer is seen.
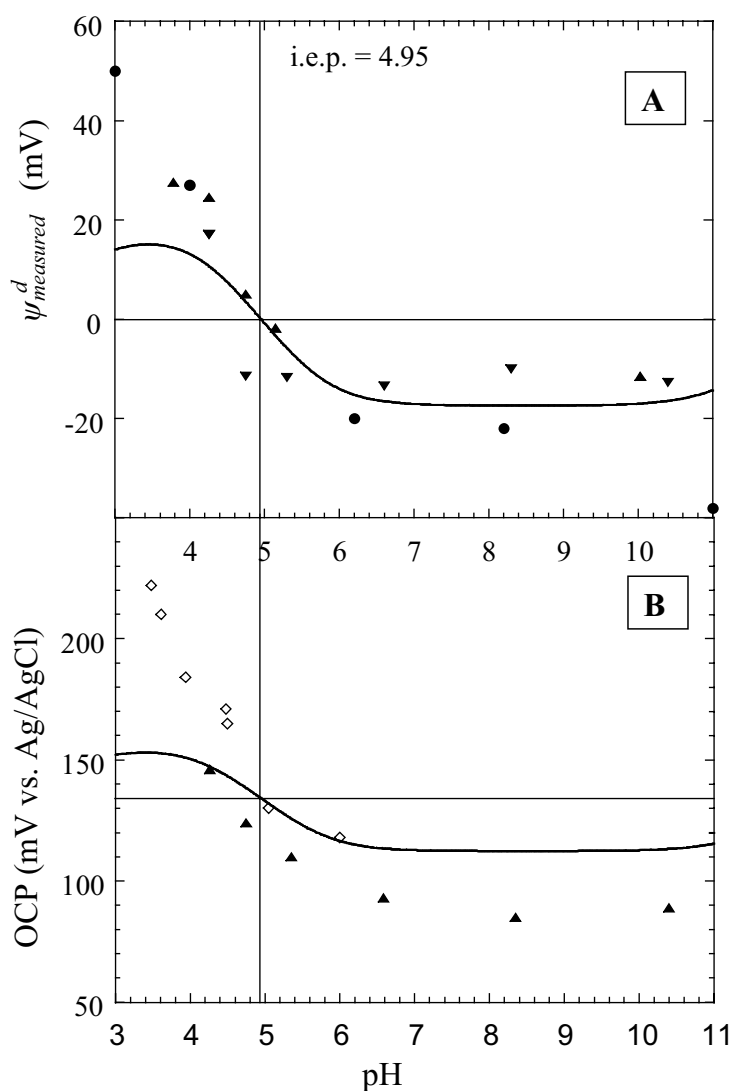
Figure 2.3 A: *Double layer potentials ($\psi^d_{measured}$) of the gold/electrolyte interface in 1 mM KNO₃ with respect to the solution as calculated from DLVO theory and the measured AFM force-distance curves. The iso-electric point is at pH = 4.95 ± 0.15.* ▼ *= $\psi^d_{measured}$, measured in a series from pH 10 to pH 4.* ▲ *= $\psi^d_{measured}$, measured from pH 3.5 to pH 10.* ● *= data of Giesbers et al for a gold-coated silicon wafer in 1 mM KCl[7].* ***B:*** *Open circuit potential (OCP) with respect to a Ag/AgCl reference electrode as a function of pH in 1 mM KNO₃.* ▲ *= OCP, measured in a series started at pH 10, and* ◇ *= when started with a fresh surface for each pH. The solid curves give the best fit of the amphifunctional model as described in section 2.3.3.*

2.3.2 Double layer potential of gold at externally applied potential

At various pH values the potential ($\Delta\Phi$) applied to the gold/solution interface was varied, keeping the salt concentration and pH constant. Figure 2.4 shows a typical set of force curves measured at pH 4.7. The inset shows ψ^d, obtained from fitting the

force data to double layer theory. An overview of the ψ^d values obtained as a function of $\Delta\Phi$ at all pH values studied is given in Figure 2.5A. The lines in this picture are only meant to guide the eye. It can be seen from this picture that ψ^d is determined by both the solution pH and the externally applied potential.
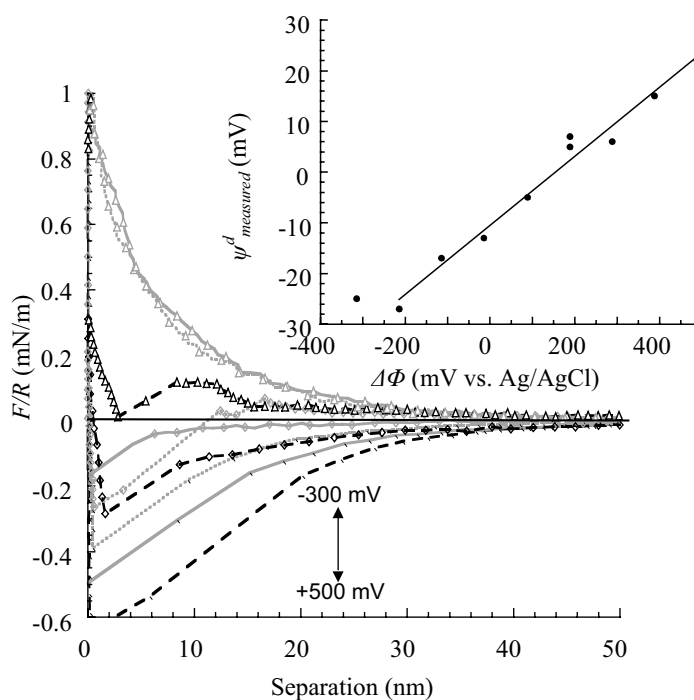
Figure 2.4: Force curves obtained at different externally applied potentials of the gold in 1 mM KNO₃ at pH 4.7. The inset shows the corresponding $\psi^d_{measured}$ values calculated from AFM measurements using DLVO theory. $\Delta\Phi$ changed in steps of 100 mV.

The variations in double layer potential found by either changing the solution pH or applying an external potential are in the same order of magnitude. Both effects are rather small – a change of several tens of millivolts in the potential and pH range studied. This is in line with the results of Hillier et al[11] and Wang and Bard[12]. Fréchette and Vanderlick[13], however, have found a larger spread in double layer potential of ca 150 mV over an external potential range of 400 mV.

With respect to adsorption studies, it should be noted that molecules adsorbing on the surface experience the double layer potential on a much smaller length scale than the radius of the colloidal probe. Since the gold substrate is polycrystalline and has a certain degree of surface roughness, the *local* potential can differ substantially from the smeared-out diffuse double layer potential as experienced by the colloidal probe. The various low index faces of gold crystals exhibit different potentials of zero charge (see, e.g., Ref. 23 and references therein). The effect of surface roughness is outlined below.

17
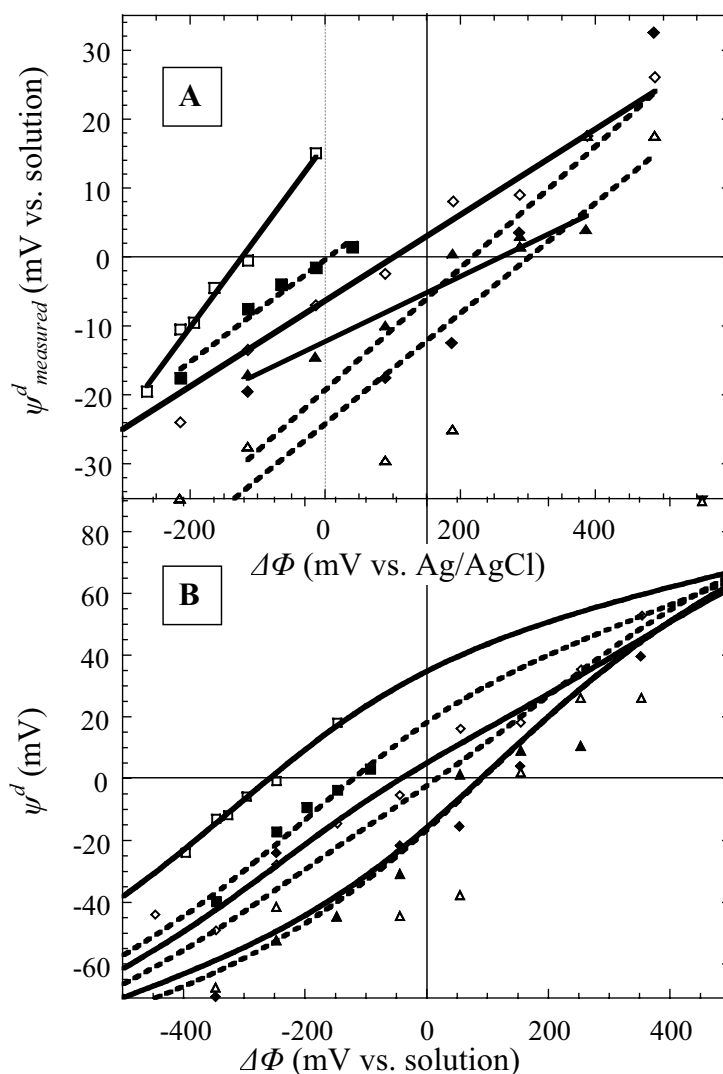
Figure 2.5 A: *Double layer potential ($\psi^d_{measured}$) as a function of the applied potential ($\Delta\Phi$) at different pH values.* □ *pH 3.5,* ■ *pH 3.9,* ◇ *pH 4.7,* ◆ *pH 5.1,* △ *pH 6.4,* ▲ *pH 6.8. The lines are only meant to guide the eye.* **B:** *Similar as figure 2.5A, here the data are adjusted as described in the text and the curves are fits according to the amphifunctional double layer model.*

2.3.3   Analysis in terms of an amphifunctional double layer model

The dependency of ψ^d on both the pH and the external potential was analysed using the model developed by Duval et al[16] This model combines the two charging mechanisms of the electrode/solution interface, i.e., charging by an external electric source and by adsorption/desorption of protons from/to the liquid. A somewhat similar model has been proposed by Smith and White[24] to describe the voltammogram of an electrode covered by a complete monolayer of molecules containing an acid group.

In the model the distribution of charge is assumed to be smeared-out over the gold surface. Here, we do not consider specific adsorption of ions from the electrolyte solution onto the gold. Briefly, the electric double layer is modelled to consist of four

elements, as schematically represented in Figure 2.6. The first corresponds to the bulk of the gold substrate. The second is a layer with oxidic binding sites for protons on the gold (referred to as the oxide layer). The third element is the Stern layer and the fourth is the diffuse part of the double layer. The solution side of the double layer (the Stern layer and the diffuse double layer) is described by classical GCS (Gouy – Chapman – Stern) theory. The pH-dependence of the surface charge is described by a two pK site-binding model. Since gold is a metallic conductor, the potential of the gold is constant throughout the entire bulk of the gold, up to the oxide layer. To calculate the potential drop over the oxide layer due to an externally applied potential, this layer is modelled as being a charge free dielectricum.
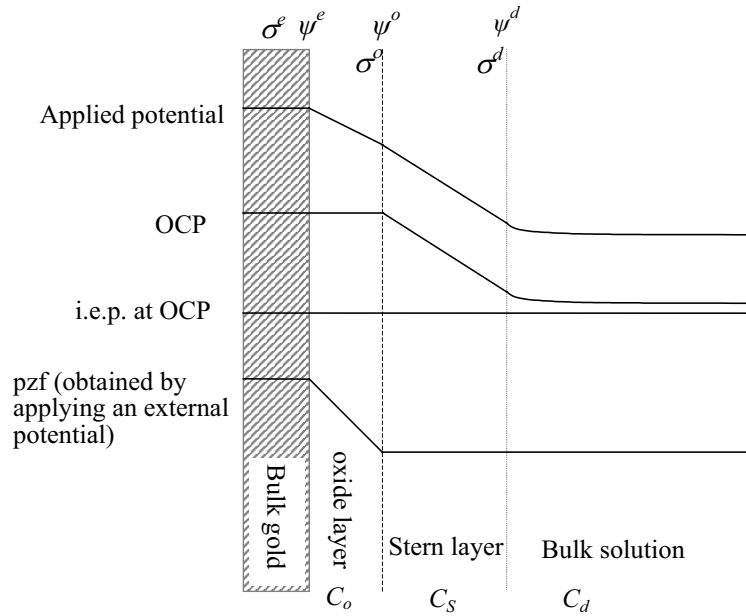
Figure 2.6: *Schematic representation of the potentials and charge distribution at the gold/electrolyte interface used in the amphifunctional double layer model.*

We used this so-called amphifunctional model to calculate ψ^d as a function of the solution properties and the externally applied potential. For more details on the model and calculations demonstrating the coupling between the two charging mechanisms and limiting cases the reader is referred to the original paper of Duval et al[16].

To fit a series of measurements at different pH values in the absence of a polarizing potential according to the amphifunctional double layer model, the only parameter to be chosen is the capacitance of the Stern layer C_s. In a review on of the gold/solution interface Vorontynsev[25] gives values between 15 and 50 $\mu F/cm^2$ for C_s from which we have chosen 30 $\mu F/cm^2$ as an average value. The number of proton binding sites (N_s), which determines the maximum charge density on the surface, and the pK values for the reactions:

$$-MOH_2^+ \underset{K_1}{\overset{}{\rightleftharpoons}} -MOH + H^+ \tag{2.2a}$$

$$-MOH \underset{K_2}{\overset{}{\rightleftharpoons}} -MO^- + H^+ \tag{2.2b}$$
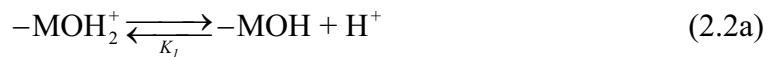
which determine the shape of the ψ^d(pH) plot - were obtained by fitting the model to the data of the double layer potential as a function of pH. The solid curve in Figure 2.3A gives the calculated curve with a value of 4.95 for both pK values (so $\Delta pK = 0$) and $N_s = 0.8 \cdot 10^{12}$ sites/cm^2. This number of binding sites would correspond to a coverage of the gold surface with oxidic groups of approximately 0.1%, based upon a density of $1.4 \cdot 10^{15}$ gold atoms per cm^2 at the Au$_{111}$ surface. Although the effect of surface roughness has not yet been taken into account in the calculation, the oxide layer seems to be well below full monolayer coverage. Such observation has been made before[16] and would deserve further study.

In the low pH range, the model does not entirely fit the measured data. To get a better match between experimental data and model calculations, it would be necessary to increase the number of proton binding sites in the model. However, this number is generally believed to decrease with decreasing pH[8,9], which is at variance with Figure 2.3A. Hence, it is likely that another double layer property is responsible for the different behaviour at low pH.

To fit a series of measurements with an externally imposed potential at the gold surface at a certain pH, we additionally need an estimate for the capacitance of the oxide layer C_o. In contrast to the open circuit situation, there is a potential drop over the oxide layer. C_o is given by the relation:

$$C_o = \frac{\varepsilon_0 \varepsilon_r}{d} \tag{2.3}$$

in which d is the thickness of the oxide layer. This thickness is determined by the Au-O-bond which is approximately 0.5 nm.

In the model $\Delta\Phi$ - like ψ^d – is defined with respect to the potential of the bulk solution ($\Delta\Phi_{Au\text{-}solution}$). Of course, in the experiments $\Delta\Phi$ is not applied with respect to the solution but with respect to the Ag/AgCl reference electrode ($\Delta\Phi_{Au\text{-}ref}$). By adding the potential difference between the reference electrode and the solution {($\Delta\Phi_{Au\text{-}ref}$) + ($\Delta\Phi_{ref\text{-}solution}$) = ($\Delta\Phi_{Au\text{-}solution}$) = $\Delta\Phi$} the applied potential is expressed with respect to the solution. The value of ($\Delta\Phi_{ref\text{-}solution}$) can be extracted from comparison of the measured potential of zero force (pzf) with the pzf calculated from the model. The pzf, defined as the applied potential for which the double layer potential equals zero, is a function of the pH and is given in Figure 2.7. In the point of zero charge, at pH = 4.95, the double layer potential equals zero. The measured pzf at this pH is 150 mV (vs. Ag/AgCl), which is close to the value of the open circuit potential (135 mV vs. Ag/AgCl), as can be seen in Figure 2.3B. Thus, all potentials applied with respect to the Ag/AgCl reference electrode are shifted by -150 mV to express these with respect to the potential of the bulk solution.
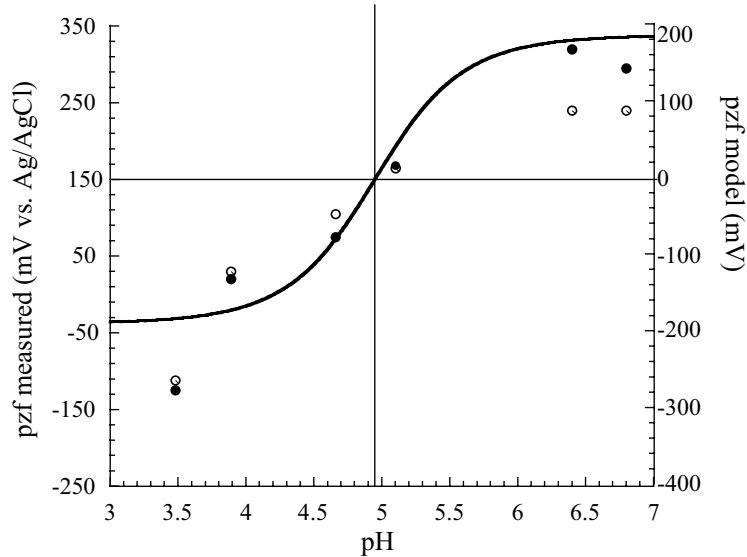
Figure 2.7: *Potential of zero force of gold in 1 mM KNO₃ as a function of the pH. The data are taken from Figure 2.5.* ● *pzf determined from Figure 2.5A;* ○ *pzf determined from the model curves in Figure 2.5B. The solid curve gives the fit of the model with $N_s = 0.8 \cdot 10^{12}$ sites/cm².*

In comparing the measured data with the model, another problem arises. The gold electrode is polycrystalline and because of surface asperities the probe does not touch the gold surface at every position. The effective double layer potential "felt" by the probe is really an ensemble of different potentials for different separations over an area of about 0.1 μm² (the electric interaction area of the probe and the surface). A first order approximation for the relation between the actual (local) double layer potential ψ^d_{local} and the measured *effective* double layer potential $\psi^d_{measured}$, which is a smeared-out, average value at the distance of closest approach, is given by:

$$\psi^d_{measured} = \frac{1}{A} \int \psi^d_{local} \cdot e^{-\kappa\delta} \mathrm{d}A \qquad (2.4)$$

in which A is the interaction area. Since the distance between the surfaces (δ) varies in this interaction area (only the larger surface asperities are touching the opposite surface), the weigh factor exp($-\kappa\delta$) is in the integral.

Equation (2.4) still assumes a locally undisturbed one-dimensional behaviour of the double layer, which is a good approximation provided that there is no significant double layer overlap between the asperities at the gold surface. That is, if the characteristic length λ between the peaks (or valleys) of the surface asperities is much larger than the double layer thickness (characterized by the Debye length κ^{-1}): $\kappa\lambda \gg 1$. From topographic images of the gold surface taken by AFM in the contact mode it was observed that λ is about 100 nm so that for $\kappa^{-1} = 10$ nm this condition is fairly well satisfied. Unfortunately, Equation (2.4) can only be applied to find the real double layer potential if the roughness profile and characteristics concerning the polycrystallinity of the surface in the interaction area are known. Since such information is not available for our Au surface, we use an even more simplified method, which involves a shift of the plane of charge (i.e., the point of zero separation

21

in the force-distance curves) over a distance Δ. In other words, we consider the distance of closest approach between the probe and gold surface to be Δ, which implies that our $\psi^d_{measured}$ values are related to the average potential at the onset of the diffuse double layer, ψ^d, by:

$$\psi^d_{measured} = \psi^d e^{-\kappa\Delta} \qquad (2.5)$$

The significance of Δ is that it replaces the ensemble of all potentials for different separations (summed over A) by a constant potential $\psi^d_{measured}$ at a mean separation Δ. The value of Δ is obtained by comparing ψ^d calculated with the amphifunctional model and the experimental value for $\psi^d_{measured}$. For one series of measurements Δ should be a constant because the whole series is taken at the same location at the gold surface. For different series, Δ may vary because the measurements refer to another area of interaction at the gold surface. It may be added that any error in determining the spring constant of the cantilever has a proportional effect on the slope of the $\psi^d - \Delta\Phi$ curves, which has an (exponential) impact on the value of Δ. The inaccuracy in the spring constant may be as much as 30% (as a result of inaccuracies in the determination of the radii of the particles used in the Cleveland method of calibration), which adds to the possible error in the estimation of Δ. Each series of measurements was performed with one cantilever.

Figure 2.5B gives the ψ^d values corrected for roughness as indicated above as well as the curves calculated with the amphifunctional model. It shows that, when the surface roughness is taken into account, the ψ^d values and their pH and $\Delta\Phi$ dependence are fairly well described by the model. In Table 1 the values obtained for Δ are listed. In the third column of Table 1 the fitted values for N_s are shown. Since in the model N_s determines the point of zero force of the curves, whereas Δ determines the slope of the curves, the two parameters are independently obtained from the experimental data.

As can be inferred from Table 1, the value of Δ varies between 2 and 11 nm. Taking into account the large error in this value due to the inaccuracy in determining the spring constant, this agrees fairly well with the observed surface roughness of 5 nm (peak-to-valley distance).

Table 1: *Values of Δ for the series of measurements in which the applied potential was varied at a range of pH values, at an electrolyte concentration of 1 mM KNO_3.*

pH	Δ (nm)	N_s ($\cdot 10^{12}$cm^{-1})
3.5	2	3
3.9	8	1.5
4.7	7	1.2
5.1	2	0.7
6.4	4	1.0
6.8	11	1.0

Wang and Bard[12] recently reported a large discrepancy between the electrically induced charge of a gold electrode and its surface charge density calculated from ψ^d values determined with colloidal probe AFM (the latter is in fact the diffuse double

layer charge). This discrepancy was mainly attributed to ion correlation and ion condensation effects. However, there is no evidence for counterion condensation from the force curves at different salt concentrations (Figure 2.2). The analysis presented here shows that the difference between electronic charge and diffuse double layer charge has to be explained in terms of surface roughness, the buffering effect of proton binding sites and the presence of a very thin dielectric layer at the surface (in our model a very incomplete oxide layer).

2.4   Conclusions

The double layer potential of gold can be varied through the solution pH as well as by an externally applied potential. Classical GCS theory alone is inadequate to describe the double layer phenomena of the gold surface. The different fits of the data in figures 2.3, 2.5B and 2.7 show that the amphifunctional model proposed by Duval et al[16] describes very well the charging behaviour of the gold/solution interface. This is true both in the presence and absence of a polarizing potential, provided surface roughness is taken into account. It appears that a very low density of proton binding sites at the gold surface causes the pH to have an effect on the double layer potential in a fairly narrow pH-range. The total variation in double layer potential is also relatively small due to this small number of oxide sites. The pH dependence correlates with a two-pK proton exchange reaction scheme with the same pK values of 4.95. The changes in ψ^d as a result of an externally applied potential are small ($\Delta\psi^d/\Delta(\Delta\Phi) \sim 0.1$) due to large potential drops over the oxide layer and the Stern layer. Moreover, due to surface roughness the potential determined with colloidal probe atomic force microscopy is generally lower than the local diffuse double layer potential.

Of course, adsorbing molecules near the gold surface experience the local potential. Therefore, heterogeneity in surface potential due to polycrystallinity of the gold and partial coverage with oxide sites also play a role in adsorption phenomena. As far as electrostatics is important in adsorption, however, we expect to be able to interpret at least the trends in kinetics and adsorbed amounts with pH and applied potential on the basis of the amphifunctional charging mechanism of the gold/solution interface.

2.5   Acknowledgements

2.6   References

1)   Haynes, C.A., Norde, W., *Colloids Surf. B* **1994**, *2*, 517.
2)   Kleijn, J.M., Norde, W. *Heterogeneous Chem. Rev.*, **1995**, *2*, 157.
3)   Burns, N.L., Holmberg, K., Brink, C., *J. Colloid Interface Sci.*, **1996**, *178*, 116.
4)   Giacomelli, C.E., Avena, M.J., Depauli, C.P., *J. Colloid Interface Sci.*, **1997**, *188*, 387.
5)   Bos, M.A., Shervani, Z., Anusiem, A.C.I., Norde, W., Kleijn, J.M., *Colloids Surfaces B*, **1994**, *3*, 91.

6) Hu, K., Fan, F.F., Bard, A.J., Hillier, A.C. *J. Phys. Chem. B*, **1997**, *101*, 8298.

7) Giesbers, M., Kleijn, J.M., Cohen Stuart, M., *J. Colloid Interface Sci.*, **2002**, 248, 88.

8) Thompson, D.W., Collins, I.R., *J. Colloid Interface Sci.*, **1992**, *152*, 197.

9) Angerstein-Kozlowska, H., Conway, B.E., Hamelin, A., Stoicoviciu, L., *J. Electroanal. Chem.*, **1987**, *228*, 429.

10) Hieda, H., Ishino, T., Tanaka, K., Gemma, N., *Jpn. J. Appl. Phys.*, **1995**, *34*, 595.

11) Hillier, A.C., Kim, S., Bard, A.J., *J. Phys. Chem.*, **1996**, *100*, 18808.

12) Wang, J., Bard, A.J. *J. Phys. Chem.* **2001**, *105*, 5217.

13) Fréchette, J., Vanderlick, T.K. *Langmuir* **2001**, *17*, 7620.

14) (a) Derjaguin, B. *Trans. Faraday Soc.*, **1940**, *36*, 203. (b) Derjaguin, B. V., Landau, L. D., *Acta Phys. Iochim.*, **1941**, *14*, 633. (c) Derjaguin, B. V., Landau, L. D. *J. Exp. Theor. Phys.*, **1941**, *11*, 802. (d) Verwey, E. J. W., Overbeek, J. T. G., *Theory of the Stability of Lyophobic Colloids*, Elsevier: New York, **1948**.

15) Giesbers, M., *Thesis Wageningen, The Netherlands* **2001**.

16) Duval, J., Lyklema, J., Kleijn, J.M., van Leeuwen, H.P. *Langmuir*, **2001**, *17*, 7573.

17) Duval, J., Kleijn, J.M., Lyklema, J., van Leeuwen, H.P., *J. Electroanal. Chem.*, **2002**, 532, 337.

18) Cleveland, J.P., Manne, S., Bocek, D., Hansma, P.K. *Rev. Sci. Instrum.*, **1993**, 403.

19) Hiemenz, P.C., *Principles of Colloid and Surface Chemistry*, Lagowski, J.J., Ed., Marcel Dekker, Inc.: New York and Basel, **1986**, Vol 4, Ch. 12.

20) Hunter, R.J., *Foundations of Colloid Science*, Oxford University Press: Oxford, **1987**.

21) Lyklema, J. In *Fundamentals of Interface and Colloid Science*, Academic press: London, **1991**, Vol I, sections 4.6 and 4.7.

22) Derjaguin, B.V. *Kolloid-Z.*, **1934**, *69*, 155.

23) Hamelin, A., Vitanov, T., Sevastyanov, E.S., Popov, A. *J. Electroanal. Chem.*, **1983**, *138*, 225.

24) Smith, C.P., White, H.S. *Langmuir*, **1993**, *9*, 1.

25) Vorotynsev, M.A., *Modern Aspects of Electrochemistry*, Bockris, J.O'M., White, R.E., Conway, B.E., Eds., Plenum Press: New York, **1986**, Ch 2, p. 177.

3 Reflectometry on a Gold Electrode: Sensitivity and Electro-Optic Effect

Abstract

In this chapter calculations and measurements are presented concerning the sensitivity of reflectometer measurements in studying the adsorption of charged polymers from aqueous solution onto a gold electrode. Furthermore, the change in reflectometer signal as a result of applying a potential to the gold electrode - the so-called electro-optic effect - is addressed. The gold electrodes used in our studies are strips of silicon wafers coated with a thin (15 nm) gold film. An even thinner (5 nm) layer of titanium is situated between the gold and the silicon, to prevent the gold from detaching. The adsorbed polyelectrolyte is quaternized polyvinyl pyridinium (PVP^+). For determining adsorbed amounts from the reflectometer signal, a sensitivity factor, A_s, is needed. A_s was calculated by modelling the system as a stack of thin layers of uniform refractive index. The influence of several parameters, such as the layer thickness of the gold and the angle of incidence of the laser beam, on the sensitivity of the reflectometer set-up was examined. In the range of potentials applied (-0.2 to +0.6 V vs. Ag/AgCl reference electrode) it was found that the electro-optic effect is significant compared to the change in the reflectometer output signal resulting from adsorption. The sensitivity factor A_s, however, is much less affected by the electro-optic effect than by the effect of inaccuracies in the system parameters. Therefore, by recording a baseline at the same applied potential as that at which adsorption is monitored, adsorption data can be obtained without interference of the electro-optic effect.

3.1 Introduction

Reflectometry is a relatively simple optical technique for directly measuring the adsorbed amount at a solid/liquid interface. It has been shown by Dijt et al[1] that under properly chosen conditions the change in the reflectometer output signal can be often virtually linear in the adsorbed amount. The proportionality factor between these two quantities is denoted as the sensitivity factor, A_s. In this chapter we present calculations and measurements concerning A_s for the adsorption of quaternized polyvinyl pyridinium (PVP^+) from aqueous solution onto a gold electrode, in this case a strip of a gold-coated silicon wafer. Our aim is to asses the effect of small variations in experimental and system parameters, such as the local gold layer thickness and the angle of incidence, on A_s. Since we are interested in manipulating the adsorption of charged molecules onto charged interfaces, one of the key variables in our adsorption studies is the externally applied potential to the gold/liquid interface. A complication is that the reflectometer output signal depends on the optical properties of the gold, which vary with the applied potential at the interface - the so-called electro-optic effect. Therefore, the influence of the electro-optic effect on the sensitivity of our reflectometer experiments is also addressed in this chapter.

For semi-conductors the electro-optic effect has been reported in literature in the 1960's[2,3]. In fact, modulation of the reflectance by applying a modulated electric field to a semi-conductor was proven to be a powerful tool for investigations of its electronic band structure[2]. Kleijn et al[4] observed that applying an external potential to a semiconductor/electrolyte interface causes a significant change in the reflectometer signal. They showed that the shift in reflectance of the interface results from a change in the concentration of charge carriers in the space-charge layer of the semi-conductor; changes in the double layer at the electrolyte side do not play a significant role.

In metallic conductors free electrons prevent the building up of an electric field. Screening of an external electric field occurs within a few atomic layers from the surface (0.05 - 0.2 nm)[5,6]. Since the depth that is probed by the light is of the order of 10 nm, it was therefore thought that electric fields would have little effect on the optical properties of metals. However, in 1966 Feinleib[5] reported a change in the reflectance spectra of metal/electrolyte interfaces as a result of electric field modulation. From simple model calculations Prostak and Hansen[7] showed that the prominent changes in the reflectance spectra observed by Feinleib are not due to modulation of the optical constants of the electrolyte but to modulation of those of the metal.

The importance of the electro-optic effect in interpreting ellipsometry results was demonstrated by Beaglehole et al[8]. They showed that the adsorption of small molecules onto gold, such as surfactants and small polymers, changes the magnitude of the electro-optic effect. This observation was attributed to the fact that smaller molecules adsorbed onto a surface, will lie in the high-electric-field region of the double layer and alter the local field and hence the surface charge for a given potential. This complicates the interpretation of such ellipsometer results seriously: the response to adsorption is in fact the sum of two effects, namely the building up of an adsorption layer *and* a change in the optical properties of the outer gold layer.

To obtain a complete picture of the significance of the electro-optic effect in our system, we performed adsorption measurements with and without an externally applied potential at the interface. From the adsorption measurements with no potential applied and using an optical model for the system, we determined A_s. Then we determined the change in reflectometer signal as a function of the applied potential without any material adsorbed at the interface. Calculations on the reflectance of the surface and measurements were combined to recalculate A_s as a function of the applied potential. Subsequently, we determined the reflectometer output signal as a function of the applied potential with a charged polymer adsorbed at the surface. By comparing these experimental results it is possible to determine whether the presence of the polyelectrolyte at the gold surface influences the electro-optic effect.
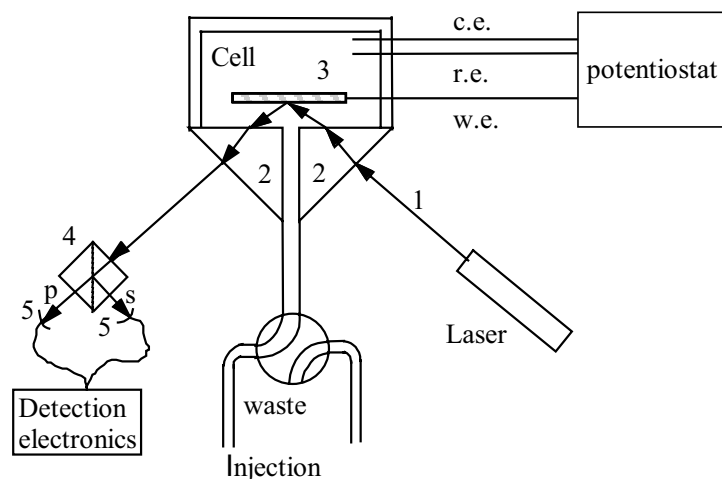
Figure 3.1: *Schematic representation of the reflectometer set-up. (1) Linearly polarized laser beam; (2) 45° glass prism; (3) adsorbent surface; (4) polarizing beam splitter; (5) photodiodes detecting the perpendicular (s) and parallel (p) components of the reflected beam; w.e. = working electrode; r.e. = reference electrode; c.e. = counter electrode.*

3.2   Theory

3.2.1   Principles of reflectometry

The reflectometer set-up with a stagnation-point flow cell that we used in our studies (see Figure 3.1) has been extensively described by Dijt et al[1] and therefore will be treated only very briefly here. Fixed-angle reflectometry measures the reflectance of a flat surface at or near the Brewster angle. A linearly polarized light beam is reflected from the surface and then split into its parallel (*p*) and perpendicular (*s*) components of which the intensities (I_p and I_s respectively) are measured continuously. Upon adsorption of molecules at the surface the ratio of these intensities changes and from this change the adsorbed amount can be obtained. The output signal *S* is defined as:

$$S = \frac{I_p}{I_s} \tag{3.1}$$

The signal that is recorded is the difference between the output signal of the reflectometer during the adsorption measurement and the output signal of the surface at the start of the experiment:

$$\Delta S = S - S_0 \tag{3.2}$$

The adsorbed amount can be calculated from the recorded results in the following way:

The reflected intensities I_p and I_s can be expressed in the incident intensities I_p^0 and I_s^0, two loss factors f_p and f_s and the reflectances R_p and R_s of the substrate:

$$I_p = f_p R_p I_p^0,$$
(3.3)

$$I_s = f_s R_s I_s^0$$
(3.4)

Combining equations 3.1, 3.3, and 3.4 results in the following relation for the output signal S:

$$S = f \frac{R_p}{R_s}$$
(3.5)

in which
$$f = \frac{f_p I_p^0}{f_s I_s^0}.$$
(3.6)

Since f does not change due to adsorption, it can be expressed as:

$$f = \frac{S_0}{\left(\frac{R_p}{R_s} \right)_0}$$
(3.7)

The output signal will alter with the adsorption of material onto the surface:

$$\Delta S = f \left\{ \left(\frac{R_p}{R_s} \right)_\Gamma - \left(\frac{R_p}{R_s} \right)_0 \right\}$$
(3.8)

Since R_p/R_s is in most cases linearly dependent on the adsorbed amount[1], the term within brackets in equation 3.8 equals: $\Gamma d(R_p/R_s)/d\Gamma$. Now equation 3.7 and 3.8 give the equation for the adsorbed amount:

$$\Gamma = \frac{\Delta S}{S_0} \frac{1}{A_s}$$
(3.9)

in which:

$$A_s = \frac{1}{(R_p/R_s)_0} \frac{\mathrm{d}(R_p/R_s)}{\mathrm{d}\Gamma} \tag{3.10}$$

S_0 is set to about 1 in each experiment by adjusting the polarisation direction of the laser beam.

3.2.2 Calculating the sensitivity factor A_s

The sensitivity factor for the system, used to determine the adsorbed amount from the reflectometer signal, was calculated using the method of Hansen which is based on the matrix formalism of Abeles[9]. The system is divided into a number of parallel flat layers and the refractive index is assumed to be constant throughout each layer. The system used in our measurements is a silicon wafer with sputtered thin layers of titanium (5 nm) and gold (15 nm) in contact with aqueous solution. This is presented schematically in Figure 3.2. The titanium serves as an adhesive between the silicon and the gold layer. In our measurements a positively charged polyelectrolyte, quaternized polyvinyl pyridine (PVP[+]), was adsorbed at the gold surface.
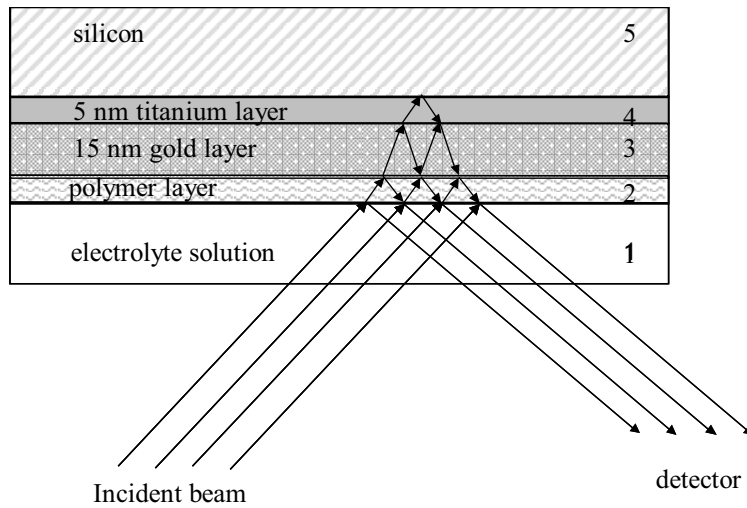
Figure 3.2: *Schematic representation of the multilayer system at which the laserbeam of the reflectometer is reflected.*

For the refractive index of the adsorbed layer some value has to be adopted. We use De Feijter's relation:

$$n_{adsorbed} = n_{solvent} + \frac{\Gamma}{d_{adsorbed}} \cdot \frac{\mathrm{d}n_{adsorbed}}{\mathrm{d}c} \tag{3.11}$$

where $n_{adsorbed}$ is the refractive index of the adsorbed layer, $n_{solvent}$ the refractive index of the solvent, Γ the total adsorbed amount, $d_{adsorbed}$ the adsorbed layer thickness, and $\mathrm{d}n_{adsorbed}/\mathrm{d}c$ the refractive index increment of the adsorbed substance. On the basis of experience a first estimation is made for the total adsorbed amount of polyelectrolyte and for the thickness of the adsorbed layer. The refractive index of the adsorbed layer

can be calculated with these parameters and equation 3.11. Using the value of $dn_{adsorbed}/dc$ for PVP^+ (with Br^- being the counterion) taken from Hoogeveen et al[10] we calculate the sensitivity factor for this system.

It should be noted that we used PVP^+ with NO_3^- being the counterion, since bromide specifically adsorbs onto gold. This may slightly change the value of dn/dc, causing an inaccuracy in the calculated value for $n_{adsorbed}$. Upon adsorption of $PVP^+NO_3^-$, which is in fact an ion exchange process at the gold surface, positively charged ions (K^+ and H^+) are exchanged for the polyelectrolyte chain. Since the gold surface is immersed in KNO_3 solution before the adsorption takes place, nitrate ions at the surface will not be replaced by another type of anion. OH^- ions at the surface might be replaced by the nitrate ions, causing a change in the refractive index of the adsorbed layer. However, this is not of significance, since the concentration of nitrate ions is hardly affected by the dissolved polyelectrolyte and since the pH of the solution in which the gold was immersed before the adsorption is the same as the pH of the solution used to perform the adsorption experiments.

The calculated sensitivity factor is used to recalculate the total adsorbed amount from our reflectometer experiments and the cycle is started anew. We iterate, keeping the thickness of the adsorbed layer at a constant value, until a constant value for the sensitivity factor is obtained. Finally, the influence of variations in the concentration of polymer in the adsorbed layer, expressed in variations in the estimated polymer layer thickness at a constant total adsorbed amount, is determined.

3.3   Experimental

Aqueous electrolyte solutions were prepared from analytical grade KNO_3 in ultrapure water. The concentration of KNO_3 was always 1 mM. Quaternized polyvinyl pyridinium bromide with a molecular mass $M_w = 12000$ g/mole was purchased from Rochrom (The Netherlands). The heterodispersity coefficient as specified by the supplier is $M_w/M_n = 1.07$. The sample was dialyzed against a solution of 1 mM KNO_3 to exchange the bromide counterion - which specifically adsorbs onto gold - for the indifferent nitrate ion. Adsorption experiments were all carried out using 5 mg/l $PVP^+(NO_3^-)$ solutions with 1 mM KNO_3 as background electrolyte. Prior to each experiment nitrogen was bubbled through the solution for at least 30 minutes to deaerate the solution and to remove dissolved CO_2. Solutions were introduced in the reflectometer using an impinging jet system as described by Dabros and van de Ven[11] and Dijt[1].

Platelets (strips) cut from silicon wafers with a 5 nm layer of titanium and a 15 nm layer of gold sputtered on top of this, were used as the substrate. These wafers were supplied by Philips Research Laboratories in Eindhoven (The Netherlands). The titanium layer serves to prevent the gold layer from detaching from the silicon wafer. The platelets were cleaned by immersion for 2 minutes into "piranha solution", i.e., a hot mixture of 30% H_2O_2 and concentrated H_2SO_4, after which the wafers were thoroughly rinsed with ultrapure water and left overnight in the electrolyte solution which was used as a blank in the corresponding adsorption experiments. Each strip was used only once. The surface roughness of the gold films, determined by AFM in the contact mode, was found to be less than 2 nm over an area of 1 μm^2.

In order to apply a potential to the surface, a three-electrode system was used. The gold-coated wafer was used as the working electrode and potentials were applied with respect to a Ag/AgCl (3 M KCl) reference electrode. The counter electrode was a platinum wire and all electrodes were put directly into the reflectometer cell (see Figure 3.1). Potentials were applied using a potentiostat (model 2059, AMEL s.r.l., Milan, Italy).

The electro-optic effect for the bare surface as well as for the PVP$^+$ covered surface was measured by first recording a baseline with no potential applied to the gold/electrolyte interface (open circuit potential). The baseline for the bare surface was recorded while 1 mM KNO_3 solution was flowing through the reflectometer cell. After two minutes a potential was applied and the reflectometer output signal was continuously recorded until the signal had become constant again. This was typically within a minute, depending on the magnitude of the potential step. Simultaneously, the current flowing through the electrode system was monitored. This current decreased to values in the order of $1 \cdot 10^{-12}$ to $1 \cdot 10^{-6}$ A. To determine the influence of the electrolyte on the electro-optic effect, the same measurements have been performed while flowing solutions of different salts and concentrations through the cell. For the PVP$^+$ covered surface, first an adsorption curve was recorded under open circuit conditions. For this, a baseline was recorded while flowing 1 mM KNO_3 solution in the cell. After two minutes polyelectrolyte solution was flushed into the reflectometer cell. The output signal of the reflectometer was recorded at intervals of 1 s. Measurements were continued until the output signal of the reflectometer did not change anymore. This was typically after six minutes. Here, only the total shift in reflectometer output signal after adsorption is considered, the kinetics of the adsorption are not within the scope of this chapter. subsequently, the electro-optic effect was measured in the same way as for the bare surface, while KNO_3 solution was flowing through the reflectometer cell.

Potentials applied at the interface were typically in the range of -0.2 to +0.6 V with respect to a Ag/AgCl (3M KCl) reference electrode. In this potential range a transient polarization current is observed after a potential step. In the steady state no significant current was measured, indicating that no redox reactions take place at the gold/electrolyte interface. The rate at which *S* reaches a constant value and the current drops to zero after a potential step is determined by the charging of the electric double layer (i.e., the development of surface charge on gold and the formation of a double layer in solution; see Kleijn et al[5] and Beaglehole et al[8]).
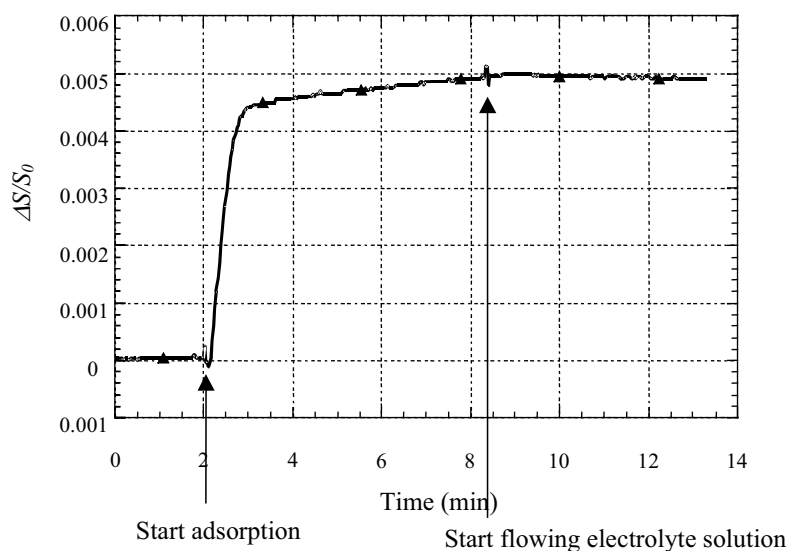
Figure 3.3: *A typical example of the reflectometer output signal while adsorbing PVP^+ (M_w = 12 kg/mole) from a 5 mg/l solution onto gold, at 1 mM KNO_3 and neutral pH without any potential applied at the interface. $S_0 \approx$ 1.*

3.4 Results and Discussion

3.4.1 Determination of A_s; no potential applied at the surface

A characteristic example of an adsorption curve, measured with reflectometry, is presented in Figure 3.3. The average total change in the reflectometer signal $(\Delta S_{tot}/S_0)$ as a result of adsorption from a 5 mg/l PVP^+ solution onto the gold surface without an applied potential is 0.0053. We will use this value to calculate A_s for this system. Other parameters we need to know to calculate A_s are the angle of incidence of the laser beam and the thickness and refractive indices of the layers as defined in Figure 3.2 at the wavelength of the light from the laser beam (632.8 nm). These are given in Table 1. It should be noted that the refractive index of gold as given in the table is for the bulk metal. It has been reported that for thin gold films the optical constants may be different[12]. The layer thickness of the adsorbed polyelectrolyte layer (1 nm) is an estimated value based on the dimensions of the polyelectrolyte and the assumption that the positively charged molecules adsorb in a flat conformation on the negatively charged surface[13] (the iso-electric point of the gold surface is at pH 5[15]). The effect of the uncertainties in the refractive index of the gold layer and in the polyelectrolyte layer thickness will be discussed later in this chapter. The refractive index of the polyelectrolyte layer is now calculated using equation 3.11. The starting value for the adsorbed amount, needed for the procedure described in the theory, is taken as 0.5 mg/m^2, which is a reasonable value for the adsorbed amount of polyelectrolytes onto a charged surface (see, e.g., Refs. 1, 10, 13, 14). The refractive index of the adsorbed layer then has a starting value of 1.438, which is also a reasonable value for an adsorbed polymer layer, based on experience (see, e.g., refs. 1,10). The angle of incidence of the laser beam used in the experiments is 70°. Using a computer program based on the matrix method of Abeles we first calculate A_s for this set of parameters and we then recalculate the adsorbed amount and - using that

value for Γ - the refractive index of the adsorbed layer. After a few iterations we find $n_{adsorbed} = 1.42$, $A_s = 0.0095$ m^2/mg and $\Gamma = 0.42$ mg/m^2. Hoogeveen et al[10] found for the adsorption of PVP$^+$ onto silica in the same reflectometer set-up a value for A_s in the range of 0.019 to 0.027 m^2/mg, which is considerably higher than our value. However, according to Dijt et al[1] a minimum value of $A_s = 0.005$ m^2/mg is needed for accurate measurements; this condition has been met.

Table 1: *Parameters used to calculate the sensitivity factor A_s of the reflectometer for the adsorption of PVP$^+$*.

Material:	Layer thickness (nm)	Refractive index at 632.8 nm[17]	Refractive index increment[10] (cm^3/g)
Silicon	-	3.8	-
Titanium	5	2.22 + 2.99i	-
Gold	15	0.1 + 3.6i	-
Polyelectrolyte	1	1.42	0.21
Solution	-	1.333	-

3.4.2   Determination of the influence of the polyelectrolyte layer thickness on A_s

For the thickness of the polyelectrolyte layer we assumed a value of 1 nm. Although polyelectrolytes adsorbing onto oppositely charged interfaces are generally believed to have a very flat conformation[13], the appearance of several loops, increasing the average layer thickness of the adsorbed layer is very well possible. It is also very likely that the number of loops in the adsorbed polyelectrolyte increases when the charge of the surface decreases or becomes of the same charge sign as the polyelectrolyte. Therefore we repeated the calculations described in the previous section, using various values for the thickness of the adsorbed layer, implying also different values for the refractive index of this layer. The results are presented in Figure 3.4. This plot shows that the value assumed for the layer thickness of the adsorbed polyelectrolyte has a clear influence on the value calculated for A_s. Increasing the layer thickness to 3 nm - many loops are needed to establish such an increase in the *average* layer thickness - results into an increase of A_s from 0.0095 to 0.0102, which is ca. 10%. This effect is smaller for molecules which do not adsorb in such thin layers, as was described by Dijt et al[1]. For adsorbed layers of more than ca. 3 nm, an increase in thickness has a much smaller effect on A_s. In the adsorption of e.g., proteins, A_s will not significantly change when the thickness of the adsorbed layer increases or decreases a little bit. However, for the adsorption of polyelectrolytes onto charged interfaces, as described in this chapter, we expect that the charge of the gold surface will have an effect on the adsorbed layer thickness, and thus on A_s. This effect is at the most 10% of the total change in reflectometer signal.
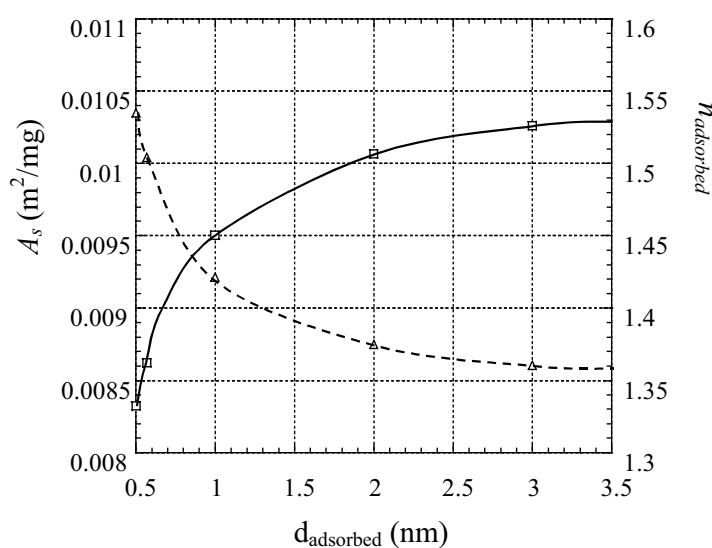
Figure 3.4*: Calculation of the sensitivity factor (□, solid curve) as a function of the layer thickness of the adsorbed polyelectrolyte at constant adsorbed amount, and the corresponding change in refractive index of the polyelectrolyte layer (△, dashed curve). $\Gamma = 0.5$ mg/m².*

3.4.3 The influence of the angle of incidence and the gold layer thickness on A_s

The reflectometer set-up is aligned at an angle of incidence of 70°, the Brewster angle of the silicon/water interface. To check the influence of the angle of incidence and the layer thickness of the gold on A_s, we calculated the reflectance and the sensitivity factor as a function of those variables. The results are shown in Figure 3.5. Curves are calculated for an adsorbed amount of $\Gamma = 0.42$ mg/m², which was obtained in the previous section. Thicknesses and refractive indices of the layers are given in table 1.

It appears that the optimal angle of incidence for our system is around 78° rather than the 70° we have been using and which is used in our laboratory for oxidized silicon wafers. Although A_s is still large enough to perform accurate measurements, small changes in the angle of incidence will have a pronounced effect on the sensitivity of the reflectometer set-up. When aligning the reflectometer set-up, the estimated error in the angle of incidence is 0.5°, which gives rise to an uncertainty in A_s of ± 3.4%. It is therefore very important not to change the settings during one series of measurements, to ensure that the trend of the measurements is not obscured.

Figure 3.5*: Reflectivity for layers of PVP$^+$ adsorbed from aqueous solution on gold-coated wafers. In A and B we give the reflectivities R_p and R_s of silicon covered with 5 nm titanium and (A) 15 nm or (B) variable gold layer, at (A) variable or (B) fixed (70°) angle of incidence. Curves C and D show the sensitivity factor A_s as a function of (C) the angle of incidence (θ_i) and (D) the gold layer thickness (d_{Au}), respectively.*
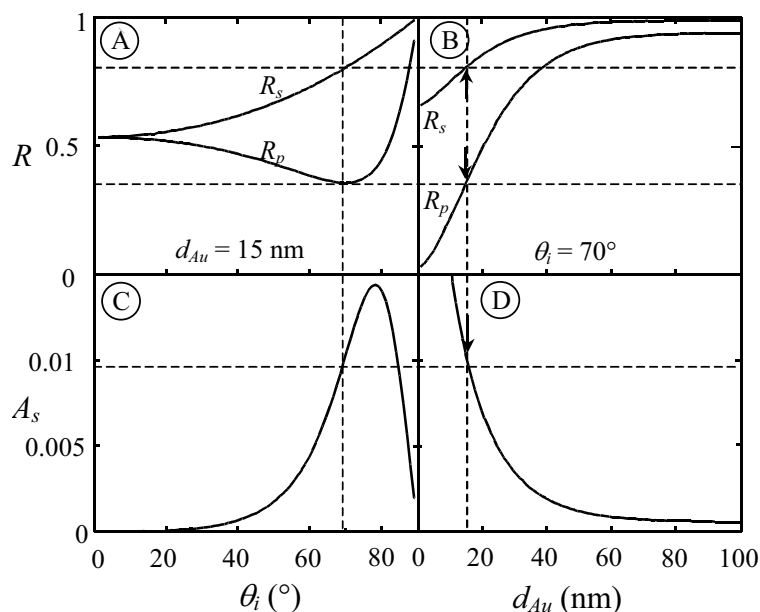
From Figure 3.5D we can see that the thinner the gold layer is, the higher the value obtained for A_s. Therefore we have chosen a value of 15 nm, which is the lowest value at which a complete closed layer of gold can be fabricated. The disadvantage of choosing this value is that the dependence of A_s on the gold layer thickness is rather large. In our experiments we see that when we use strips which have been cut from one single wafer, the relative output signal of the reflectometer S, and thus the sensitivity factor A_s, may vary as much as 5%; for strips of different wafers this may increase up to a value of 20%. This corresponds to a variation in layer thickness of ± 1 nm (for strips cut from 1 wafer) or 5 nm (for strips from different wafers), which is slightly more than the specifications of the manufacturer. Since for every adsorption experiment the strip is taken out and replaced by a new one, such deviations cannot be avoided and therefore cause scatter in the data points, even within one series of measurements.

3.4.4   The influence of the adsorbed amount on A_s

To check the linearity of the output signal with the adsorbed amount Γ, we varied the adsorbed amount in our calculations and plotted the resulting change in A_s as a function of Γ in Figure 3.6A. The adsorbed amount is expressed in the layer thickness d of the adsorbed polyelectrolyte layer, at a constant value for the refractive index of the adsorbed layer. If S were perfectly linear with Γ, A_s would be independent on Γ. It appears that A_s is not exactly constant with increasing adsorbed amount, but when comparing it to the effect of variations in the gold layer thickness, see Figure 3.6B, this error is negligible.
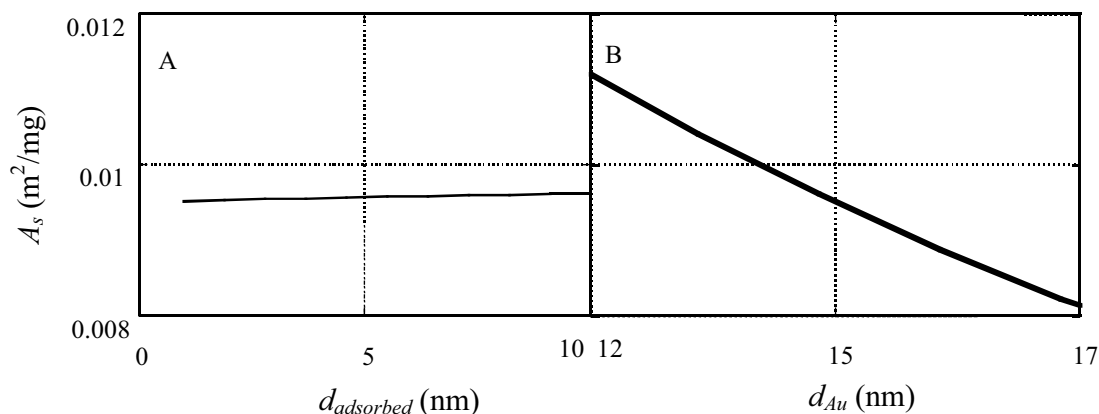
Figure 3.6: *A: Calculation of the sensitivity factor A_s as a function of the total adsorbed amount, compared to, B, the dependence on the gold layer thickness. The adsorbed amount was varied by varying the thickness of the adsorbed layer at a constant refractive index of 1.42.*

3.4.5 *Applying a potential over the gold/electrolyte interface: electro-optic effect*

When a potential is applied to the gold surface, the output signal *S* of the reflectometer changes due to changes in the refractive index in the outer part of the gold layer[7]. Additionally, changes in the refractive index of the gold layer lead to a change in the sensitivity of the reflectometer set-up. We measured S_0 (i.e., the reflectometer signal in the absence of an adsorption layer) as a function of the applied potential, which is given in Figure 3.7 by the curve indicated with "A". In these measurements the value S_0 at the open circuit potential S_0(OCP) equals 1.000 and there in a deviation ΔS_0 given by $\Delta S_0 = S_0 - S_0$(OCP). The picture shows that ΔS_0 is positive for applied potentials below the OCP and negative at potentials higher than the OCP. Furthermore, the relation between ΔS_0 and applied potential is more or less linear, with a bend around 230 mV vs. the Ag/AgCl/3 M KCl reference electrode.
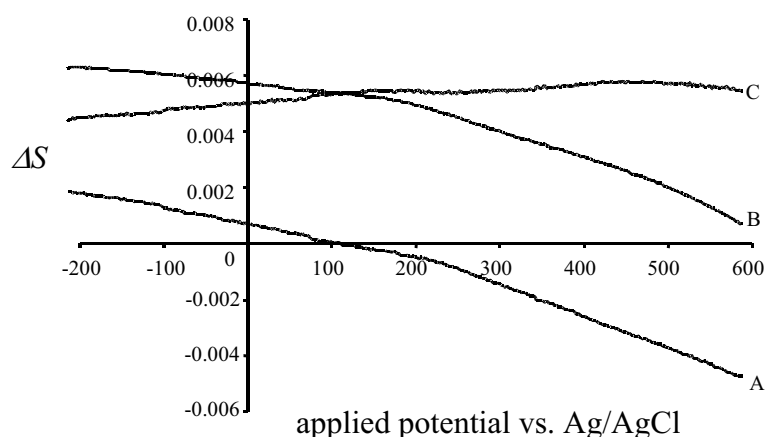
Figure 3.7: *Reflectometer output signal for (A) the bare gold surface and (B) the gold surface covered with PVP^+. The curve labelled C denotes the difference between the two curves. During measurements a solution of 1 mM KNO_3 at a constant flow of 1 ml/min was flushed through the cell.*

In order to better understand the electro-optic effect and by what experimental variables it may be affected, we conducted similar measurements at various salt concentrations and using several different types of salt. The results are depicted in Figures 3.8 and 3.9. It was found that the electro-optic effect does not depend on the electrolyte concentration, except when KCl is used. Furthermore, the type of electrolyte has only a marginal influence – again with the exception of KCl – although the refractive index increments of the salts are quite different (e.g., for a 1 M solution of KNO_3 Δn amounts to 95 x 10^{-4}, while this is 242 x 10^{-4} for $MgSO_4$[17]). We therefore conclude that the electro-optic effect is not a result of adjustments in the diffuse double layer in solution, but results from changes in the optical properties of the outer gold layer, as already suggested by Prostak and Hansen[7]. These changes must be directly related to the local electric field strength. The strong influence of KCl is probably due to the formation of $AuCl_4$ complexes at the surface.

Except for KCl, the curves obtained for the various salts and at different concentrations all show a bend in the ΔS_0 – potential curve at the same potential. Calculations using a model for the electric double layer as described in Ref. 15 show that the position of this bend corresponds approximately to the applied potential where the electric field at the gold changes its direction (i.e., $\psi^i - \psi^o = 0$, the potential of zero charge, see Figure 2.6). At the positive side of this potential the electro-optic effect is somewhat stronger than at the negative side.
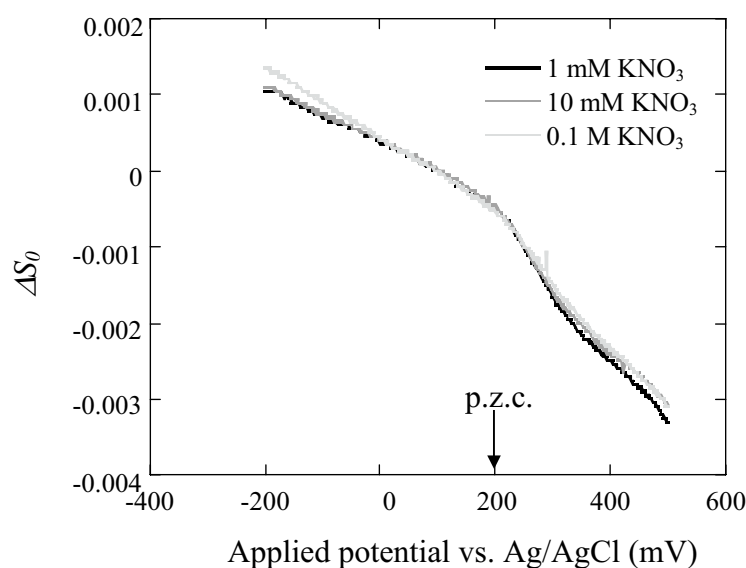
Figure 3.8: Electro-optic effect. Influence of the salt concentration.

Kolb and Franke[6,16] have reported very similar results for the optical excitation energy of the electronic surface states of gold in 0.5 M $NaClO_4$ aqueous solutions as a function of applied potential. The excitation energy varies linearly with applied potential, but the slope of the curve for potentials positive of the potential of zero charge is considerably higher than for potentials below the pzc. This is ascribed to specific adsorption of ClO_4^- ions above the potential of zero charge, leading to a high electric field gradient near the metal surface that is felt by the electronic surface states. We found, however, no dependence of the electro-optic effect on the

concentration KNO_3, K_2SO_4 or $MgSO_4$ in the range of 1 mM to 0.1 M, which seems to contradict specific adsorption of the anions of these salts. Furthermore, the difference in slopes of the two linear parts of our curves is much smaller than that reported by Kolb and Franke. A possible explanation is that in our case the higher slope at positive potentials is caused by specific interaction of OH^- with the gold surface.
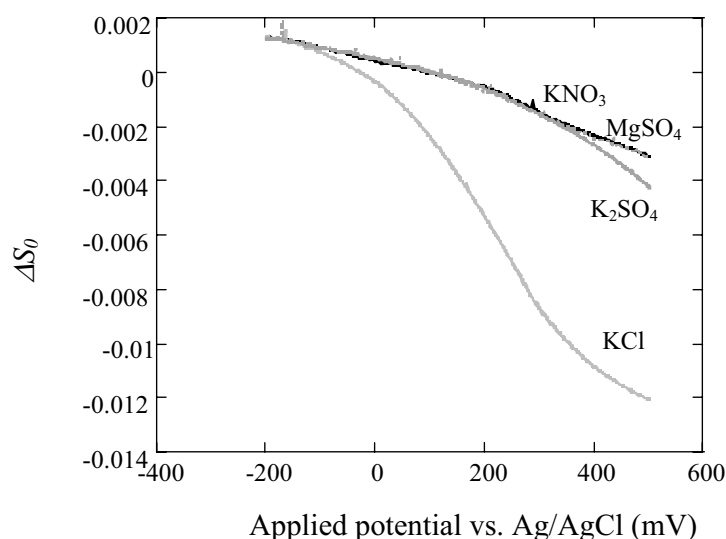
Figure 3.9: *Electro-optic effect in 0.1 M salt.*

The electro-optic effect measured here is much smaller than observed for semiconductors (see, e.g., Ref. 4). At –200 mV (vs. Ag/AgCl/3 M KCl) the shift in S_0 is only ca +0.2 %, while at +600 mV it is -0.5 %. However, in comparison to the change in reflectometer signal upon adsorption, which is typical in the order of 0.5 % as can be seen from Figure 3.3, it cannot be ignored.

Using the optical model of Hansen we examined the effect of applying a potential to the gold film on the *sensitivity* of the reflectometer signal for adsorption. From the reflectometer signal as measured at –200 mV and +600 mV (without adsorption layer), and assuming that the factor *f* as defined in equation 3.6 is a constant system parameter, we calculated the corresponding new values for $[R_p/R_s]_o$. Subsequently, we changed the real and imaginary parts of the refractive index ($n_{Au}(re)$ and $n_{Au}(im)$, respectively) of the gold film to see the relation between $[R_p/R_s]_o$ and these optical parameters. These relations are shown graphically in Figure 3.10. Table 2 shows what change in real or imaginary part of the refractive index is necessary to obtain the corresponding electro-optic effect as measured at -200 mV and at +600 mV, respectively. In the real system only the optical properties of the outer layer of the gold change, and probably both $n_{Au}(re)$ and $n_{Au}(im)$ change at the same time. However, the effect on the sensitivity factor A_s of the system must be between the values calculated for the effective changes in the gold film for $n_{Au}(re)$ and $n_{Au}(im)$ separately. The results presented in table 2 show that A_s changes less than 1% as a result of the electro-optic effect. This is negligible compared to other uncertainties in the measurements, such as, e.g., fluctuations in the thickness of the gold film. In conclusion, provided that a base-line is measured at the same applied potential as at

which adsorption takes place, interference of the electro-optic effect on the adsorption measurements can be ignored.

Table 2: *Changes in the reflectometer signal due to the electro-optic effect*

applied potential	S	R_p/R_s	n_{Au} (re)[*]	n_{Au} (im)[*]	$A_{s,re}$[**]	$A_{s,im}$[**]
no potential applied	1.0000	0.4427	0.10	3.60	0.00952	0.00952
-200 mV	1.0018	0.4435	0.09	3.61	0.00950	0.00949
+600 mV	0.9953	0.4406	0.12	3.57	0.00957	0.00959

[*] The values for n_{Au} *(re)* and n_{Au} *(im)* given for applied potentials of -200 mV and +600 mV indicate how either the real or the imaginary part of the refractive index should be changed to account for the effect. For explanation see text.
[**] The subscripts *re* and *im* denote that the change in A_s is a result of the change in $n_{Au}(re)$ or $n_{Au}(im)$.

We determined the electro-optic effect also in the presence of an adsorption layer of PVP$^+$ (M_w = 12400 g/mole). The results are represented by curve B in Figure 3.7. During the potential scans the adsorbed amount remained constant. This follows from the observation that the curve can be cycled without any hysteresis. However, the difference between the curves A and B is not independent of the applied potential, but gradually increases up to 15% when going from –200 mV to +600 mV (curve C). Assuming that A_s does not change by more than 1% due to the electro-optic effect, the increase must stem from other changes in the system. As noted before, the conformation of the adsorbed polyelectrolyte may change when the charge density at the gold surface changes. At potentials lower than ca. +200 mV, the pzc of the gold, the surface is negatively charged, above this potential it is positively charged. Therefore, it is likely that the thickness of the adsorbed PVP+ layer increases with applied potential, because the molecules go from a flat conformation to a conformation with more loops sticking out into the solution. An increase in layer thickness at constant adsorbed amount (which corresponds to a decrease in refractive index of the adsorbed layer) causes A_s to increase by ca 10% (see Figure 3.4). This explains the largest part of the increase in curve 2.7C.
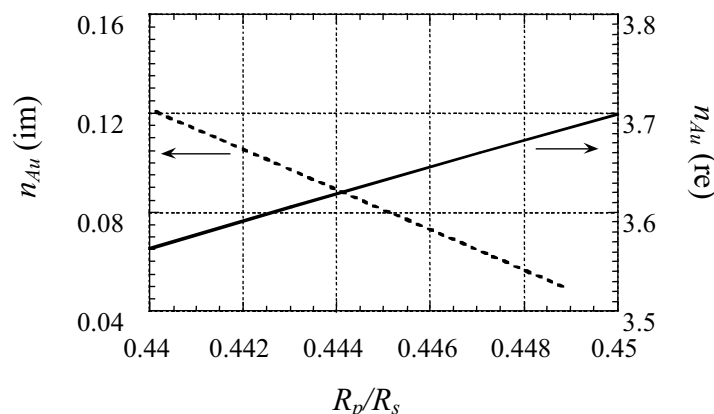

Figure 3.10: *The change in R_p/R_s as a function of the assumed refractive index of the gold.*

3.5   Conclusions

We have calculated the sensitivity factor for measurements on the adsorption of PVP$^+$ on gold-coated wafers in our reflectometry set-up. The value obtained is rather low, but still sufficient for accurate measurements. Variations in several system parameters give rise to substantial variations in the value calculated for A_s. We calculated that an error of 0.5˚ in the angle of incidence of the laser beam causes a change in A_s of 3%. The alignment of the reflectometer does not change during the experiments, so the error in the angle of incidence causes a *systematic* error in the calculation of the total adsorbed amount from the change in the reflectometer signal. It was also found that A_s is independent of the total adsorbed amount, as long as the density of the adsorbed layer remains constant. The gold layer thickness varies with approximately 1 nm for strips cut from one wafer and circa 5 nm between different wafers. This gives rise to an error in the total adsorbed amount of 5 - 20%, which explains scatter in the data points. Also, when the thickness of the adsorbed polymer increases from 1 nm to 3 nm, at a constant adsorbed amount, an error of 10% is made in the estimation of A_s. The polymer layer density, expressed in a layer thickness at a constant adsorbed amount, is likely to change with the potential of the gold surface. At negative potentials, the layer will be flat and at positive potentials, the layer will be extended in the solution, resulting in a lower density in the adsorbed layer and thus in an increased layer thickness. Since the density of the adsorbed layer varies systematically with the applied potential, the variation in A_s as a result of this, causes a systematic error in the *trend* in the experiments of approximately 10%.

In fact this variation in adsorption layer thickness has probably been observed in measuring the electro-optic effect of the gold. The effect of changes in the optical properties of the system with applied potential on the sensitivity factor is rather small (about 1%), especially when it is compared to the effect of the gold layer thickness on A_s. However, the difference in reflectometer output signal between a bare gold surface and a PVP$^+$ covered gold surface is not constant, but increases as a function of the applied potential by 15% when going from -200 mV to +600 mV. The increase in the layer thickness of the adsorbed polyelectrolyte - at a constant adsorbed amount resulting in a decrease in the refractive index of the layer - is most likely the largest part of this effect. It was concluded that by recording a baseline at the same potential as the experiment one avoids large effects on the reflectometer output signal as a result of the electro-optic effect. Unfortunately, data scatter as a result of variations in the gold layer thickness and the density of the adsorbed layer cannot be avoided and, under certain conditions (e.g., when strips of different wafers are used), may reach levels of 20 - 30% in the data points.

3.6   Acknowledgements

3.7   References

1) Dijt, J.C., Cohen Stuart, M.A., Hofman, J.E., Fleer, G.J., *Colloids Surf.*, **1990**, 51, 141.
2) Seraphin, B.O., Hess, R.B., *Phys. Rev. Letters*, **1965**, 14, 138.
3) Shaklee, K.L., Pollak, F.H., Cardona, M., *Phys. Rev. Lett.*, **1965**, 15, 883.
4) Kleijn, J.M., Cohen Stuart, M.A., de Wit, A., *Colloids Surf. A*, **1996**, 110, 213.
5) Feinleib, J., *Phys. Rev. Lett.*, **1966**, 16, 1200.
6) Kolb, D.M., *Angew. Chem. Int. Ed.*, **2001**, 40, 1162.
7) Prostak, K., Hansen, W.N., *Phys. Rev.*, **1967**, 160, 600.
8) Beaglehole, D., Webster, B., Werner, S., *J. Colloid Interface Sci.*, **1998**, 202, 541.
9) Hansen, W.N., *J. Optical Soc. Am.*, **1968**, 58, 380.
10) Hoogeveen, N.G., Cohen Stuart, M.A., Fleer, G.J., *J. Colloid Interface Sci.*, **1996**, 182, 133.
11) Dabros, T., van de Ven, T.G.M., *Colloid Polym. Sci.*, **1983**, 261, 694.
12) Heavens, O.S., *Optical properties of thin solid films*, **1955**, Butterworths Scientific Publications, London.
13) Fleer, G.J., Cohen Stuart, M.A., Scheutjens, J.M.H.M., Cosgrove, T., Vincent, B., *Polymers at Interfaces*, **1993**, Chapman & Hall, London, Chapter 7.
14) Bajpai, A.K., *Prog. Polym. Sci.*, **1997**, 22, 523.
15) Barten, D., Kleijn, J.M., Duval, J., van Leeuwen, H.P., Lyklema, J., Cohen Stuart, M.A., *Langmuir,* **2003**, 19, 1133; Chapter 2 of this thesis.
16) Kolb, D.M., Franke, C., *Appl. Phys. A.*, **1989**, 19, 379.
17) Weast, R.C. (Ed.), Handbook of Chemistry and Physics 73rd edition, **1990**, CRC Press, West Palm Beach, Florida.

4 Adsorption of a Linear Polyelectrolyte on a Gold Electrode[*]

Abstract

The adsorption of quaternized poly-2-vinyl pyridine (PVP$^+$), which has a fixed charge per monomer, onto a gold electrode was investigated using reflectometry. The double layer charge and potential of the gold substrate were controlled by means of either the solution pH or by applying an external potential. The adsorption process was monitored for various molecular masses and concentrations of PVP$^+$, and as a function of the electrolyte concentration, the pH of the solution, and the externally applied potential on the gold electrode. The adsorption isotherms and the dependence on the background electrolyte concentration point to a high non-electrostatic affinity of PVP$^+$ for the gold surface. The results for the two charging mechanisms (pH or applied potential) are very similar when compared by plotting the adsorbed amounts as a function of the double layer potential of the gold. The total adsorbed amount decreases linearly with the double layer potential of the gold. Adsorption takes place up to a relatively high double layer potential, in line with a relatively high contribution of non-electrostatic interactions. The electrostatic barrier for adsorption is always low, since in practically all measurements the initial adsorption rate is completely determined by the transport of molecules towards the gold surface, even near the threshold potential for adsorption.

4.1 Introduction

The study presented here is part of a systematic study into the adsorption from solution of charged macromolecules onto a solid surface as a function of the electric potential of the solid/liquid interface. The potential is either controlled by an *externally* applied potential across the solid/liquid interface or through the solution conditions, i.e., pH and electrolyte concentration. In the case of external potential control, the properties of the solution and thus of the adsorbing macromolecules remain constant during the experiments. The goal of this study is to elucidate the role of electrostatics in the adsorption process of macromolecules and to be able to discriminate between effects of the potential of the adsorbent surface and effects of intrinsic changes within the adsorbing molecule on the adsorption behaviour. The motivation of this study is our interest in the effect of electrostatics on adsorption phenomena, in particular the possibilities for manipulating the adsorption of charged macromolecules - including proteins - by applying a potential across the solid/liquid interface. Here, we report on the adsorption behaviour of a strong, linear polyelectrolyte with a constant charge per monomer, quaternized poly-2-vinylpyridine (PVP$^+$). Samples of different molecular masses were used and the experiments were carried out as a function of the polyelectrolyte concentration, salt concentration, solution pH, and the applied potential across the solid/liquid interface.

Studies in which the adsorption process of charged macromolecules has been investigated as a function of an externally applied potential across the solid/liquid interface are scarce and the results are far from unambiguous[1-8]. This is caused by various complications met in such measurements, such as (i) the occurrence of redox reactions which limit the potential range in which adsorption can be studied, (ii) the fact that the imposed potential is not the same as that experienced by the adsorbing species at the electrode/electrolyte interface (especially when using a semi-conductor as the substrate), (iii) in addition to this, more often than not the surface potential is partly determined by the association or dissociation of surface groups and/or specific adsorption of electrolyte ions, and (iv) in the case that optical detection methods (e.g., ellipsometry or reflectometry) are used, interference of electro-optical effects (change of optical properties of the adsorbent with potential) hampers interpretation of the change in signal upon adsorption[5,9]. For example, Bos et al[3] investigated the effect of the applied potential on protein adsorption onto indium tin oxide (ITO) using reflectometry and found that that effect was very small. ITO is an oxidic semi-conductor; its surface potential in equilibrium with an aqueous electrolyte solution is determined by the (de)protonation of surface hydroxyl groups. From calculations using an amphifunctional model for the electric double layer for electrified interfaces with functional groups, developed in our laboratory[10], it follows that when a potential is applied across a semi-conductor/solution interface only a small part of the potential drop is found in the solution. Furthermore, in particular potential ranges (dependent on the pH) the applied potential is buffered by protonation and deprotonation of the surface groups. Therefore, the applied potential is hardly sensed by adsorbing macromolecules. This has been experimentally confirmed in a study by Hillier et al[11] in which the double layer potential of the semi-conductor titanium oxide in aqueous solution was determined from AFM force measurements. Morrissey et al[1] investigated the adsorbed amount of blood proteins on a platinum electrode by means of ellipsometry. These authors varied the potential of the electrode in the positive direction *after* adsorption of protein had taken place at the equilibrium potential. Like Bos et al, they found hardly any influence of the applied potential, until a certain "onset potential" was reached (0.4 – 0.8 V vs. SCE) above which additional adsorption took place; desorption as a result of changes in the potential was never observed. It is not clear to which extent redox reactions or an electro-optical effect have played a role in this study. In a study of the adsorption onto gold and stainless steel of a protein (bovine serum albumin, BSA), a surfactant (sodium dodecyl sulphate, SDS) and a polyelectrolyte (polyethylenimine, PEI) Beaglehole et al[5] found that the adsorbed layers are not sensitive to the applied potential, and only in one case reversible desorption with varying potential was observed. This study was performed using an ellipsometer and electro-optical effects were accounted for.

To avoid the problem of large potential drops in the outer layers of the adsorbent, we have chosen gold as the adsorbing interface. Force measurements between a silica probe on an AFM tip and the gold surface as a function of both the pH and the applied potential across the gold/solution interface showed that the double layer potential of gold can be regulated by applying an external potential as well as by changing the solution pH[12]. The latter effect is attributed to a small number of oxidic sites on the gold surface resulting from the adsorption and partial discharge of water or hydroxyl groups from the solution, which can take up or donate a proton. It was also found that the variation in double layer potential due to applying an external potential across the

solid/liquid interface is in the same order of magnitude as the variation in the double layer potential by changing the solution pH, which facilitates the comparison between the two types of experiments.

4.2 Experimental

4.2.1 Materials

Quaternized poly-2-vinyl pyridine (poly-1-methyl 2-vinyl pyridinium, PVP^+) (Rochrom, The Netherlands) with bromide as the counterion was used to perform the adsorption experiments. The molecular structure of PVP^+ is shown in Figure 4.1. PVP^+ carries a constant charge of one elementary charge per segment. We used PVP^+ with molecular weights M_w of 2.8, 11.6, and 120 kg/mol. The heterodispersity coefficients M_w/M_n as specified by the supplier are 1.13, 1.07 and 1.03, respectively. Since bromide adsorbs specifically onto the adsorbent gold, the counterion was replaced by nitrate by means of dialysis against a solution of 1 mM potassium nitrate.
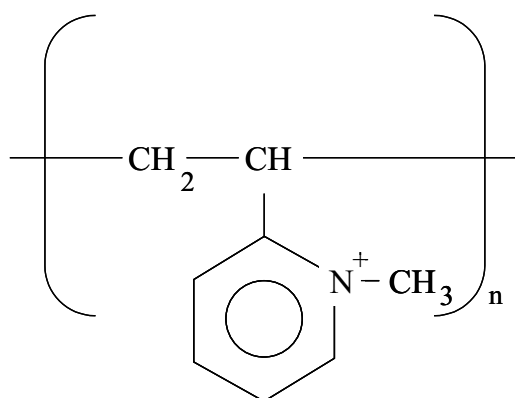
Figure 4.1: Structural formula of quaternized poly-2-vinyl pyridine (poly-1-methyl 2-vinyl pyridinium, PVP^+).

All solutions were prepared using ultrapure water (Richard van Seenus Technologies bv, Almere, The Netherlands). Unless specified otherwise, the background electrolyte was 1 mM KNO_3 and generally the pH was between 5.5 and 6.4 (checked carefully before each measurement). The pH of the solutions was adjusted using aliquots of aqueous solutions of nitric acid (HNO_3). Since the KNO_3 concentration was not adjusted for the addition of HNO_3, the total ionic strength varies slightly with pH (only significant at low pH). For the series as a function of pH and in which external potentials were applied across the gold/electrolyte interface, the solutions were deaerated just before measurements.

Platelets (strips) cut from silicon wafers with a 5 nm layer of titanium and a 15 nm layer of gold sputtered on top of this were used as the substrate. The gold-coated wafers were supplied by Philips Research Laboratories in Eindhoven (The Netherlands). The titanium layer serves to prevent the gold layer from detaching from the silicon wafer. The strips were cleaned by immersion for 2 minutes into "piranha

solution", i.e., a hot mixture of 30% H_2O_2 and concentrated H_2SO_4, after which they were thoroughly rinsed with ultrapure water and left overnight in the electrolyte solution which was used as a blank in the corresponding adsorption experiments. Each strip was used only once. The surface roughness of the gold films, determined by AFM in the imaging mode, was found to be less than 2 nm over an area of 1 μm^2. Potentials were applied using a potentiostat (model 2059, AMEL s.r.l., Milan, Italy). A platinum wire served as the counter electrode and a Ag/AgCl (in 3 M KCl) was used as the reference electrode. All electrodes were put directly in the reflectometer cell. A schematic representation of the experimental set-up is shown in Figure 4.2.
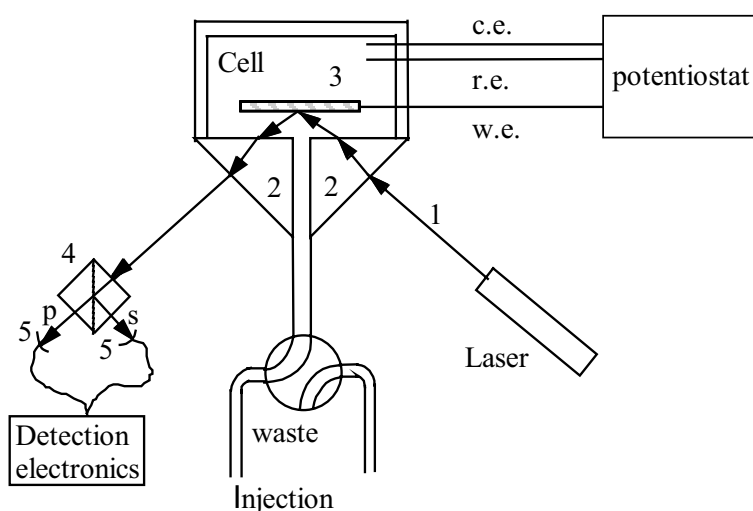
Figure 4.2: Schematic representation of the experimental set-up. (1) Linearly polarized laser beam; (2) 45° glass prism; (3) adsorbent surface ; (4) beam splitter; (5) photodiodes detecting the perpendicular (s) and parallel (p) components of the reflected beam; (6) detection electronics, (7) switch valve, w.e. = working electrode; r.e. = reference electrode; c.e. = counter electrode.

4.2.2   Methods

The adsorption measurements were carried out using a reflectometer with a stagnation-point flow cell as described by Dijt et al[13]. The reflectometer set-up is placed in a cabinet, in which the temperature is 26°C ± 0.5°C, due to heating-up by the laser. The transport of particles to a surface via an impinging jet system has been described by Dabros and van de Ven[14] and is not discussed in detail here. The adsorbed amount, Γ, is determined from the sensitivity factor for the system, A_s, and the change in the reflectometer signal, ΔS, using the relation

$$\Gamma = \frac{\Delta S}{S_0} \frac{1}{A_s} \tag{4.1}$$

in which S_0 is the reflectometer signal for the bare gold surface. A_s was calculated using the method of Hansen[15], which is based on the matrix formalism of Abeles. In this method the system is divided into a number of parallel flat layers of constant

refractive index. The parameters used in the calculation are the layer thickness of the gold film (15 nm), and of the titanium layer (5 nm), the complex indices of refraction of these layers at the wavelength of the laser beam (0.1 + 3.6i and 2.22 + 2.99i, respectively[16]), the indices of refraction of silicon (3.8) and the aqueous solution (1.333)[16], and the angle of incidence θ (71°) and the wavelength of the laser beam (632.8 nm). The refractive index of the adsorbed layer is calculated using the refractive index of the solution, the thickness of the adsorbed layer (assumed to be 1 nm, see next section) and the refractive index increment of PVP[+], for which a value of 0.21 cm^3/g has been adopted[17]. For this set of parameters the sensitivity factor A_s equals 0.0095 m^2/mg. this is rather low, but still sufficient to perform accurate measurements[13]. More details concerning the determination of A_s have been given in Chapter 3.

4.2.3 Reproducibility

The reproducibility of reflectometer experiments is largely determined by the dependence of A_s on the system parameters which may vary from experiment to experiment. This has been extensively described elsewhere[18] and we will discuss it only briefly here.
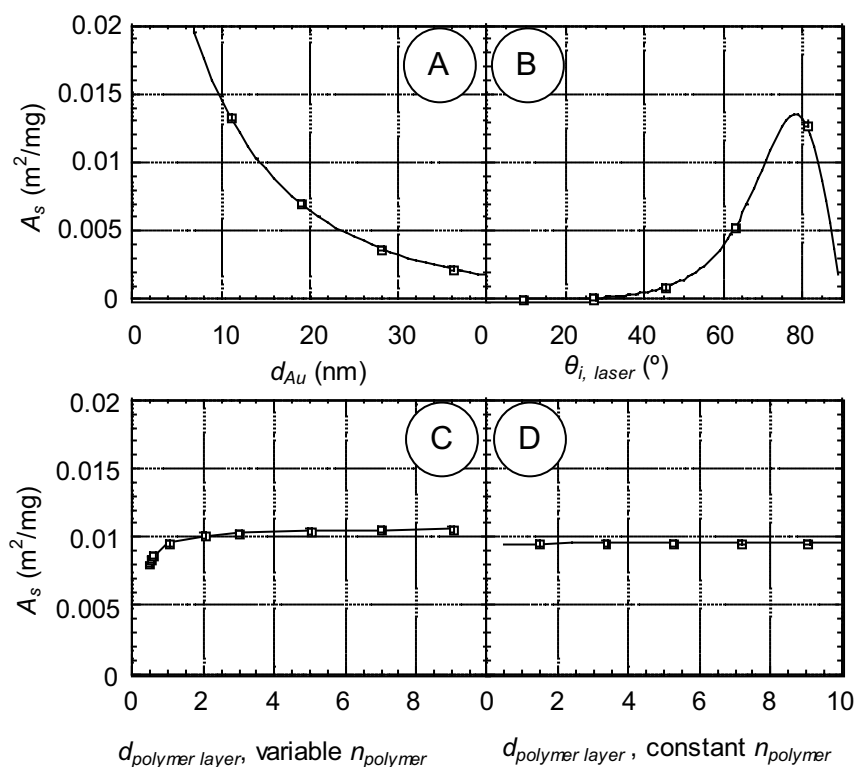

Figure 4.3: Sensitivity of the reflectometer for the adsorption of PVP[+] on gold as a function of (A) the gold layer thickness, (B) the angle of incidence of the laser beam, (C) the thickness of the polymer layer at constant adsorbed amount, and (D) the total adsorbed amount.

Figure 4.3 shows A_s as a function of (a) the gold layer thickness, (b) the angle of incidence of the laser beam, (c) the density of the adsorbed layer, expressed in a layer thickness with a constant adsorbed amount and thus a variable index of refraction, and (d) the adsorbed amount, expressed in a layer thickness with a constant refractive index. This picture shows that a slight variation in the gold layer thickness has a profound effect on A_s. The gold layer thickness on one gold-coated wafer varies with approximately 1 nm difference over the entire wafer, which gives rise to a variation in A_s of ± 5%. The variation in the gold layer thickness between different gold-coated wafers can be as much as 5 nm and thus causes variations up to 20%. The angle of incidence also has a relatively large influence on A_s, an error of 0.5° leads to an error in A_s of ± 3.4%[18]. However, the angle of incidence is the same in all experiments, which implies that the trends in the experiments are not affected by this error. The thickness of the adsorbed layer is also a source of uncertainty in determining A_s. For a complete adsorption layer with an adsorbed amount of $\Gamma \sim 0.4$ mg/m^2 we estimated the layer thickness to be approximately 1 nm, which is based both on experience and on the observation that polyelectrolytes tend to adsorb in a flat conformation onto charged surfaces[19]. The influence of the total adsorbed amount on A_s at a constant density of the adsorbed layer (i.e., constant refractive index, see Figure 4.3D) is very little and will be ignored.

When a potential is applied to the gold surface, the reflectometer signal changes due to changes in the dielectric constant of a thin outer layer of the gold[18,20,21]. To minimize the effect of this change, a baseline is always recorded at the same potential as the actual adsorption process. The effect on the *sensitivity* of the reflectometer set-up is less than 1%[18] and will be ignored.

Other sources for inaccuracies in the measurements are, e.g., the temperature and the flow rate in the reflectometer cell. These were kept virtually constant - the fluctuation in the flow rate is approximately 1% and the temperature is 26 ± 0.5°C. In conclusion, the main cause for scatter in the output of the experiments is the variation in the gold layer thickness. Therefore all experiments were performed 3 to 4 times and averaged. If possible, measurements of one series were performed using strips from the same gold-coated wafer. Taking the average of the 3 - 4 measurements reduces the error in the adsorbed amount in one series of measurements to ±2%, if a single gold-coated wafer is used. This increases up to ±7% if more than one wafer is used.

4.3   Results and Discussion

4.3.1   Variation of the polyelectrolyte concentration

In Figure 4.4, the total adsorbed amount Γ and the initial adsorption rate $(d\Gamma/dt)_0$ of PVP$^+$ on gold at pH 5.5 is given. At this pH the gold surface is negatively charged, the pzc is at pH 4.9[12,23]. For all the molecular weights used, the adsorbed amount is independent of the concentration of PVP$^+$ in the solution, indicating that we are at the plateau level of the adsorption isotherm. This suggests a high affinity of the polyelectrolyte for the gold surface. At this low salt concentration, Γ varies only weakly with M_w because the molecules adsorb in a flat conformation[19].
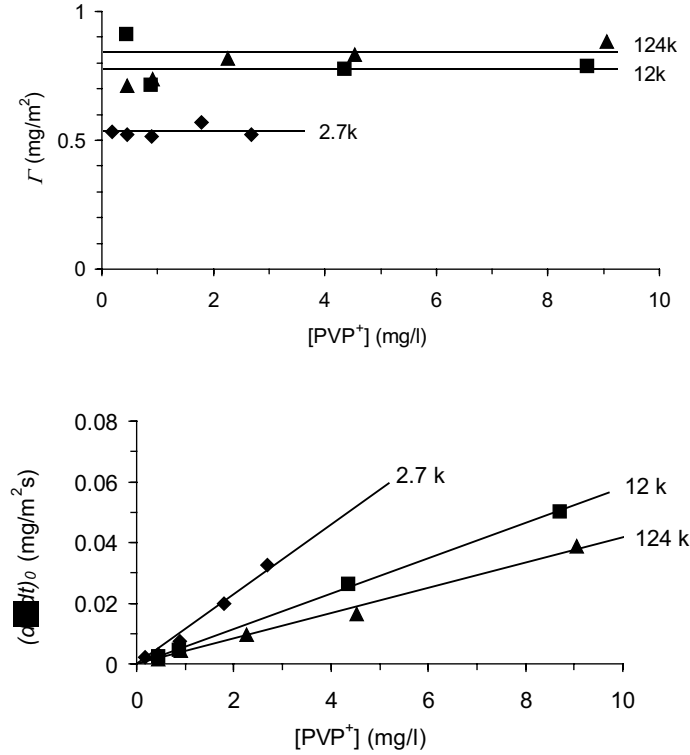
Figure 4.4: *Adsorbed amount Γ and initial adsorption rate $(d\Gamma/dt)_0$ of PVP^+ onto gold as a function of the polyelectrolyte concentration for various molecular weights, as indicated (2.7k = 2.7 kg/mole etc.). The background electrolyte is 1 mM KNO_3.*

The initial adsorption rate increases linearly with PVP^+-concentration. For the 124k PVP^+ the adsorption rate is the same as for the adsorption of this polymer on titanium oxide[17]. Apparently, the rate is independent on the nature of the substrate. This suggests that the adsorption process is transport limited. In that case the rate $(d\Gamma/dt)_0$ equals the limiting flux of PVP^+ to the surface, which is given by[13,14]:

$$\frac{d\Gamma}{dt} = k \cdot \left(C_b - C_s \right) \qquad (4.2)$$

with

$$k = 0.776 v^{\frac{1}{3}} R^{-1} D^{\frac{2}{3}} \left(\overline{\alpha}\, Re \right)^{\frac{1}{3}} \qquad (4.3)$$

Here, C_b is the PVP^+-concentration in the bulk solution, C_s the PVP^+-concentration near the gold surface (the subsurface concentration), v the kinematic viscosity of the solution, R the radius of the tube of the impinging jet system, D the diffusion coefficient of the PVP^+-molecule, and Re the Reynolds number given by

$$Re = \frac{UR}{v} \qquad (4.4)$$

where U is the mean fluid velocity at the end of the inlet tube. The parameter $\bar{\alpha}$ reflects the intensity of the flow near the surface, which depends on the Reynolds number and on the geometry of the cell. The latter is characterized by the ratio h/R, where h is the distance between the surface and the end of the inlet tube. If we assume transport limitation in the first stages of the adsorption process, (i.e., when the subsurface concentration is still equal to zero), we can compare the measured initial adsorption rate to the calculated initial adsorption rate (i.e., the flux of PVP$^+$ to the surface).

The polyelectrolyte solutions used here are very dilute ($1 - 10$ mg/l), which allows us for most parameters to use the values of pure water. The kinematic viscosity ν then is 10^{-6} m^2/s, $R = 0.5 \cdot 10^{-3}$ m, and $U = 0.021$ m/s. In our system $h/R = 1.7$, $Re = 10.6$ and $\bar{\alpha} = 6$[14]. Assuming that $(d\Gamma/dt)_0$ is transport limited, we can calculate the diffusion coefficient of the PVP$^+$ molecules of different molar masses from the experimental data using equations ($2 - 4$). From the data in Figure 4.4, we obtain for $M_w = 2.68$ kg/mole $D = 8.0 \cdot 10^{-11}$ m^2/s, for $M_w = 12$ kg/mole $D = 2.9 \cdot 10^{-11}$ m^2/s, and for $M_w = 124$ kg/mole $D = 1.7 \cdot 10^{-11}$ m^2/s. These results are plotted on a log-log scale in Figure 4.5. For spherical particles with a radius a in solution at low concentrations the diffusion coefficient is given by the Stokes-Einstein equation:

$$D = \frac{kT}{f} = \frac{kT}{6\pi\eta a} \tag{5.5}$$

in which f is the friction coefficient and η the viscosity of the solution. For a random coil conformation of the polyelectrolyte chains, the radius of the coil is linear with the square root of the length of the chains[19], i.e., the square root of M_w, and therefore D is inversely proportional to the square root of M_w ($\log D \sim -\frac{1}{2} \log M_w$).

The solid line in Figure 4.5 has a slope of $-\frac{1}{2}$. The data points agree well with this line, indicating that transport limitation does indeed apply to our system. Moreover, the calculated values for the diffusion coefficient agree well with the diffusion coefficients found for other polymers with approximately the same molecular mass (see, e.g., Ref. 22).

4.3.2   Variation of the electrolyte concentration

In aqueous solutions of KNO$_3$ at neutral pH, the gold surface is negatively charged[12,23]. At a low salt concentration the associated double layer extends relatively far into the solution; the effect of the surface charge is felt by the polyelectrolyte molecules over a large distance (several tens of nanometers). The polyelectrolyte coils are highly charged, causing a strong repulsion between the charges on the chain and thus causing the polyelectrolyte to swell. At low salt concentration, the polyelectrolyte will adsorb in a flat conformation on the surface and the adsorbed amount will be relatively low. For a review on the adsorption of linear polyelectrolytes, see, e.g., Refs. 24 and 25.
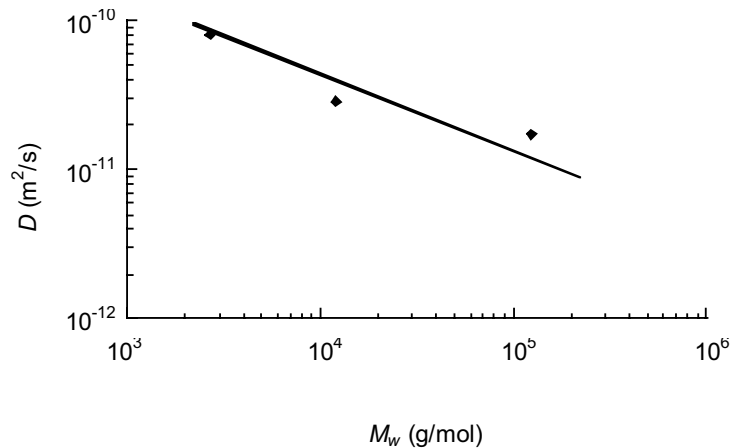
Figure 4.5*: The diffusion coefficient of PVP$^+$ calculated from the initial adsorption rate as a function of the molar mass of the molecule.*

Figure 4.6 shows the adsorption of PVP$^+$ of two different molar masses onto gold as a function of the electrolyte concentration in the solution. The concentration PVP$^+$ of the molecule with M_n = 12 kg/mole is 1 mg/l, the concentration PVP$^+$ with a molecular weight of 124 kg/mole is 5 mg/l. The initial adsorption rate does not change with the electrolyte concentration, again in line with a transport-limited adsorption process. The total adsorbed amount is proportional to the square root of the electrolyte concentration. A similar trend has been found, for example, for the adsorption of poly(styrene sulfonate) onto polyoxymethylene, titanium and silica[26,27].

Increasing the electrolyte concentration has two effects: the double layer thickness decreases and the number of counter charges in the polyelectrolyte coil increases. Since the surface and the polyelectrolyte have opposite charge signs, the first effect causes the attractive forces between the two to decrease. The second effect makes the repulsion inside the polyelectrolyte chain smaller. As a result of both effects, the polyelectrolyte chains have less tendency to adsorb in a flat conformation. Due to the flat conformation of the adsorbed molecules in the low salt concentration range (lower than 1 mM), Γ is practically independent on the molar mass (see Figure 4.6). At higher salt concentrations, we see that Γ increases with increasing molar mass of PVP$^+$. The adsorbed molecules have more loops in this region, which allows more material to attach to the surface. For larger molecules, this effect is stronger than for smaller molecules.

By self-consistent-field model calculations[19] it has been shown that for *pure electrosorption*, the adsorbed amount of polyelectrolyte decreases with increasing salt concentration. This is because at higher salt concentrations the small ions progressively contribute to the charge compensation of the surface. When electrosorption is enhanced by surface affinity, either a maximum appears in the total adsorbed amount with increasing electrolyte concentration, or the total adsorbed amount increases monotonically with increasing salt concentration, depending on the strength of the non-electrostatic interactions. In our experiments, we found that Γ increases strongly with electrolyte concentration, indicating a strong non-electrostatic contribution to the adsorption process.
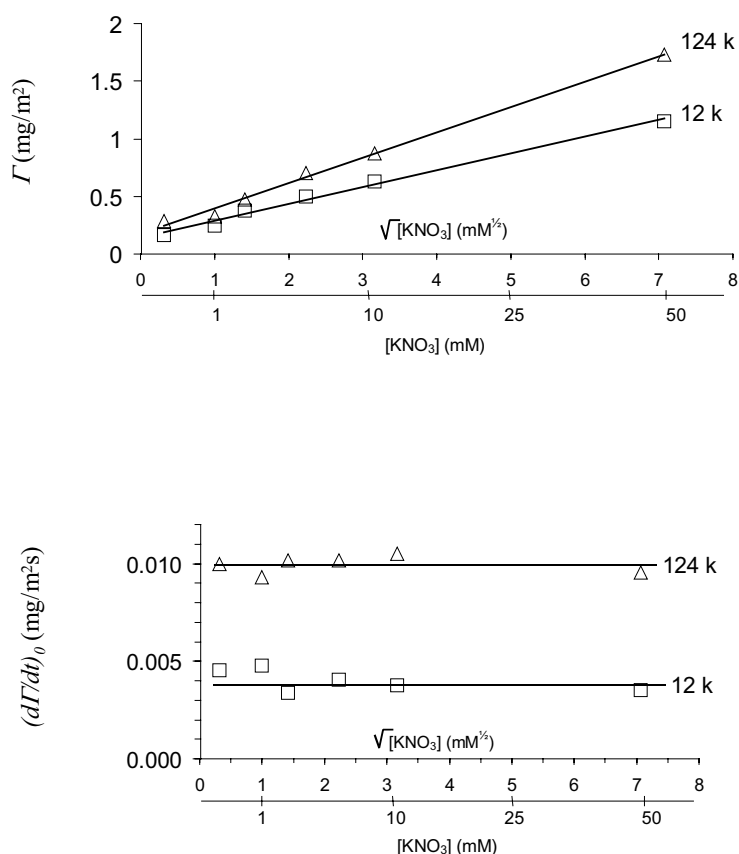
Figure 4.6: Total adsorbed amount and initial adsorption rate of PVP$^+$ as a function of the salt concentration in the solution at neutral pH. The concentration of PVP$^+$ (12 k) = 1 mg/l; PVP$^+$ (124 k) = 5 mg/l.

2.1.1 Variation of the solution pH

We studied the adsorption of PVP$^+$ onto gold in the range of pH 3.5 to 6. In this pH range the potential of the gold surface depends on pH, while above pH 6, the potential is practically constant (see ref. 12). The total charge on the polyelectrolyte is independent of the solution pH. The electrolyte concentration was not corrected for the pH and therefore varies slightly with pH. The total adsorbed amount and the initial adsorption rate are given in Figure 4.7. There seems to be a slight increase in the adsorbed amount upon increasing the pH. The initial adsorption rate is independent of the pH as expected for a transport-limited process. Although the trend in the adsorption data is not very distinct, it is quite clear that PVP$^+$ adsorbs onto the gold surface, even when the surface potential of the gold has the same sign as the polyelectrolyte charge, which is the case at pH values lower than pH 4.9 (the iso-electric point of the gold surface[12]). This again points to a strong non-electrostatic driving force for adsorption of PVP$^+$ onto gold.
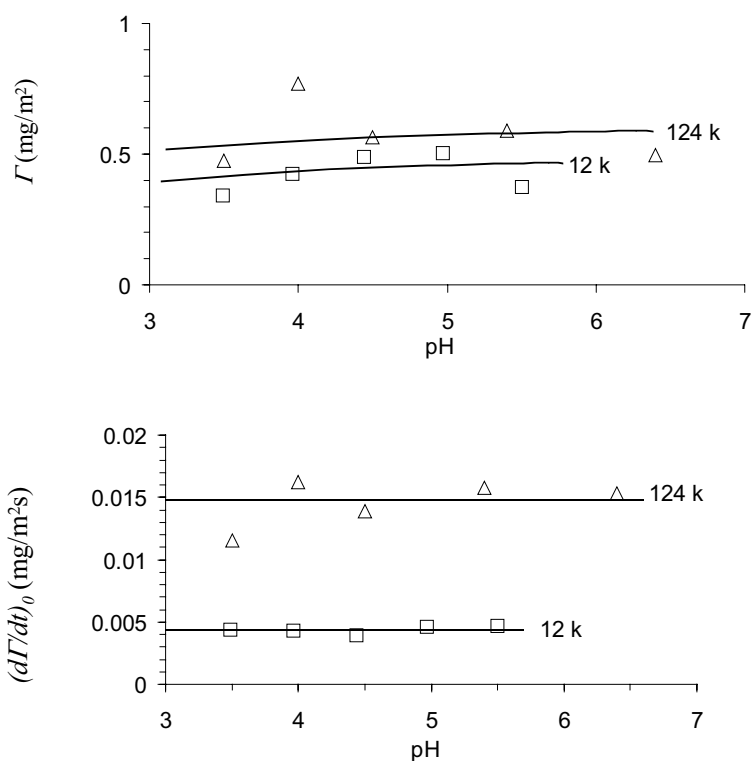
Figure 4.7: Total adsorbed amount and initial adsorption rate as a function of the pH of the solution. The concentration of PVP^+ (12 k) = 1 mg/l; PVP^+ (124 k) = 5 mg/l. The background electrolyte is 1 mM KNO_3.

In a previous chapter we analysed the effect of the thickness of the adsorbed layer on the sensitivity factor A_s of our system[18]. This is also depicted in Figure 4.3C. It was found that if the thickness of the adsorbed layer is small (< ca. 2 nm) A_s increases with increasing layer thickness (at constant adsorbed amount). In Figure 4.7 this has not been accounted for, since we do not know the thickness of the adsorbed layer as a function of the pH of the solution. In calculating A_s we assumed a flat conformation for the adsorbed molecules. However, it is likely that, at pH values where the gold surface is positively charged, the adsorbed PVP^+ molecules extend into the solution. Therefore, the thickness of the adsorbed layer may be less resulting in a higher sensitivity factor A_s. As a consequence, we may systematically overestimate the total adsorbed amount at pH values where the surface is positively charged. As can be seen from Figure 4.3C, this may add up to 10% of the value for the total adsorbed amount. The same holds, of course, when the surface is positively charged by applying sufficiently positive external potentials.

2.1.2 Variation of the applied potential

The total adsorbed amount and the initial adsorption rate of PVP^+ onto gold were also measured as a function of the potential externally applied to the gold. The results of these experiments are shown in Figure 4.8. The total adsorbed amount decreases approximately linearly with the applied potential. Deviations from a straight line are somewhat larger for the polyelectrolyte with the highest molecular weight, but these are still within the range of experimental error (more than one wafer was used for these experiments). Varying the external potential over the range -200 mV to +600

mV vs. Ag/AgCl/3M KCl after adsorption has taken place (while flushing with electrolyte solution) does not lead to desorption. The initial adsorption rate is determined by the transport of molecules towards the surface, practically up to the potential above which no adsorption takes place anymore.
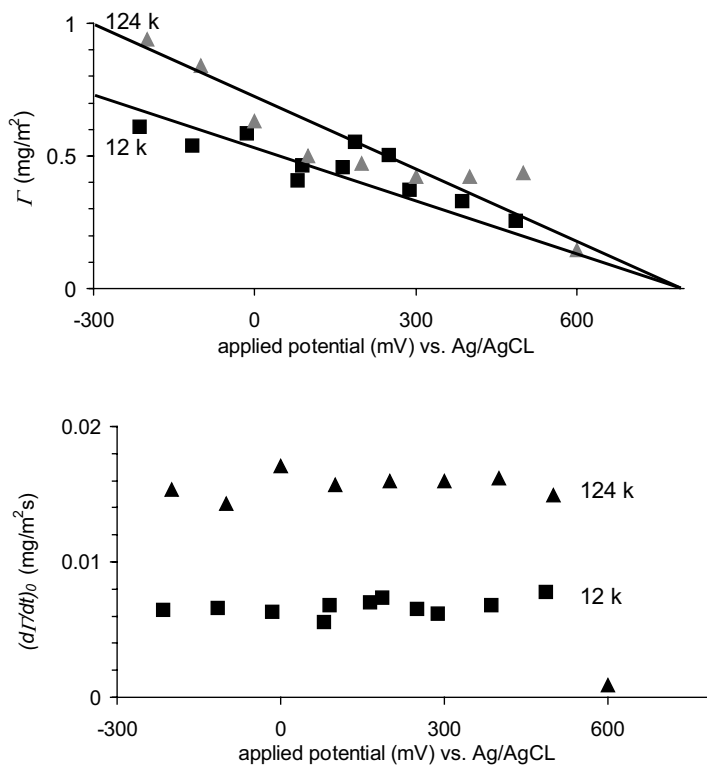
Figure 4.8: *Total adsorbed amount and initial adsorption rate as a function of the applied potential across the solid/liquid interface. The concentration of PVP$^+$ (■) 12 k = 1 mg/l; (▲) 124 k = 5 mg/l. The background electrolyte is 1 mM KNO$_3$, the pH of the solution is 6.4.*

4.3.5   Adsorption of PVP$^+$ as a function of the double layer potential

In an earlier study[12] we determined the double layer potential ψ^d of gold in aqueous solutions using colloidal probe AFM. The double layer potential is defined as the potential difference between the outer Helmholtz plane and the bulk solution. It should be noted that the values for ψ^d as determined from interaction curves between a gold substrate and a silica probe, are in fact smeared-out, average values of the potential at the distance of closest approach. For a discussion see Ref. 12. It was found that the double layer potential of gold is linearly dependent on the solution pH in the range of pH 3 – pH 5.5, with the iso-electric point at pH 5. The double layer potential ψ^d in this region ranges from +50 mV at pH 3 to –10 mV at pH 5.5. At pH values higher than pH 5.5, the double layer potential levels off to a value of –17 mV. These results are given in Figure 4.9. The dependence of the double layer potential of the gold surface on pH is attributed to oxidic surface sites. Since it changes with pH only in a relatively small pH-range, it was concluded that the number of these proton binding sites is very small. Furthermore, from analysis of the ψ^d data in terms of an amphifunctional double layer model[12], it has been found that the number of such sites

is in the order of 10^{16} m^{-2}, which corresponds to a coverage of approximately 0.1%. The open circuit potential (OCP) follows the same trend with pH as ψ^d and has a value of ca. 135 mV vs. Ag/AgCl/3M KCl at the point of zero charge of the gold surface (pH 4.9)[12].
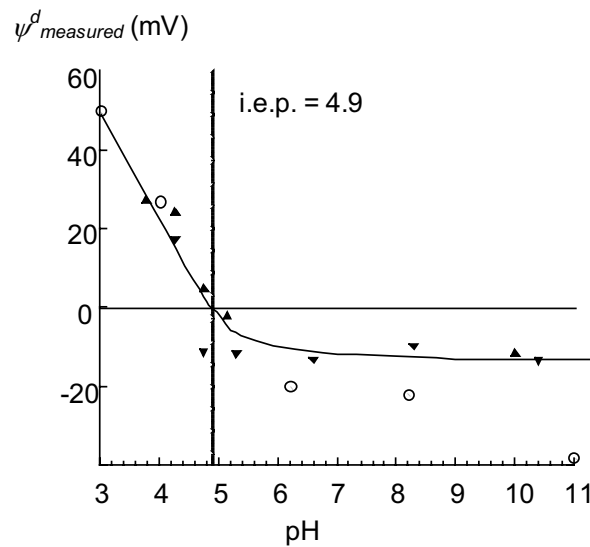
Figure 4.9: *The double layer potential, ψ^d of gold as a function of the pH. ▼ = pH 11-3; ▲ = pH 3-11; ○ = data Giesbers et al[23]. Background electrolyte is 1 mM KNO₃ (results from Chapter 2) and 1 mM KCl (Giesbers et al).*
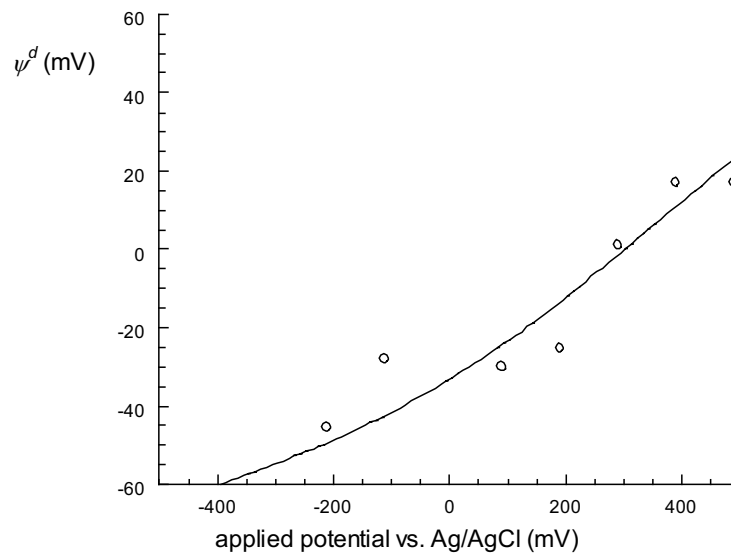
Figure 4.10: *Double layer potential ψ^d of gold as a function of the applied potential at pH = 6.4. (Data taken from ref. 12) The line is a fit to the amphifunctional double layer model as described in references 10 and 12.*

In the same study[12], we also determined the double layer potential of gold as a function of the applied potential at various pH values. Figure 4.10 shows the results of this study at pH = 6.4. The data points are indicated by the circles, the solid line is a fit to the above-mentioned amphifunctional double layer model. This diagram shows a

more or less linear change of the double layer potential of gold with the applied potential.

Figure 4.11 shows the total adsorbed amount and the initial adsorption rate of PVP^+ on gold as a function of the double layer potential. In this figure data obtained by varying the pH as well as by varying the applied potential have been collected. The total adsorbed amount decreases monotonically to zero as a function of the double layer potential of gold. Whether this potential is determined by the pH of the solution or by an external source has no significant influence on the adsorbed amount.

By means of streaming potential measurements Hoogeveen et al[28] determined the zeta-potential of adsorbed PVP^+-layers on TiO_2 at the pH values at which adsorption had taken place. They found that after adsorption of PVP^+ onto TiO_2, the zeta-potential is approximately 50 mV for every pH, although the total adsorbed amount increases with increasing pH. The double layer potential - which corresponds closely to the zeta-potential - of TiO_2 is a function of the pH. These observations suggest that PVP^+ adsorbs onto the substrate up to a certain value of the double layer potential, irrespective of the potential of the bare surface. The same holds for our system. The threshold value of the double layer potential above which adsorption no longer takes place, seems to be higher for gold than for TiO_2 (for the latter a value of ca. 50 mV has been reported[28]), which implies a higher non-electrostatic contribution to the adsorption energy.

In principle, the two methods for charging the gold surface could have a different effect on the adsorption behaviour of the PVP^+. When the double layer potential is determined by the solution pH, the surface charge at the gold surface might adjust itself upon adsorption of a charged polymer. In the case where the double layer potential of gold is determined by an external source, the potential in the bulk of the gold is kept constant and surface charge regulation is expected to be more limited. However, this difference is obviously too subtle to have a noticeable influence on the adsorption behaviour of PVP^+ onto the gold substrate. It has not been observed in AFM force measurements either. The interaction between the gold surface and a silica probe shows the same degree of charge regulation, no matter if an external potential is applied or not[12,23].

Cohen Stuart et al[29] developed a kinetic model for polyelectrolyte adsorption, which is based on the assumption that a polyelectrolyte encounters a barrier in its motion towards a like-charged surface. The height of the barrier, which is of electrostatic origin, is calculated using self-consistent-field (SCF) theory. In their calculations the presence of countercharges in the polyelectrolyte coil was not taken into account. The results suggest that with increasing surface charge, the height of the electrostatic barrier quickly becomes large enough to slow down and stop the adsorption process. In our experiments, we found that the initial adsorption rate, even at low electrolyte concentrations and near the threshold potential above which no adsorption takes place, is independent of the double layer potential of the gold. This is in contradiction with the predictions of Cohen Stuart et al, and probably partly due to condensation of counterions on the polyelectrolyte chain. Counterion condensation ("strong screening") occurs when the linear distance between the individual charges on the chain is smaller than the Bjerrum length[30] (0.7 nm, which is the distance between two oppositely charged ions with an electrical attraction energy just as large as the

thermal energy of the pair, 2 kT). The distance between the individual charges in the PVP^+-chain is in this order of magnitude and hence counterions will bind strongly at the polyelectrolyte chain. Therefore, the effective charge of the polyelectrolyte chain is relatively small and the electrostatic barrier low. Although we have no quantitative estimate of the barrier, our data show that the initial adsorption can take place at a transport limited rate under practically all circumstances examined by us.
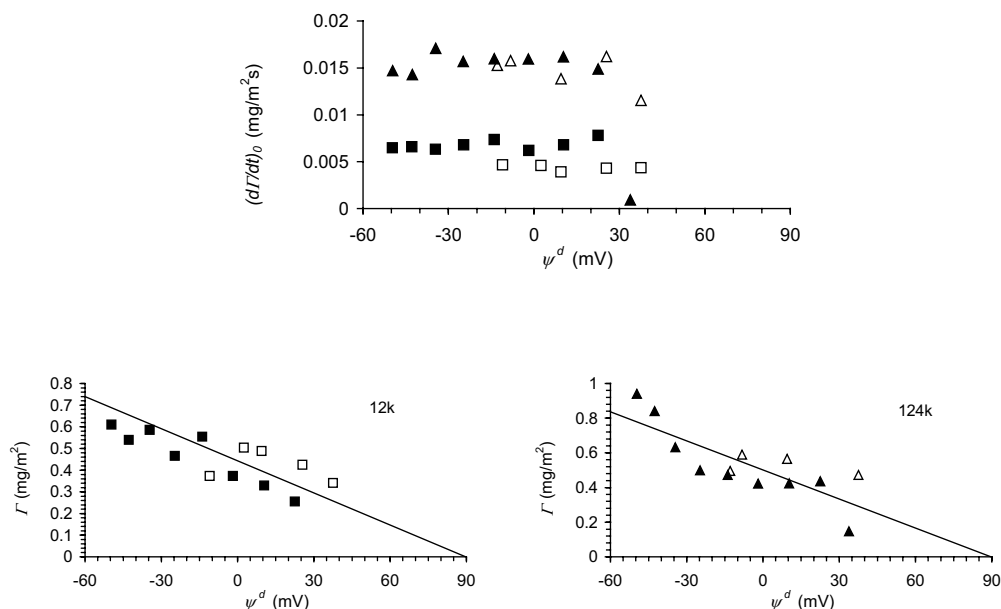
Figure 4.11: *Total adsorbed amount and initial adsorption rate as a function of the double layer potential. The open symbols represent the measurements in which the double layer potential was varied using the solution pH, and the closed symbols represent the measurements in which the double layer potential was varied using an external source. The concentration of PVP^+ (12 k) = 1 mg/l; PVP^+(124 k) = 5 mg/l. The background electrolyte is 1 mM KNO_3.*

4.4   Conclusions

The adsorption of the linear, strong polyelectrolyte PVP^+ from aqueous solution onto gold can be characterised as electrosorption enhanced by a relatively high non-electrostatic affinity. The total adsorbed amount is independent of the PVP^+ concentration, indicating that we are already at the plateau level of the adsorption isotherm at very low concentrations and thus that the affinity of the polymer for the surface is relatively high, as is quite common for macromolecules.

Increasing the electrolyte concentration causes a strong increase in the total adsorbed amount. At low salt concentration there is little difference in adsorbed amount (mass per unit area) for different molecular masses of the polymer, because the molecules are adsorbed in a flat conformation. At high salt concentration, the polyelectrolyte adsorbs in loops and trains and this results into higher adsorbed amounts for PVP^+ of higher molecular weight. The strong increase in the total adsorbed amount with increasing salt concentration again indicates that the electrosorption is enhanced by

specific (i.e., non-electrostatic) interactions between the polyelectrolyte and the surface.

The adsorbed amounts slightly increase with increasing pH and the total adsorbed amount decreases monotonically to zero with the externally applied potential. However, changing the external potential after adsorption has taken place, never leads to desorption. The results of the two series of experiments, i.e., variation of pH and of external potential, were compared by plotting both data sets as a function of the double layer potential of the gold. No significant difference was found between the results obtained using these two different ways to control the double layer potential. As expected, the adsorbed amount decreases with increasing potential. The threshold potential above which no adsorption takes place, is relatively high, in line with a high (non-electrostatic) affinity for the gold surface. Surprisingly, the adsorption kinetics are determined completely by the flux of molecules to the surface, even at low electrolyte concentrations and near the threshold potential for adsorption. This implies that the electrostatic barrier for adsorption is always relatively low.

4.5 References

1) Morrissey, B.W., Smith, L.E., Strömberg, R.R., Fenstermaker, C.A., *J. Colloid Interface Sci.*, **1976**, 56(3), 557.
2) Kawaguchi, M., Hayashi, K., Takahashi, A., *Macromolecules*, **1988**, 21, 1016.
3) Bos, M.A., Shervani, Z., Anusiem, A.C.I., Giesbers, M., Norde, W., Kleijn, J.M., *Colloids Surf. B*, **1994**, 3, 91.
4) Khan, G.F., Wernet, W., *Thin Solid Films*, **1997**, 300, 265.
5) Beaglehole, D., Webster, B., Werner, S., *J. Colloid Interface Sci.*, **1998**, 202, 541.
6) Holmström, N., Askendal, A., Tengvall, P., *Colloids Surf. B*, **1998**, 11, 265.
7) Zhou, A., Xie, N., *J. Colloid Interface Sci.*, **1999**, 220, 281.
8) Zhou, A., Xie, Q., Wu, Y., Cai, Y., Nie, L., Yao, S., *J. Colloid Interface Sci.*, **2000**, 229, 12.
9) Kleijn, J.M., Cohen Stuart, M.A., de Wit, A., *Colloids Surf. A*, **1996**, 110, 213.
10) Duval, J., Lyklema, J., Kleijn, J.M., van Leeuwen, H.P., *Langmuir*, **2001**, 17, 7573.
11) Hillier, A.C., Kim, S., Bard, A.J., *J. Phys. Chem.*, **1996**, 100, 18808.
12) Barten, D., Kleijn, J.M., Duval, J., van Leeuwen, H.P., Lyklema, J., Cohen Stuart, M.A., *Langmuir*, **2003**, 19, 1133.
13) Dijt, J.C., Cohen Stuart, M.A., Hofman, J.E., Fleer, G.J., *Colloids Surf.* **1990**, 51, 141.
14) Dabros, T., van de Ven, T.G.M., *Colloid Polym. Sci.*, **1983**, 261, 694.
15) Hansen, W.N., *J. Optical Soc. Am.*, **1968**, 58, 380.
16) Weast R.C. (Ed.), Handbook of Chemistry and Physics 73rd edition, **1990**, CRC press, West Palm Beach, Florida.
17) Hoogeveen, N.G., Cohen Stuart, M.A., Fleer, G.J., *J. Colloid Interface Sci.*, **1996**, 182, 133.
18) Chapter 3 of this thesis.

19) Fleer, G.J., Cohen Stuart, M.A., Scheutjens, J.M.H.M., Cosgrove, T., Vincent, B., *Polymers at Interfaces* **1993**, , Chapman & Hall, London.

20) Feinleib, J., *Phys. Rev. Lett.*, **1966**, 16, 1200.

21) Prostak, A., Hansen, W.N., *Physical Review*, **1967**, 160, 600.

22) Bandrup, J., Immergut, E.H., Eds., *Polymer Handbook*, **1989**, John Wiley and Sons, New York.

23) Giesbers, M., Kleijn, J.M., Cohen Stuart, M.A., *J. Colloid Interface Sci.*, **2002**, 2448, 88.

24) Fleer, G.J., *Food Polymers, Gels and Colloids*, **1991**, E. Dickinson Ed., Royal Society of Chemistry, 34.

25) Bajpai, A.K., *Prog. Polym. Sci.*, **1997**, 22, 523.

26) Marra, J., van der Schee, H.A., Fleer, G.J., Lyklema, J., *Adsorption form solution*, **1983**, R.H. Ottewill, C.H. Rochester, A.L. Smith Eds., Academic Press, 245.

27) Papenhuizen, J., Fleer, G.J., Bijsterbosch, B.H., *J. Colloid Interface Sci.*, **1985**, 104, 530.

28) Hoogeveen, N.G., Cohen Stuart, M.A., Fleer, G.J., *Colloids Surf. A*, **1996**, 117, 77.

29) Cohen Stuart, M.A., Hoogendam, C.W., de Keizer, A., *J. Phys.: Condens. Matter*, **1997**, 9, 7767.

30) Odijk, T., *Chem. Phys. Lett.*, **1983**, 100, 145.

5 Adsorption of a Dendritic Polyelectrolyte on a Gold Electrode

Abstract

The adsorption of the dendritic polyelectrolyte 1,4-diaminobutane poly(propylene imine) (DAB-dendr-$(NH_2)_{64}$) from aqueous electrolyte solution onto a gold electrode was investigated as a function of the double layer potential of the substrate by means of reflectometry. The dendrimer has a pH-dependent positive charge. The double layer charge and potential of the gold/electrolyte interface was manipulated either by means of the solution properties or by means of an externally applied potential. The results of the experiments are rather surprising and in some cases difficult to interpret. The total adsorbed amount increases with increasing dendrimer concentration up to the random sequential adsorption (RSA) jamming limit. At a concentration of about 10 mg/l the initial adsorption rate as a function of the dendrimer concentration shows a sudden decrease in the slope of the line by a factor of three. Neither the total adsorbed amount nor the initial adsorption rate vary with concentration background electrolyte. The initial adsorption rate increases with increasing electrostatic repulsion between dendrimer and substrate, i.e., with decreasing pH or increasing applied potential. The pH has no effect on the total adsorbed amount. However, as a function of the applied potential the total adsorbed amount decreases linearly, which is very similar to the adsorption behaviour of PVP^+, a linear polyelectrolyte with a fixed charge, onto gold (Chapter 4). On the basis of the complete set of results, it is concluded that electrostatic interactions do not significantly affect the adsorption process of the dendrimer onto gold. Probably, e.g., the density of oxidic binding sites at the gold surface, which is dependent on pH, is an important parameter.

5.1 Introduction

Poly(propylene imine) dendrimers are synthetic polyelectrolytes with a highly branched structure. They are synthesized in a stepwise manner, resulting in successive generations[1,2]. Starting from a 1,4-diaminobutane (DAB) core and adding propylene imine branches to it by an iterative procedure, a highly symmetric, monodisperse, tree-like macromolecule with a regular structure is formed. A two-dimensional picture is given in Figure 5.1. At the branching points in the core tertiary amine groups are formed and their number is equal to $2^{n+1} - 2$ (n = generation number). At the outer shell of the dendrimer, 2^{n+1} primary amine end groups are situated. All amine groups are ionisable, resulting in a polyelectrolyte which is fully charged at pH 3 and fully uncharged at pH 11 (see Figure 5.2). Most properties, such as the acid-base properties[3,4] and the protonation mechanism[5], structure, intermolecular interactions and structure-property relations[6-8] of dendrimers are well-studied and adsorption studies on, for example, glass and silica[9,10] have been reported in literature.
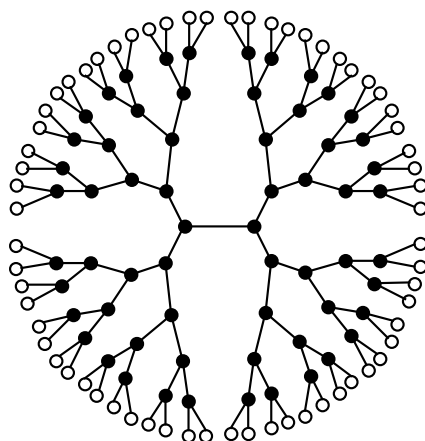
Figure 5.1: *Schematic representation of the fifth generation poly(propylene imine) dendrimer DAB-64. Closed symbols are tertiary amines, open symbols represent primary amines. The connecting lines represent the carbon backbone of the dendrimer.*
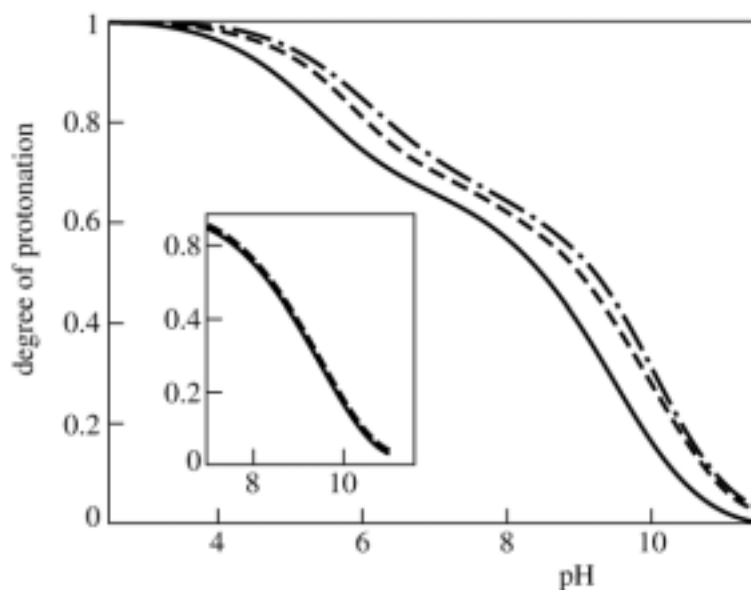
Figure 5.2*: Titration curves of DAB-64 at a concentration of 80 mM amine groups plotted as the degree of protonation versus pH in KCl as background electrolyte. Ionic strengths: 0.1 (—), 0.5(---), and 1.0 M (— -). In the inset, the effect of different cations, Na^+ (—) and K^+ (---), is shown for a ionic strength of 0.1 M. Redrawn from van Duijvenbode et al[3].*

One goal of this thesis is to get more insight into the role of electrostatics in the adsorption behaviour of charged macromolecules and the possibilities to control their adsorption by varying the interfacial potential. In Chapter 4, we have presented the results on the adsorption behaviour of a linear polyelectrolyte (i.e., quaternized poly(vinyl pyridine), PVP^+). By also investigating the adsorption of DAB-64, for which - as stated before - the contribution stemming from conformational changes is much less important, we hope to be able to discriminate between effects of such changes and electrostatic interactions.

Here, we present a systematic study of the adsorption from solution of a fifth generation poly(propylene imine) dendrimer onto a gold electrode. The dendrimer has $2^{5+1} = 64$ end groups and will be indicated as DAB-64 from now on. The structure of the dendrimer is very stable. On the basis of X-ray reflectivity studies on polyamidoamine dendrimers[11] and computer simulations on model dendrimers[12], van Duijvenbode et al[9] conclude that a dendrimer is not able to stretch fully along a surface. The dendrimers can be compressed slightly, but the additional surface coverage per molecule is hardly comparable to what a flexible chain can do. The number of contacts between the dendrimer and the surface will therefore stay relatively low. Linear chain polyelectrolytes usually have the conformation of a random coil and adsorption means a loss in conformational entropy, which always opposes adsorption (see Chapter 1 and Ref. 13). However, even a small reduction of the Gibbs energy per adsorbed segment adds up to a considerable amount per molecule, since the molecule is very large. In the case of DAB-64 adsorbing onto a solid surface, the entropy loss due to conformational changes (opposing adsorption) is small. On the other hand, the number of contacts between the dendrimer and the solid surface is also small, meaning that the sum of the contributions of each adsorbed segment to the reduction of the Gibbs energy is much less than in the adsorption of a linear polyelectrolyte. In view of all this, the balance of forces determining the adsorption behaviour in the present experiments is very different from what has been examined in the previous chapter.

Like in the previous chapter, the results of adsorption experiments in which the potential of the gold/electrolyte interface is varied through the solution properties are compared to results obtained as a function of an externally applied potential. In contrast to PVP$^+$, which is a strong polyelectrolyte, the charge of the dendrimer depends on the solution pH. Therefore, by changing the pH of the solution we do not only change the electric properties of the substrate, but also those of the adsorbing molecules. For our adsorption studies we have chosen gold as the sorbent because it is a metallic conductor and because it is not very reactive, i.e., over a relatively large potential range no electrochemical surface reactions occur. The choice for gold as the adsorbing surface is motivated more extensively in Chapter 2.

5.2   Experimental

The measurements described in this chapter are performed using the same methods as described in the previous chapter, using the same type of gold-coated silicon wafers (Philips Research Laboratories, Eindhoven, the Netherlands), reflectometer set-up for the adsorption experiments, and potentiostat for applying potentials across the gold/electrolyte interface. The parameters used to calculate the sensitivity factor for the reflectometer experiments A_s (see Chapter 3), are given in Table 1. The thickness of the adsorbed layer is based upon the dimensions of the dendrimer as reported in literature[7]. For this set of parameters A_s is 0.0075 m^2/mg, which is rather low. However, Dijt et al[11] give a minimum value of 0.005 for performing accurate measurements.

Table 1: *Parameters used to calculate the sensitivity factor A_S, according to the method described in Chapter 3.*

Thickness of the gold film	15 nm
Refractive index of the gold film[11]	0.1 + 3.6 i (at a wavelength of 632.8 nm)
Thickness of the titanium film	5 nm
Refractive index of the titanium film[11]	2.22 + 2.99 i (at a wavelength of 632.8 nm)
Refractive index of the silicon[11]	3.8
Refractive index of the aqueous solution[11]	1.333
Thickness of the adsorbed layer of DAB-64[5]	3 nm
Refractive index increment of DAB-64[7]	0.17 cm^3/g
Angle of incidence	71°
Wavelength of the laser beam	632.8 nm

The dendrimer 1,4-diaminobutane poly(propylene imine) (DAB-*dendr*-$(NH_2)_{64}$) was used as obtained from Sigma-Aldrich Chemie GmbH (Germany). A schematic picture of the dendrimer is shown in Figure 5.1. The supporting electrolyte in all experiments is KNO_3. Adsorption studies were carried out at various dendrimer concentrations, electrolyte concentrations, solution pH values, and as a function of the potential applied across the gold/electrolyte interface. The pH of the solutions was adjusted using aliquots of aqueous solutions of nitric acid (HNO_3). The electrolyte concentration was 1 mM, unless specified otherwise. This concentration was not corrected for the pH adjustments, so that the total ionic strength varies slightly with pH. All solutions were prepared using ultrapure water (Richard van Seenus Technologies bv. Almere, The Netherlands).

In Chapter 3, the sensitivity factor and reproducibility of the adsorption experiments performed with our reflectometer set-up have been extensively described. This was done for the adsorption of a linear polyelectrolyte onto the gold-coated wafers. When the polyelectrolyte and the surface are oppositely charged, the conformation of the adsorbed polyelectrolyte is very flat, resulting in a layer thickness of approximately 1 nm. When the charge signs of the polyelectrolyte and the surface are the same, more loops occur in the conformation of the adsorbed chains and the thickness may increase up to approximately 3 nm. In this range, the sensitivity factor A_s is strongly dependent on the thickness of the adsorbed layer (see Figure 3.4). The structure of the dendrimer, on the other hand, is very stable and deformation upon adsorption from solution onto a solid surface is minimal. The thickness of the adsorbed layer therefore does not change very much and is expected to be always around 3 nm, the diameter of the molecule[5]. Therefore the dependence of A_s on the thickness of the adsorbed layer is very small (see Figure 3.4). The contribution of variations in the dendrimer layer thickness to inaccuracies in the measurements is therefore negligible. The largest source of scatter in the data points originates from variations in the layer thickness of the gold on the coated wafer (see Chapter 3). Since all adsorption measurements are performed 3 - 4 times, this scatter in the data points is ± 2 - 10% (depending on whether strips of one or more wafers have been used in the series of measurements).

5.3 Results and Discussion

5.3.1 Adsorption of DAB-64 onto gold as a function of its concentration

The total adsorbed amount, Γ, and the initial adsorption rate, $(d\Gamma/dt)_0$, of DAB-64 onto gold-coated silica wafers were measured as a function of the concentration of dendrimer in solution. The results of these experiments are presented in Figure 5.3. It should be noted that the pH of the solutions was not adjusted and the solutions were not deaerated prior to use. This results in solutions of varying pH, namely 6 at the lowest dendrimer concentration, pH 7.5 at a concentration of 10 mg/l, and pH 9 at the highest dendrimer concentrations. In this pH range the double layer potential of the gold substrate as determined by colloidal probe AFM in Chapter 2 is virtually constant and negative.[12] Van Duijvenbode et al[3] have determined the degree of protonation of DAB-64 as a function of the pH of the solution, and found that the proton charge of the dendrimer decreases slightly between pH 6 and 7.5 and decreases much stronger at pH values above 7.5. Titration curves at various KCl concentrations are shown in Figure 5.2.
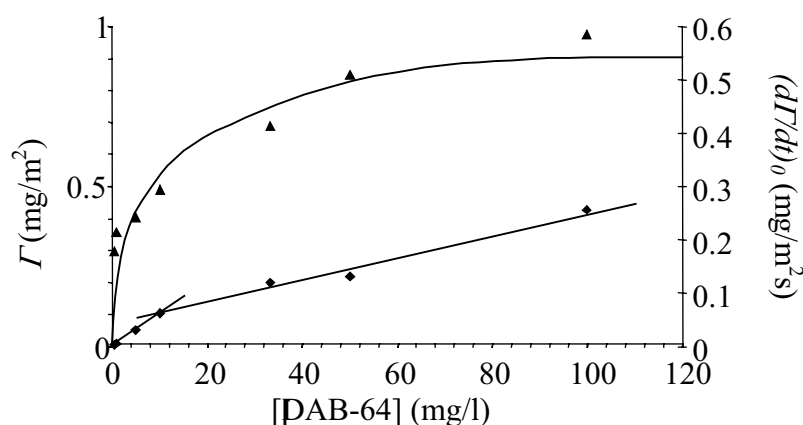
Figure 5.3: *Total adsorbed amount (▲) and initial adsorption rate (◆) of DAB-64 onto gold as a function of the concentration of dendrimer in the bulk solution. (Background electrolyte = 1 mM KNO₃, pH not adjusted (see text))*

The degree of surface coverage at the highest concentrations of dendrimer is about 52%, calculated from the adsorbed amount (ca. 1 mg/m^2), and the molecular weight and size of DAB-64 (M_w = 7168 g/mole, radius of gyration R_g = 1.4 nm)[7]. This is close to the jamming limit in the RSA (Random Sequential Adsorption) model[17]. The applicability of this model is corroborated by the fact that we do not find any desorption upon flowing the background electrolyte solution through the reflectometer cell, i.e., the binding is quite irreversible. The maximum adsorbed amount we find on gold is much higher than that on glass reported by Van Duijvenbode et al[9], who found a maximum degree of coverage of 10 - 15%.

The initial adsorption rate increases linearly with the dendrimer concentration in the range of 0.5 to 10 mg/l. At concentrations higher than 10 mg/l, the initial adsorption

rate continues to increase approximately linearly with the dendrimer concentration, but the slope is a factor of 3 lower than in the low concentration range. The adsorption rate $d\Gamma/dt$ is given by[11,14]:

$$\frac{d\Gamma}{dt} = k \cdot (C_b - C_s) \qquad (5.1)$$

with

$$k = 0.776 \nu^{\frac{1}{3}} R^{-1} D^{\frac{2}{3}} (\bar{\alpha}\, Re)^{\frac{1}{2}} \qquad (5.2)$$

Here, C_b is the DAB-64-concentration in the bulk solution, C_s the DAB-64 concentration near the gold surface (the subsurface concentration), ν the kinematic viscosity of the solution, R the radius of the tube of the impinging jet system, D the diffusion coefficient of the DAB-64, and Re the Reynolds number. When the flux to the surface is the limiting factor in the adsorption process, the subsurface concentration of DAB-64, C_s, is zero and $d\Gamma/dt$ equals the limiting flux of DAB-64 to the surface. Then $d\Gamma/dt \cdot C_b^{-1}$ is equal to the constant k. The diffusion coefficient of DAB-64 measured with pulsed-field gradient NMR at pH 7 and 0.1 M NaCl is $1\cdot10^{-10}$ m²/s. We can calculate the limiting flux of dendrimers to the surface using this value. With $n = 10^{-6}$ m²/s, $R = 0.5$ mm, $Re = 10.6$, and $\bar{\alpha} = 6$ [11], we find that for concentrations below 10 mg/l the initial adsorption rate is somewhat lower (by a factor of ca 2), but still in the same order of magnitude as the limiting flux. This indicates that on the one hand the transport of molecules towards the gold surface does affect the adsorption rate, but that on the other hand other steps in the adsorption process, e.g., attachment to the surface, also play a role. At dendrimer concentrations higher than 10 mg/l the initial adsorption rate is approximately 6 times lower than the flux calculated from the literature value of D.

A similar observation, i.e., a fairly sharp decrease in the slope of the initial adsorption rate as a function of the dendrimer concentration has been observed by Van Duijvenbode et al[10], for the adsorption of dendrimers on glass from 0.1 M NaCl solutions of pH 7. However, the initial adsorption rates they have measured were always far below the limiting flux to the surface, and, moreover, independent of the generation of dendrimers ($n = 2, 3, 4, 5$). This implies that aggregation of the dendrimers in solution cannot be the cause of this phenomenon, because the adsorption kinetics are not related to the transport of molecules towards the surface. From conductivity measurements on dendrimer solutions we have found no indication whatsoever that the compound forms aggregates at concentrations around 10 mg/l and higher. It seems more likely that a surface process influences the initial adsorption rate, but it is presently unclear what that process might be.

5.3.2 Variation of the electrolyte concentration

The electrolyte concentration of the solution was varied, while keeping the dendrimer concentration constant. The total adsorbed amounts and the initial adsorption rate are given in Figure 5.4. The experiments were carried out at bulk dendrimer concentrations of 33 mg/l (Figure 5.4A) and 3 mg/l (Figure 5.4B). It appears that the ionic strength does not have much systematic influence on the adsorption behaviour. From model calculations on linear polyelectrolytes it has been shown that in the case of pure electrosorption the adsorbed amount decreases with increasing ionic strength, while the adsorbed amount shows a maximum or a monotonical increase when non-electrostatic attraction plays a role[15]. Such calculations have not yet been performed for dendrimers or polyelectrolyte stars. In the adsorbed amounts measured here at a concentration of 33 mg/l there seems to be a maximum, although the variations are hardly more than the experimental error. In any case, the adsorbed amounts are very high, almost equal to the RSA limit, which makes any significant increase with electrolyte concentration not to be expected.
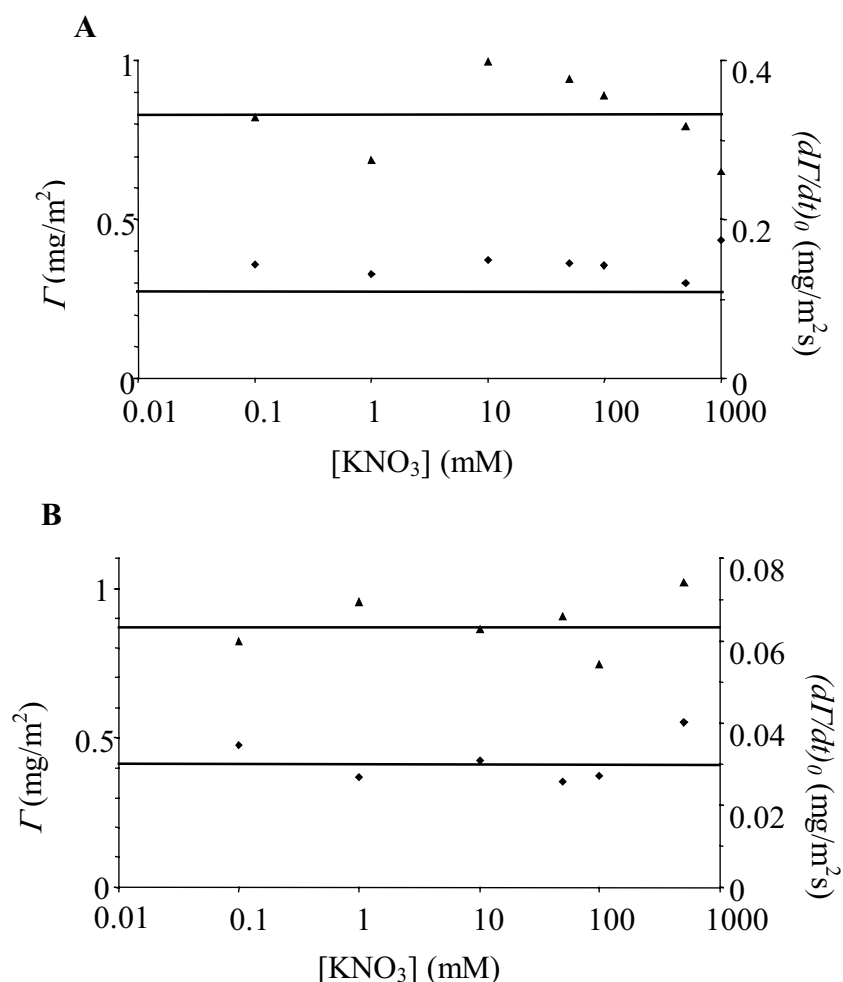

Figure 5.4: *Total adsorbed amount (▲) and initial adsorption rate (◆) of DAB-64 onto gold as a function of the ionic strength. **A:** At a bulk dendrimer concentration of 33 mg/l, pH = 6.5. **B:** At a bulk dendrimer concentration of 3 mg/l, pH = 6.0.*

The initial adsorption rate is unaffected by the electrolyte concentration. At the lowest concentration of dendrimer (3 mg/l) this was expected, since we observed that the adsorption rate at this dendrimer concentration is for the most part transport limited. At a dendrimer concentration of 33 mg/l, the initial adsorption rate is also independent of the electrolyte concentration. If at this concentration something else than the transport of the dendrimers towards the gold surface is rate limiting (e.g., the attachment to the surface), this step in the adsorption process is not influenced by the electrolyte concentration. From these results it can be concluded that electrostatics is not a dominant factor in the adsorption.

5.3.3 Variation of the pH of the solution

The total adsorbed amount and the initial adsorption rate as a function of the solution pH are presented in Figure 5.5. The iso-electric point (i.e.p.) of the gold is indicated in the figure. The total adsorbed amount is independent of the solution pH. Although the degree of protonation of the dendrimer varies with pH, the effective charge within the molecule is probably fairly constant. Over the whole pH range (i.e., pH 3.5 - 8) the primary amino groups (the end groups) are charged; the internal charge is probably effectively screened by counterions in the dendrimer[9,16]. Figure 5.5 shows that at low pH, where the gold substrate and the dendrimer are oppositely charged, the total adsorbed amount is approximately equal to that at high pH, where the gold and the dendrimer have the same charge sign. This show again that the total adsorbed amount is not - or only slightly - determined by the electrostatic interactions between the molecules and the substrate.
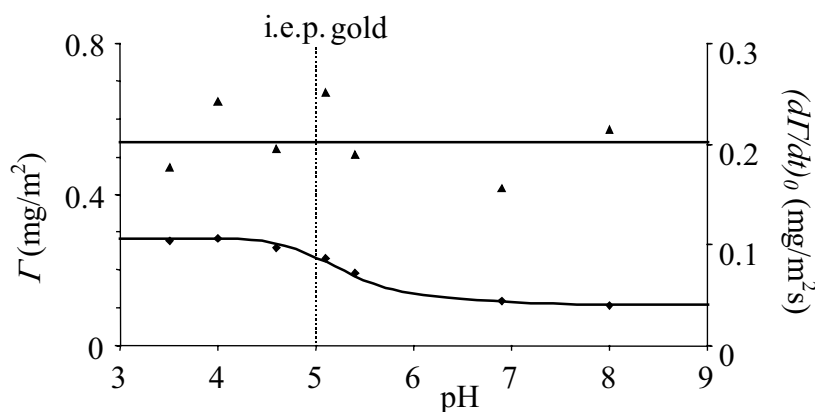
Figure 5.5: *Total adsorbed amount (▲) and initial adsorption rate (◆) of DAB-64 onto gold as a function of the solution pH (concentration DAB-64 = 5 mg/l, background electrolyte = 1 mM KNO$_3$,). The solid lines are just to guide the eye.*

The initial adsorption rate decreases with increasing pH (almost threefold) in a relatively small pH range around the iso-electric point of the gold surface from rather high to values similar to those presented in Figure 5.3. We have seen that at this dendrimer concentration (5 mg/l) at pH 6 the initial adsorption rate is determined both by the flux of the molecules to the surface, and by another step in the process, e.g., attachment to the surface. Apparently, at lower pH values, this other step in the process does not play a role anymore and the diffusion coefficient determines the initial adsorption rate. When we calculate the diffusion coefficient from the

measurements at low pH (using equations 5.1 and 5.2), we obtain a value of $1.8 \cdot 10^{-10}$ m^2/s, which is even slightly higher than the diffusion coefficient measured with pulsed field gradient NMR ($1 \cdot 10^{-10}$ m^2/s). Considering these results, we infer that changes in the initial adsorption rate most likely stem from changes at the gold surface as a function of the solution pH and *not* from changes in the electrostatic interactions between the dendrimer and the gold.

5.3.4   *Applying an external potential*

The total adsorbed amount and the initial adsorption rate at a constant pH of 6.9 as a function of the applied potential are given in Figure 5.6. At this pH the degree of protonation of the dendrimer equals 0.67. The total adsorbed amount decreases strongly with increasing applied potential at the gold surface. The total adsorbed amount at an applied potential of ca. +200 mV (which is approximately equal to the open circuit potential of the gold surface at this pH) is the same as in previous measurements (see fig. 5.3, 5.4 and 5.5). At lower applied potentials, the surface coverage increases, again up to approximately the jamming limit in the random sequential adsorption model. Apparently, the dendrimers can get closer together at the gold surface when the electrostatic interaction between the dendrimer and the gold surface is increased. Increasing the applied potential results in a linear decrease in the adsorbed amount of the dendrimer. The trend in the adsorbed amounts resembles very closely the results measured for PVP^+ adsorption on gold (see Chapter 4). Desorption as a result of changing the applied potential from low to higher values has not been observed.
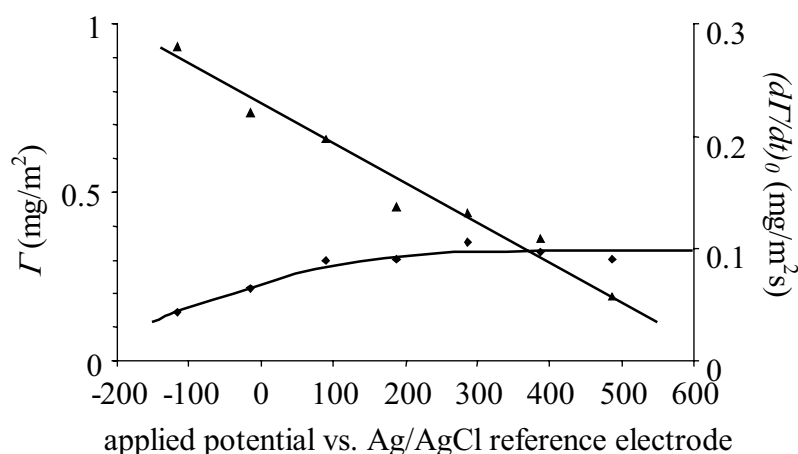
Figure 5.6: *Total adsorbed amount (▲) and initial adsorption rate (◆) of DAB-64 onto gold as a function of the applied potential across the gold/electrolyte interface. (Background electrolyte = 1 mM KNO_3, pH = 6.9).*

The initial adsorption rate decreases with decreasing applied potential in the range below the potential of zero charge of the gold surface, which is at an applied potential of approximately +300 mV[12]. This behaviour resembles that for PVP^+ described in the previous paragraph. Again, changes in the gold surface are believed to be responsible for the decrease in the initial adsorption rate. This will be further discussed in the next section.

5.3.5 Adsorption of dendrimer onto gold as a function of the double layer potential

The double layer potential of the gold as a function of the applied potential across the gold/electrolyte interface and as a function of the pH of the solution has been determined using colloidal probe AFM[12] and the results have been presented in Chapter 2. Here, we use these data to compare the results of the measurements in which the pH of the solution was varied to those in which a potential was applied at the gold/solution interface. The total adsorbed amount and the initial adsorption rate as a function of the double layer potential of the gold surface are presented in Figure 5.7, which comprises the results from the previous two sections.
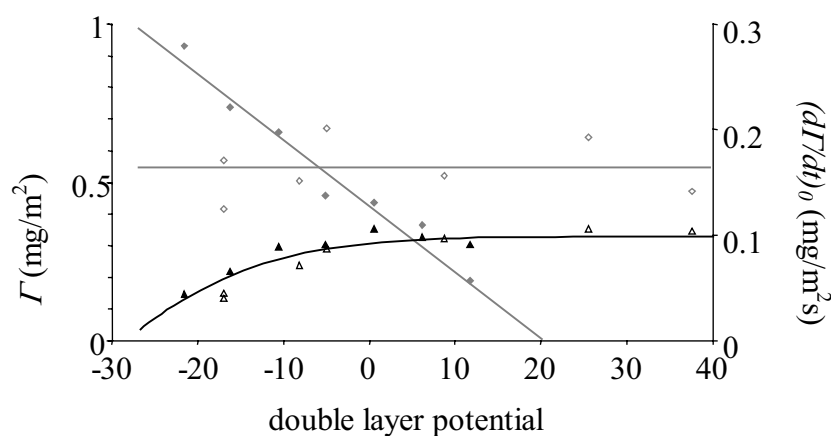
Figure 5.7: *Total adsorbed amount (◆,◇) and initial adsorption rate (▲,△) of DAB-64 onto gold as a function of the double layer potential of the gold. The concentration of dendrimer was always 5 mg/l. The open symbols represent results form the experiments in which the pH was varied under open circuit conditions, the closed symbols represent those in which a potential was applied at the gold surface at pH 6.9. The lines are just to guide the eye.*

The total adsorbed amounts measured as a function of solution pH (Figure 5.5), and those measured as a function of the applied potential (Figure 5.7) show completely different behaviour. This is in sharp contrast to the adsorption of PVP^+ onto gold under the same conditions (described in Chapter 3), for which the two types of experiments (changing the pH and applying a potential) give very similar $\Gamma(\psi^d)$ curves. Important differences between PVP^+ and DAB-64 are the conformation (PVP^+ has a random coil conformation in solution, while DAB-64 is always more or less spherical), and the charge (the charge of PVP^+ is fixed, whereas the charge on DAB-64 is pH dependent and adjustable). As a result of its flexible conformation, PVP^+ adsorbed onto gold can have much more binding contacts with the gold substrate than DAB-64. Of course, also chemical differences between the two adsorbates may play an important role. From the results presented earlier in this chapter, it is clear that electrostatics do not play a decisive role in the adsorption of the dendrimer, while for PVP^+ the adsorption can be characterized as electrosorption enhanced by specific interactions.

Looking at the adsorption kinetics, it is clear that PVP^+ attaches more easily (faster) to the gold surface than the dendrimer: for PVP^+ the initial adsorption rate was under practically all experimental conditions equal to the flux of molecules to the surface,

while for the dendrimer this is only the case at low pH or high applied potential. It is remarkable that the initial adsorption rates of DAB-64 – quite different from its adsorbed amounts - show the same trend as a function of double layer potential under pH control and when the external potential is varied. At positive double layer potentials, the initial adsorption rate is constant and equal to, or close to, the transport-limited value. At negative double layer potentials, the initial adsorption rate decreases with decreasing double layer potential, even though the dendrimer is positively charged and the electrostatic interactions become more attractive.

A possible explanation for some of the results described above, is that there are two types of binding sites for the dendrimer at the gold surface: oxidic binding sites (which are also responsible for the pH dependent behaviour of the double layer potential of the gold) and metallic ('bare' gold) sites. (In view of the high maximum adsorbed amounts, near the RSA jamming limit, the oxidic surface sites, which have under the conditions of our experiments a low density, cannot be the only binding sites for the dendrimer.) The dendrimer molecules would bind preferably to the oxidic sites, like also proposed for adsorption onto glass by Van Duijvenbode et al[3]. In Chapter 2, we found strong indications that below the iso-electric point of the gold surface (pH 5), the number of oxidic sites increases with decreasing pH, while above the iso-electric point of the gold surface, it is practically constant. We have no indication that the applied potential at a fixed pH has influence on the number of oxidic sites, although it seems likely that it increases at higher applied potentials. The increase in the *initial* adsorption rate of the dendrimers would then be the result of an increasing number of oxidic sites.

The total adsorbed amount as a function of pH is constant. For adsorption from a 5 mg/l DAB-64 solution (Figure 5.7), the surface coverage is ca 30%, which means that the contribution of binding to oxidic sites (considerably less than 1% of the surface sites, see Chapter 2) to the total adsorbed amount is small and therefore cannot lead to a significant variation with pH. The variation in the total adsorbed amount with applied external potential is in line with our first expectations, but is difficult to explain in view of the rest of the results, which all point to a very limited role of electrostatic interactions in the adsorption process. Possibly the binding of the dendrimer to the metallic sites becomes stronger when the applied potential becomes more negative, without affecting the kinetics. Clearly, this cannot be a long-range electrostatic effect, but would rather be equivalent to a change in chemical affinity. This conclusion seems to be supported by the fact that we did not observe any desorption upon decreasing the applied potential.

5.4 Conclusions

When changing the dendrimer concentration from 1 mg/l to 100 mg/l the total adsorbed amount increases to a plateau level very close to the jamming limit of the RSA model. Flushing with electrolyte solution does not lead to desorption on the time-scale of our experiments.

The initial adsorption rate increases linearly with dendrimer concentration. However, the slope of this line decreases rather abruptly by a factor of three at a dendrimer concentration of approximately 10 mg/l. A similar phenomenon was observed by van

Duijvenbode et al[10] for the adsorption of different generations of dendrimers on glass. The origin of this sharp decrease in the slope of the initial adsorption rate as a function of the dendrimer concentration is not clear. It is not related to a change in the flux of molecules towards the surface, like would occur in the case of aggregation. In the low concentration range, the initial adsorption rate is somewhat lower than but still in the same order as the limiting flux. Therefore, the initial adsorption rate is not only determined by the supply of molecules to the surface but also by another step in the adsorption process, e.g., attachment to the surface. At dendrimer concentrations above 10 mg/l, the initial adsorption rate is much lower than the transport-limited value.

Varying the electrolyte concentration at relatively low (3 mg/l) and high (33 mg/l) dendrimer concentrations does not affect either the total adsorbed amount or the initial adsorption rate. This is a strong indication that electrostatics is not a dominating factor in the adsorption process. Furthermore, the total adsorbed amount is independent of the solution pH, which affects both the potential of the gold substrate and the charge on the dendrimers. Neither do the initial adsorption rates as a function of pH and as a function of applied potential follow the electrostatic interactions, on the contrary. When these initial adsorption rates are plotted as a function of the double layer potential of the gold surface, they show exactly the same behaviour: for negative values of the double layer potential the initial adsorption rate decreases with increasing absolute value of the double layer potential; at positive double layer potentials the initial adsorption rate is equal to the transport-limited flux towards the surface, whereas at negative values it is substantially lower. In view of all this, it is surprising that the total adsorbed amount as a function of externally applied potential does seem to follow the electrostatic interactions, i.e., it shows a linear decrease with increasing applied potential, similar to what was found for the adsorption of PVP$^+$ onto gold in Chapter 4. However, from the complete sets of results we conclude that electrostatic interactions have no significant effect on the adsorption of DAB-64 on gold. Thus, the effect of the applied potential on the adsorbed amounts must be an indirect one, e.g., stemming from an increase in binding strength between dendrimer and metallic surface sites or a decrease in molecular cross section ("footprint") with decreasing applied potential.

The changes in the initial adsorption rate as a result of changing the solution pH most likely stem from (chemical) changes of the gold surface as a function of the solution pH. As described in Chapter 2, the density of oxidic sites at the gold surface probably increases with decreasing pH. If the dendrimers preferably bind to these sites, this may explain the increase in initial adsorption rate with decreasing pH. However, the density of these sites is always so low, that it does not significantly affect the total adsorbed amount.

The trend in initial adsorption rate as a function of applied potential can perhaps be explained in the same way, although we have found no indication that the density of oxidic sites changes over the potential range studied here.

5.5 Acknowledgements

Mr. Wim Threels in the Department of Physical Chemistry and Colloid Science at Wageningen University is gratefully acknowledged for performing conductivity measurements on dendrimers in solution.

5.6 References

1) Brabander, de, E.M.M., Meijer, E.W., *Angew. chem., Int. Ed.*, **1993**, 32, 1308.
2) Brabander, de, E.M.M., Brackman, J., Mure-Mak, M., Man, de, H., Hogeweg, M., Keulen, J., Scherrenberg, R., Coussens, B., Mengerink, Y., Wal, van der, S., *Macromol. symp.*, **1996**, 102, 9
3) Duijvenbode, van, R.C., Borkovec, M., Koper, G.J.M., *Polymer*, **1998**, 39, 2657.
4) Kabanov, V.A., Zezin, A.B., Rogacheva, V.B., Gulyaeva, Zh.G., Zansochova, M.F., Joosten, J.G.H., Brackman, J., *Macromolecules*, **1998**, 31, 5142.
5) Koper, G.J.M., van Genderen, M.H.P., Elissen-Román, C., Baars, M.W.P.L., Meijer, E.W., Borkovec, M., *J. Am. Chem. Soc.*, **1997**, 119, 6512.
6) Ramzi, A., Scherrenberg, R., Brackman, J., Joosten, J., Mortensen, K., *Macromolecules*, **1998**, 31, 1621.
7) Scherrenberg, R., Coussens, B., Vliet, van, P.G., Edouard, Brackman, J., Brabander, de, E., *Macromolecules*, **1998**, 31, 456.
8) Ramzi, A., Scherrenberg, R., Joosten, J., Lemstra, P., Mortensen, K., *Macromolecules*, **2002**, 35, 827.
9) Duijvenbode, van, R.C., Koper, G.J.M., Böhmer, M.R., *Langmuir*, **2000**, 16, 7713.
10) Duijvenbode, van, R.C., Koper, G.J.M., Böhmer, M.R., *Langmuir*, **2000**, 16, 7720.
11) Dijt, J.C., Cohen Stuart, M.A., Hofman, J.E., Fleer, G.J., *Colloids Surf.*, **1990**, 51, 141.
12) Barten, D., Kleijn, J.M., Duval, J., Leeuwen, van, H.P., Lyklema, J., Cohen Stuart, M.A., *Langmuir*; **2003**, 19, 1133.
13) Weast R.C. (Ed.), *Handbook of Chemistry and Physics 73rd edition*, **1990**, CRC Press, West Palm Beach, Florida.
14) Dabros, T., van de Ven, T.G.M., *Colloid Polym. Sci.*, **1983**, 261, 694.
15) Fleer, G.J., Cohen Stuart, M.A., Scheutjens, J.M.H.M., Cosgrove, T., Vincent, B., *Polymers at Interfaces*, **1993**, Chapman & Hall, London.
16) Klein Wolterink, J., Leermakers, F.A.M., Fleer, G.J., Koopal, L.K., Zhulina, E.B., Borisov, O.V., *Macromolecules*, **1999**, 32, 2365.
17) Bartelt, M.C., Privman, V., *Int. J. Mod. Phys.*, **1991**, 5, 2883.

6 Adsorption of a Structure-Stable Protein on a Gold Electrode

Abstract

In order to determine the role of electrostatic interactions in the adsorption from aqueous solution of the structure-stable ('hard') protein lysozyme onto gold, we examined this process by means of reflectometry. The charge and potential of the gold substrate were controlled by either varying the solution pH or by externally applying a potential. The adsorption process was monitored for various concentrations of protein and background electrolyte, pH values and applied potentials across the gold/electrolyte interface. The initial adsorption rate is substantially lower than the transport-limited flux to the surface indicating that the rate-limiting adsorption step is a surface process. Since it is not affected by the electrolyte concentration, electrostatics do not play a role in this step. Comparison of the results obtained using each of the two ways to control the electric properties of the substrate, show that the influence of electrostatics on the adsorption is minor. The adsorbed amounts are determined by the area per molecule ('footprint') occupied at the gold surface, which in turn is determined by the potential-dependent interfacial tension. The approach followed in this study can be successfully applied to discriminate between various contributions to the process of protein adsorption, i.e., electrostatic and non-electrostatic interactions between protein and substrate, electrostatic repulsion between adsorbing protein molecules and structural rearrangements within the protein.

6.1 Introduction

The adsorption of proteins from aqueous solution onto solid surfaces is a widely studied subject. Protein adsorption, either desired or not, plays a very important role in many systems. The manufacturing of diagnostic tests and biosensors, and the stabilizing of colloidal dispersions in pharmaceuticals and food products are examples in which the adsorption of proteins has an important function. Undesired protein adsorption is illustrated by fouling of food processing equipment, artificial kidney devices and cardiovascular implant materials. Although a lot of effort has been invested in understanding protein adsorption, the description of protein adsorption in literature is still highly qualitative and in order to predict the adsorption behaviour of a specific protein at best a few rules of thumb are available. It is widely recognised that there is a strong correlation between the structural stability of a protein in solution and its interfacial behaviour (see, e.g., Refs. 1-3) . The adsorption of proteins with a high internal stability - so-called "hard" proteins - is governed by hydrophobic and electrostatic interactions between protein and sorbent surface. These proteins adsorb on hydrophobic surfaces irrespective of the sign of the surface charge and

presumably undergo structural changes upon adsorption. On hydrophilic surfaces they only adsorb if there are favourable electrostatic interactions. Proteins with a low internal stability - so-called "soft" proteins - tend to adsorb on all surfaces, due to a gain in conformational entropy involving a loss of (secondary) structure, and this gain then dominates over any unfavourable effects of hydrophilic dehydration of the sorbent surface and protein, and over the electrostatic interactions. More hydrophobic surfaces induce larger perturbations in the conformation of an adsorbing protein molecule. In the systematic studies that form the basis of these insights the hydrophobicity of the surface generally has been varied by choosing materials of different chemical nature or by surface modification like silanisation, while the surface charge and potential as well as the charge on the protein molecules have often been varied through the solution pH (see, e.g., Refs. 4-9). However, changing the composition of the solution to manipulate the electrostatics also changes other properties of the adsorbing protein, in particular its structural stability. Therefore, in this way it is hardly possible to attribute the observed effects to changes in electrostatic interactions alone.

Applying an external potential to the adsorbent is probably the only reliable way to control the electrostatic properties of the surface without changing the composition of the solution and thus without changing the properties of the protein molecules in solution. Bos et al.[10] studied the adsorption process of several proteins onto an indium tin oxide (ITO) electrode. The structural stability of the various proteins varied from very low (e.g., bovine serum albumin, α-lactalbumin) to relatively high (e.g., lysozyme, ribonuclease A, superoxide dismutase). It was found for all proteins that applying an external potential to the ITO had very little effect on the adsorption behaviour, whereas changing the pH of the solution had quite a large effect. Only at high pH values the total adsorbed amounts of the most structure-stable proteins (among which lysozyme) were influenced by the applied potential. The pronounced differences found by Bos et al.[10] between the effect of changing the pH and varying the applied potential may be explained by the large effect of the solution pH on the conformational stability and charge of the protein molecules. On the other hand, the effect of the applied potential may have been small due to a large potential drop inside the semiconductive ITO, leaving only a small part of the applied potential at the solution side of the electric double layer. Hu et al.[11] showed that for a semiconducting surface (TiO_2) the influence of an applied potential on the diffuse double layer potential is very limited, typically less than 10% of the applied potential.

There are only a few other studies concerning the adsorption of proteins from aqueous solution onto electrodes. Razumas et al.[12] reported a minimum in the adsorption of insulin on a Pt electrode near the potential of zero charge of platinum. Morrissey et al.[13] investigated the effect of varying the potential on the adsorbed amounts of blood proteins on platinum *after* adsorption had taken place. Over the largest part of the studied potential range the effect was negligible, only above a certain threshold potential (400 – 800 mV vs. SCE, depending on the protein) additional adsorption took place. In a comparable study Beaglehole et al.[14] found that the adsorbed amount of bovine serum albumin (BSA) on gold and on stainless steel was not affected by changing the potential.

In this chapter reflectometry is employed to study the adsorption of lysozyme, a relatively structure-stable protein, from aqueous solution onto gold as a function of the solution pH, as well as the applied potential. The aim of the investigation is to determine the importance of electrostatic interactions in comparison to other factors, among which changes in structure (stability) of the protein molecules. From the above, it is clear that for a good interpretation in terms of electrostatics and for comparison of results obtained at variable pH and at variable externally imposed interfacial potential, it is necessary to have knowledge concerning the electric potential of the substrate relative to the solution under all relevant experimental conditions.

We have chosen gold as the substrate because it is a metallic conductor, which ensures that the potential in the bulk is constant up to the very close vicinity of the solid/solution interface. Furthermore, for gold in contact with water there is a relatively large potential range in which no electrochemical reactions take place. In an earlier paper[15] we reported on the double layer properties of gold in aqueous electrolyte solutions and showed that these can be manipulated by both the solution pH and the applied potential. By measuring the double layer interaction between the gold surface and a silica probe using an atomic force microscope, we were able to establish the dependence of the double layer potential of the gold surface on the pH and on the externally applied potential at different pH values.

Lysozyme is a globular, single-domain protein with a molecular weight of 14 600 g mole^{-1}. The protein is found in a variety of vertebrate cells and secretions, such as spleen, egg white, milk, nasal mucus and tears. Its function is to hydrolyse glucosidic bonds in the proteoglycan layer of bacteria, resulting to the destruction of bacterial cell walls. In 1962 lysozyme became the first enzyme of which the molecular structure had been determined by X-ray crystallography[16] (see Figure 6.1). A number of physical-chemical properties of lysozyme is listed in Table 1. The protein has a pH-dependent charge (given in Figure 6.2) resulting from association and dissociation of about 20 acidic and basic amino acid residues. In comparison to other proteins it has a rather stable structure, reflected in, for example, its heat of denaturation (see Ref 9). The rigidity of lysozyme is imposed by four disulfide bridges[17]. The stability of the protein decreases with decreasing pH[18].
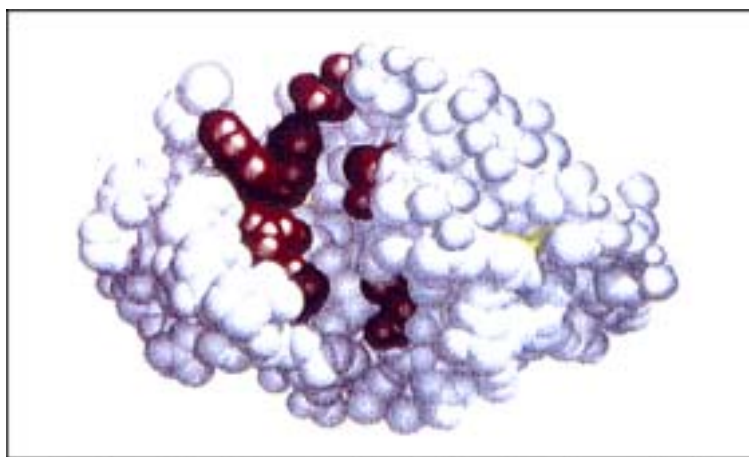

Figure 6.1: Space-filling model of a lysozyme molecule.

77
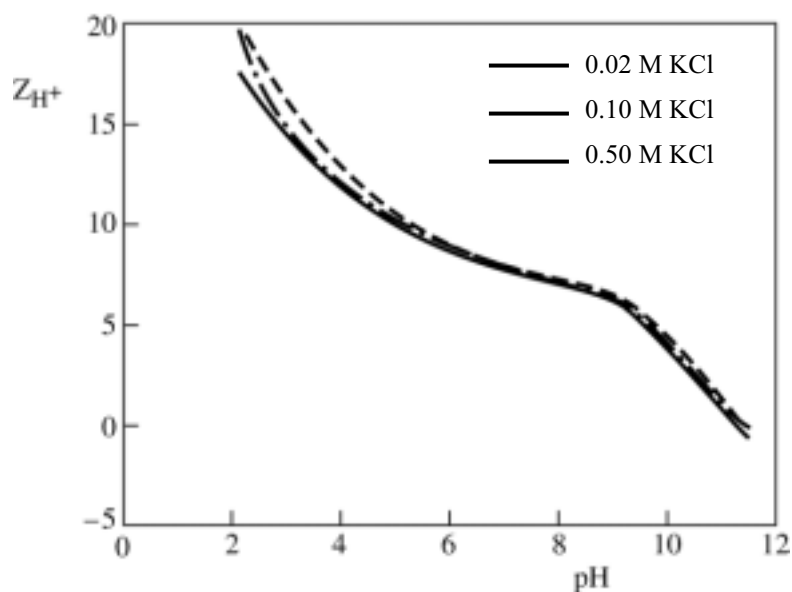
Figure 6.2: *Titration curves of lysozyme at various KCl concentrations. Z_{H+} is the net number of proton charges per molecule. Redrawn from ref 22.*

Table 1: *Physical-chemical properties of lysozyme*

Molar mass (g mole^{-1})[19]	14 600
Dimensions (nm)[19]	4.5 x 3.0 x 3.0
Diffusion coefficient (m^2 s^{-1})[19]	1.04 x 10^{-10}
Iso-electric point[19]	pH 11
Fraction of polar groups at water accessible surface[20]	0.59

The adsorption of lysozyme from aqueous solutions onto solid surfaces has been studied by several groups (e.g., Refs. 5,6,8-10,21-26), using various techniques and under a range of conditions. At high bulk concentrations (> 1 g/l) adsorption in more than one layer is often observed, particularly on silica (e.g., Refs. 21,23 and 26). There is no evidence for structural changes in lysozyme on adsorption onto the hydrophilic silica surface at ambient temperatures at pH 7[6,23]. However, at the surface, structural rearrangements take place more easily, i.e., at lower temperatures, than in bulk solution[23]. At pH 4 - 5 structural changes take place, as reflected in a lower fraction of α-helix in the adsorbed protein molecules and the extent of these changes increases with decreasing surface coverage[6]. It is generally concluded that electrostatic interactions are a dominant factor in lysozyme adsorption onto hydrophilic surfaces. Exceptions are the earlier mentioned study of Bos et al.[10], which is the only one conducted at an electrode (i.e., at variable externally imposed interfacial potential) and the study of Burns et al.[24], who investigated the adsorption of lysozyme as a function of the acid-to-base functional group ratio on a plasma polymer surface. In the latter study it was found that lysozyme adsorbs in higher amounts than the soft protein HSA (human serum albumin) regardless of solution pH and surface charge.

6.2   *Experimental*

6.2.1   *Materials*

Lysozyme from hen's egg (Sigma) was used without further purification to perform the adsorption experiments. Analytical grade KNO_3 was used as the background electrolyte. Adsorption studies were carried out at various solution pH values, electrolyte concentrations, lysozyme concentrations and as a function of the potential applied at the gold/electrolyte interface. The pH of the solution was adjusted using aliquots of aqueous solutions of nitric acid (HNO_3). The background electrolyte was 1 mM KNO_3, unless specified otherwise. This concentration was not corrected for the pH adjustments, so that the total ionic strength varies slightly with pH. All solutions were prepared using ultrapure water (Richard van Seenus Technologies bv. Almere, The Netherlands) and deaerated with nitrogen gas just prior before use.

Silicon wafers with a 5 nm layer of titanium and a 15 nm layer of gold sputtered on top of this were used as the substrate and were supplied by Philips Research Laboratories in Eindhoven (The Netherlands). The titanium layer is to prevent the gold layer from detaching from the silicon wafer. Strips of the gold-coated wafers were cleaned by immersion into "piranha solution", i.e., a hot mixture of 30% H_2O_2 and concentrated H_2SO_4, for 2 minutes, after which they were thoroughly rinsed with ultrapure water and left overnight in the electrolyte solution which was used as a blank in the particular adsorption experiments. Each strip was used only once. The surface roughness of the gold films, determined by AFM in the imaging mode, was found to be less than 2 nm over an area of 1 μm^2. Potentials were applied using a potentiostat (model 2059, AMEL s.r.l., Milan, Italy). A strip of the gold-coated wafer served as the working electrode, a platinum wire as the counter electrode and a Ag/AgCl (in 3 M KCl) was used as the reference electrode. All electrodes were put directly in the reflectometer cell.

6.2.2   *Methods and reproducibility*

In Chapter 4, we described adsorption measurements of a polyelectrolyte onto gold using reflectometry. The sensitivity factor A_s, used to calculate adsorbed amounts from the reflectometer output signal, and the reproducibility of the measurements have been extensively described in Chapter 3. Here we use the same system to measure the adsorption of lysozyme onto gold; A_s and the reproducibility are discussed only very briefly. The parameters needed to calculate A_s are given in Table 2. The refractive index increment *dn/dc* used for lysozyme was estimated from the values for several other proteins. The value for A_s obtained from these parameters is 0.0085 m^2/mg.

Unlike polyelectrolytes, proteins do not adsorb in a completely flat conformation. If they change their conformation, they unfold only partly. The structure of lysozyme is considered to be relatively stable and rearrangements in the structure upon adsorption from solution onto a solid surface are expected to be limited. We therefore assume that the thickness of the adsorbed layer does not change very much and varies between 2 and 4.5 nm. The lower limit allows for some structural changes at the surface, the upper limit is for adsorption of the molecules in an 'end-on' orientation. In Chapter 3 it was shown that in this range the dependence of A_s on the thickness of

the adsorbed layer is minimal. The contribution of variations in the protein layer thickness to uncertainties in the measurements is therefore negligible.

Table 2: *Parameters necessary to calculate the sensitivity factor A_s for the reflectometer measurements*

Thickness of gold film, d_{Au}	15 nm
Thickness of Ti film, d_{Ti}	5 nm
Thickness adsorbed layer, $d_{adsorbed}$	3 nm
Refractive index gold, n_{Au} (at 632.8 nm)[27]	$0.1 + 3.6i$
Refractive index titanium, n_{Ti} (at 632.8 nm)[27]	$2.22 + 2.99i$
Refractive index silicon, n_{Si}[27]	3.8
Refractive index solution, $n_{solution}$[27]	1.333
Refractive index increment lysozyme, $dn/dc_{lysozyme}$	0.185
Angle of incidence of laserbeam, θ_i	71°

Other sources for inaccuracies in the measurements are, e.g., the temperature and the flow rate in the reflectometer cell. These were kept constant - the fluctuation in the flow rate is approximately 1% and the temperature is $26 \pm 0.5°C$. The main cause for scatter in the output of the experiments is the variation in the gold layer thickness. Therefore all experiments were performed 3 to 4 times and averaged. Measurements of one series were performed using one gold-coated wafer only, if possible. Some series, however, required the use of two wafers, which introduces a much larger error. The error in the adsorbed amount in one series of measurements is as low as $\pm 2\%$ if strips of the same gold-coated wafer are used. This increases up to 10% if more than one wafer is used (see Chapter 3).

6.3   Results and Discussion

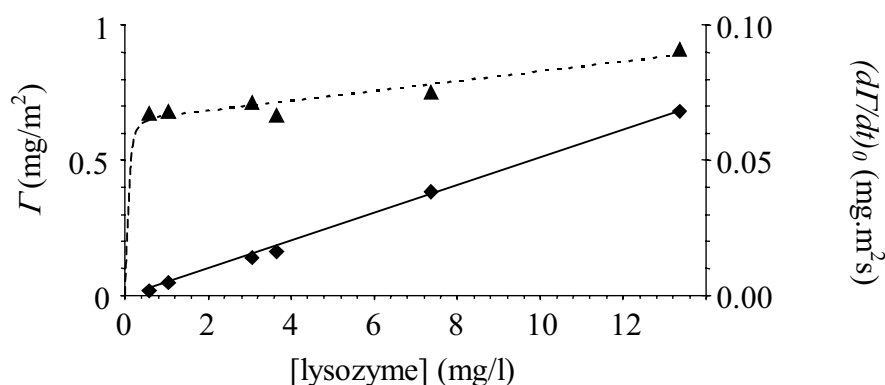### 6.3.1   Variation of the concentration of lysozyme

Figure 6.2: *Adsorption of lysozyme onto gold at neutral pH ($\pm$ 5.6) as a function of the concentration of lysozyme. Background electrolyte: 1 mM KNO₃. ▲=total adsorbed amount, ◆=initial adsorption rate.*

Figure 6.2 shows the total adsorbed amount and the initial adsorption rate of the adsorption of lysozyme onto gold at neutral pH as a function of the concentration of lysozyme in the solution. The adsorption rate $d\Gamma/dt$ is given by[28]:

$$\frac{d\Gamma}{dt} = k \cdot (C_b - C_s) \qquad (6.1)$$

with

$$k = 0.776 v^{\frac{1}{3}} R^{-1} D^{\frac{2}{3}} (\overline{\alpha} Re)^{\frac{1}{3}} \qquad (6.2)$$

in which C_b is the lysozyme concentration in the bulk solution, C_s the lysozyme concentration near the gold surface (the subsurface concentration), v the kinematic viscosity of the solution, R the radius of the tube of the impinging jet system, D the diffusion coefficient of the lysozyme, and Re the Reynolds number given by

$$Re = \frac{UR}{v} \qquad (6.3)$$

where U is the mean fluid velocity at the end of the inlet tube. The parameter $\overline{\alpha}$ reflects the intensity of the flow near the surface, which depends on the Reynolds number and on the geometry of the cell. The latter is characterized by the ratio h/R, with h the distance between the surface and the inlet tube. The protein solutions used here are very dilute (1 – 10 mg/l), which allows us for most parameters to use the values of pure water. In that case, the kinematic viscosity v is 10^{-6} m^2/s, $R = 0.5 \cdot 10^{-3}$ m, and $U = 0.021$ m/s. In our system, $Re = 10.6$ and $\overline{\alpha} = 6$ [28]. In the case that the adsorption is transport limited, $d\Gamma/dt$ equals the flux of lysozyme to the surface. If we assume transport limitation in the first stages of the adsorption process when the subsurface concentration is still equal to zero, we can compare the measured initial adsorption rate to the calculated initial adsorption rate (i.e., the flux of lysozyme to the surface). The diffusion coefficient, calculated from the measurements using equations (6.1)-(6.3), assuming transport limitation is $2.35 \cdot 10^{-11}$ m^2/s. This value is only 23% of the value of $1.04 \cdot 10^{-10}$ m^2/s reported in Ref. 19, indicating that instead of bulk transport another step in the adsorption process, e.g., the rate of attachment of the molecules to the surface, determines the initial adsorption rate.

Figure 6.2 further shows that the adsorbed amount rapidly increases with concentration lysozyme in solution at low concentrations (characteristic for a high-affinity isotherm) and then increases more gradually. In the concentration range studied here, the plateau of the adsorption isotherm is not reached yet. The measured adsorbed amounts are all considerably below the estimated monolayer coverage, which amounts to 1.8 – 2.7 mg m^{-2} depending on the orientation of the adsorbed protein molecules ('side-on' or 'head-on', respectively). Desorption upon rinsing with the electrolyte solution was never observed.

6.3.2 Adsorption of lysozyme onto gold as a function of the electrolyte concentration.

The total adsorbed amount of lysozyme on the gold substrate and the initial adsorption rate are given in Figure 6.3 as a function of the electrolyte concentration. The initial adsorption rate is independent of the electrolyte concentration, indicating that the rate-limiting step is not affected by electrostatic interactions. The adsorbed amounts are fairly constant or increase very gradually over the KNO_3 concentration range from 0.1 to 100 mM; from around 100 mM, the increase of Γ with increasing electrolyte concentration is more pronounced. Possibly this trend results from the screening of repulsive interactions between the adsorbing molecules. This result is at variance with earlier work of Buijs and Hlady[8] and Ball and Ramsden[25] who found that the adsorption of lysozyme on different substrates (of varying hydrophobicity and charge) decreases with increasing electrolyte concentration. This was explained by a change in structural stability of the protein with increasing salt concentration, affecting the affinity for adsorption.
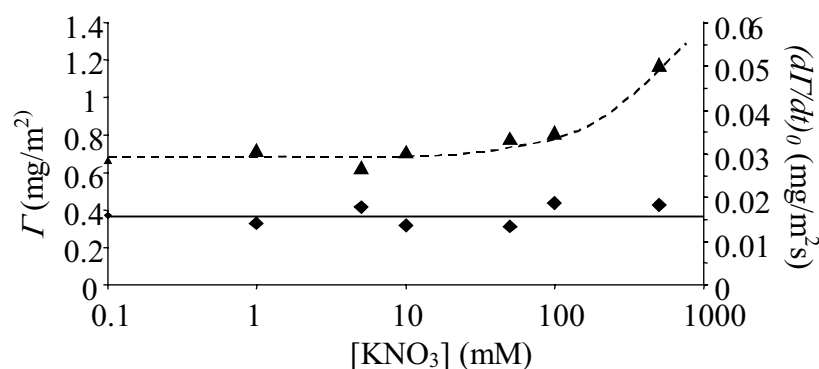
Figure 6.3: *Adsorption of lysozyme from a 3 mg/l solution onto gold at neutral pH as a function of the electrolyte concentration.* ▲*=total adsorbed amount,* ◆ *=initial adsorption rate. The solid line gives the value for* $d\Gamma/dt$ *obtained from the previous figure. The dotted line is just to guide the eye.*

6.3.3 Adsorption of lysozyme onto gold as a function of the solution pH

The effect of the solution pH on the total adsorbed amount and the initial adsorption rate is presented in figure 6.4. The iso-electric point of the gold surface[15,29] and that of lysozyme are indicated in the graph. In the pH range up to pH 5, Γ increases with increasing pH. Then, Γ remains approximately constant up to pH 7. At pH 11, Γ has increased up to a value of 1.8 mg/m^2, which corresponds to a full monolayer with the proteins adsorbed "side-on". At this pH the structural stability is at its maximum and the net charge of the protein in solution is zero. This allows the molecules to adsorb closely together in their compact, native conformation.
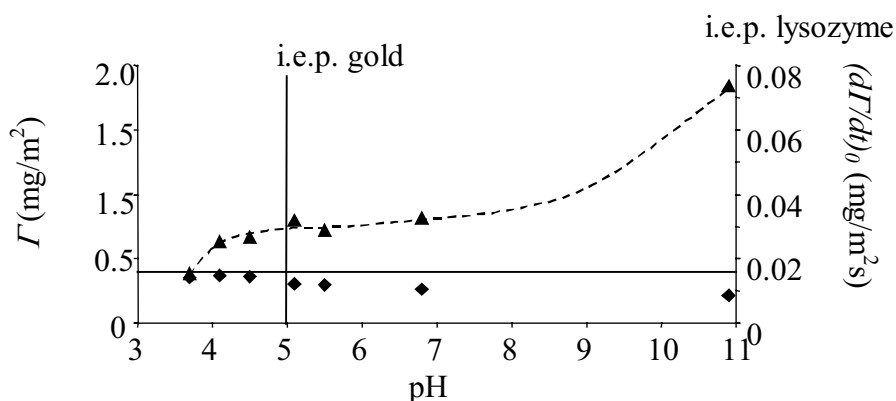
Figure 6.4*: Adsorption of lysozyme from a 3 mg/l solution onto gold as a function of the pH of the solution (1 mM KNO₃).* ▲=*total adsorbed amount,* ◆=*initial adsorption rate. The solid line gives the value for (dΓ/dt)₀ obtained from the previous figure. The dotted line is just to guide the eye.*

The decrease in adsorbed amount at pH < 5 may reflect the increasing electrostatic repulsion between the adsorbing molecules. It is also possible that the decreasing structure stability plays a role and that conformational rearrangements result in a larger adsorption area per protein molecule. By comparing the results from these experiments with the results of the next paragraph, in which the double layer potential of the gold is varied without varying the solution properties, it is possible to draw a conclusion about the relative importance of electrostatic interactions in the adsorption process. This will be further discussed in section 6.3.5.

Below the iso-electric point of the gold the initial adsorption rate is somewhat higher than above this pH value. Since the protein and the gold surface are both positively charged below pH 5 and have an opposite charge sign at higher pH values, this trend in $(dΓ/dt)_0$ cannot result from changes in the electrostatic interactions between the protein and the gold surface. This is line with the observation that the electrolyte concentration does not affect the initial adsorption rate (see section 6.3.2).

6.3.4 Adsorption of lysozyme onto gold as a function of the applied potential at the gold surface

The total adsorbed amount and the initial adsorption rate of lysozyme onto gold were measured as a function of the applied potential at the gold/electrolyte interface. Figure 6.5A gives the results of the reflectometer experiments at pH 6.4. The adsorbed amount $Γ$ decreases with increasing applied potential up to ca. +400 mV. Above this potential this trend is interrupted and the total adsorbed amount even slightly increases. At this pH the upper limit of the potential range in which measurements can be performed without interference of redox reactions at the gold/electrolyte interface is about +500 mV.

A

B

Figure 6.5: *Adsorption of lysozyme from a 3 mg/l solution onto gold as a function of the applied potential across the gold/solution interface (background electrolyte: 1 mM KNO₃).* ▲=*total adsorbed amount,* ◆ =*initial adsorption rate. A: pH = 6.4.* **B**: *pH = 5.0. The dotted line is just to guide the eye. The solid line is drawn at the value for (dΓ/dt)₀ obtained from Figure 6.3.*

To be able to reach higher double layer potentials of the gold, we repeated the experiments at pH 5. The results are presented in Figure 6.5B. We observe the same trend: up to an applied potential of +300 mV Γ decreases and above this potential Γ starts to increase again. To compare the results of both series of measurements, in the next section they will be presented as a function of the double layer potential of the gold surface, together with the results obtained as a function of pH at open circuit potential. The initial adsorption rate is rather constant with applied potential, at pH 6.4 as well as at pH 5.

6.3.5 *Lysozyme adsorption onto gold as a function of the double layer potential*

The total adsorbed amount, measured as a function of the applied potential across the gold/electrolyte interface and as a function of the pH of the solution is again presented in Figure 6.6A, but now as a function of the double layer potential of the gold/electrolyte interface. The double layer potential ψ^d is defined as the potential difference between the outer Helmholz plane and the bulk solution. Figure 6.6B gives the initial adsorption rate as a function of the double layer potential. The externally applied interfacial potentials and the pH values of the solution have been converted into the corresponding double layer potentials, using the results of AFM force measurements, which are described elsewhere[14].

The curves showing Γ measured at variable potential at pH 5 and at pH 6.4 overlap perfectly, when converted into one curve as a function of the double layer potential (see Figure 6.6). The proton charge of the lysozyme is somewhat higher at pH 5 than at pH 6.4 (see Figure 6.1), but apparently this does not result into a distinct difference between both curves. The curve for the total adsorbed amount obtained at variable pH under open circuit conditions is for the largest part also equal to the other two curves. Only at the lowest and highest pH values Γ deviates from the other two sets of results. The total adsorbed amount at pH 11 under open circuit conditions is much higher than at an applied potential of about 0 mV at pH 6.4, while under both conditions ψ^d is approximately -20 mV. The opposite is observed when the total adsorbed amount at pH 3 under open circuit conditions is compared to the adsorbed amount at an applied potential of approximately 450 mV at pH 6.4. Here, the corresponding double layer potential is ca. 40 mV. As stated before, at pH 11, the high amount of lysozyme adsorbed onto the gold is probably due to the high structural stability and the absence of electrostatic repulsion between the adsorbing molecules. At pH 3 the low amount of lysozyme adsorbed onto the gold is most likely the result of conformational changes upon adsorption ('spreading' of the protein) and/or a relatively large lateral electrostatic repulsion. In the intermediate region, the variation in the proton charge and structural stability with pH is apparently too small to result in a significant difference between the series of measurements, at variable pH and at variable applied potential.

Considering the measurements in which the double layer potential of the gold was varied using an applied potential and in which the solution properties - and thus the properties of the protein - are kept constant, we observe that Γ shows a minimum close to the potential of zero charge of the gold surface. Very similar data were reported in Ref. 12 for the adsorption of various types of insulin on platinum. Increasing and decreasing the double layer potential from the potential of zero charge has the same effect on the total adsorbed amount. This shows that electrostatic attraction or repulsion between the protein and the surface plays only a minor role. Since the properties of the protein molecules in solution do not vary, this behaviour must be due to changes in the nature of the gold/solution interface connected to variation of the electrode potential.

A

B

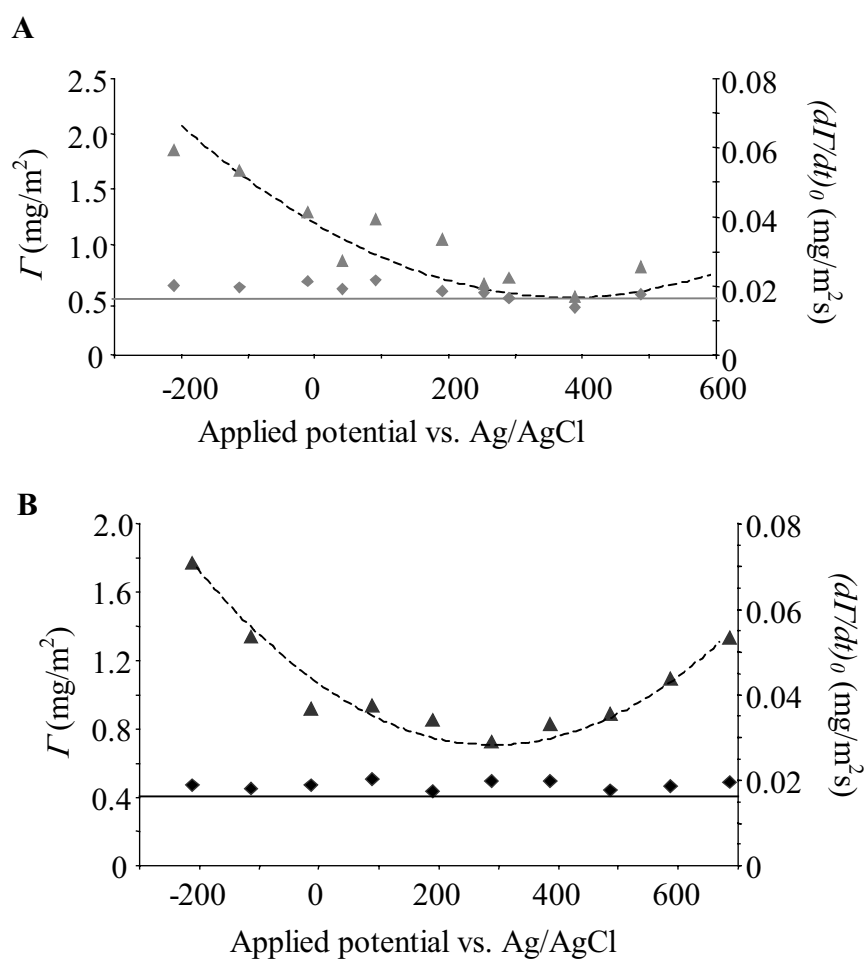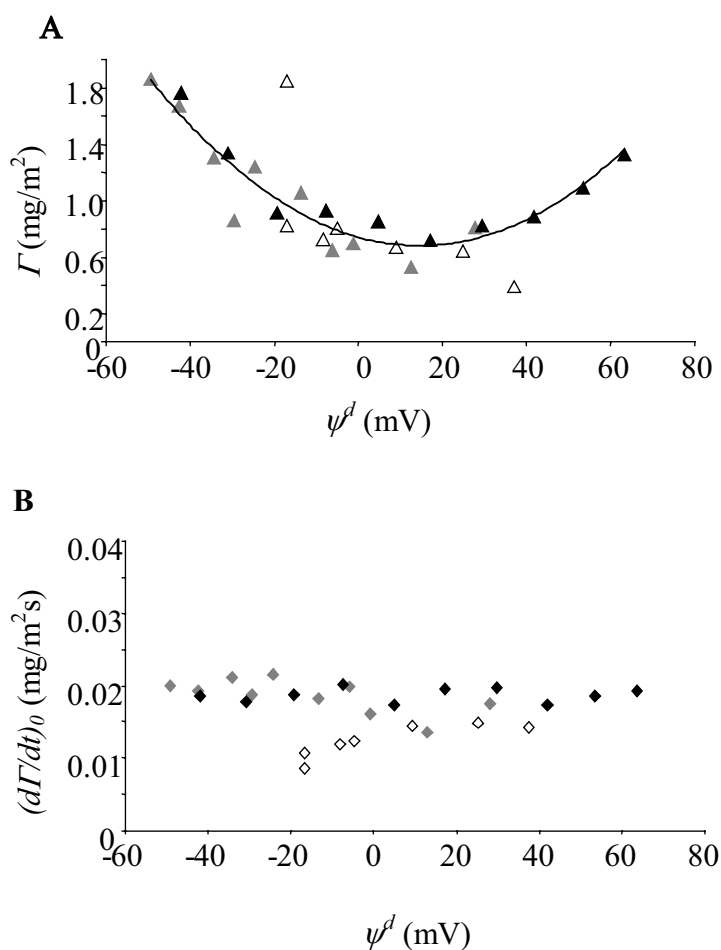*Figure 6.6: Adsorption of lysozyme from a 3 mg/l solution onto gold as a function of the double layer potential of the gold surface. The background electrolyte is 1 mM KNO₃. A: The total adsorbed amount. The closed symbols represent the results form the experiments in which a potential was applied at the gold surface at pH 6.4 (grey symbols) and at pH 5 (black symbols). The open symbols represent the data acquired at variable pH. B: The initial adsorption rate. Symbols as in Figure 6.6A.*

The shape of the curve of the total adsorbed amount in Figure 6.6 exhibits a remarkable resemblance with so-called electrocapillary curves, measured first by Lippmann back in 1873[30]. Such curves are plots of interfacial tension versus electrode potential. Lippmann thermodynamically derived an equation for the interpretation of surface tension measurements at mercury-electrolyte interfaces, now known in different forms as the Lippmann equation or electrocapillary equation[31,32].

$$\sigma^0 = -\left(\frac{\partial \gamma}{\partial E_\pm}\right)_{T,\mu_i} = \int_{E_\pm\left(\sigma^0=0\right)}^{E_\pm} C \mathrm{d}E_\pm \qquad (6.4)$$

with σ^0 the charge density on the electrode, γ the interfacial tension, $E_\pm$ the electrode potential (convention is to add a + or − in the subscript to indicate that the reference electrode responds to an anionic or a cationic component in the system), T is the

temperature, μ_i represents the chemical potentials of the electrolyte and other species in the solution and C the differential capacitance of the electrode/electrolyte interface.

At first sight, electrocapillary curves are often parabolas, like our $\Gamma(\psi^d)$ curve in Figure 6.6. If C is constant over the considered potential range the curves are perfect parabolas (as follows from the above equation), but this is generally not the case. Furthermore, an electrocapillary curve exhibits a maximum at the potential of zero charge, which shift to higher/lower electrode potentials in the case of specific adsorption of cationic/anionic components. Our curve shows a minimum, a bit at the positive side of the potential of zero charge as determined in 1 mM KNO_3 solutions without lysozyme. At the pH of the measurements lysozyme carries a positive charge, so this also corroborates the idea that the trend in adsorbed amounts is connected to variation of the interfacial tension of the electrode with potential.

Apparently, the adsorbed mass of lysozyme increases with decreasing interfacial tension, i.e., with increasing polarity of the surface. This can only be explained by surface-induced structural changes in the protein molecules, leading to a larger area per adsorbed molecule and thus lower adsorbed amounts. The extent of these structural changes increases as the surface is more 'high-energetic'. The adsorbed amount near the potential of zero charge is almost three times as low as that at a double layer potential of -50 mV. The adsorbed amount measured at -50 mV, 1.8 mg m^{-2}, corresponds to a complete monolayer of undisturbed (native) lysozyme molecules adsorbed in a 'side-on' orientation. In view of this, the observed trend in Γ as a function of pH is most likely resulting from the loss of native structure with decreasing pH, rather than being caused by increasing repulsive lateral interactions. If our conclusion that the contact area per molecule ('footprint') decreases with increasing interfacial tension is correct, one may argue that at still higher double layer potentials it becomes too small to adequately anchor the protein. A sudden decrease in adsorbed amount may be the result, in particularly at the positive side of the potential of zero charge because of repulsive electrostatic interactions between surface and protein. This cannot be confirmed here, since it is outside the accessible potential window. We know of no other studies reporting such desorption.

As we have seen in the previous section, under potential control the initial adsorption rate is rather constant in line with the conclusion that the influence of electrostatics on the adsorption process is very limited. The adsorption rate varies somewhat with pH and thus with the double layer potential of the gold (Figure 6.6B), but it does not follow the electrostatic interactions: at low pH values, corresponding to positive values for ψ^d and a relatively high positive charge on the protein molecules, the initial adsorption rate has the highest values. In the low pH range the protein can undergo more easily structural rearrangements at the surface, so it is tentatively concluded that the rate-limiting step in the adsorption involves such rearrangements.

6.4 Conclusions

The initial adsorption rate of lysozyme from aqueous KNO_3 solutions onto gold is not transport-limited, but determined by surface processes, like attachment to the surface or conformational rearrangements in the protein molecules. This is concluded from the observation that the initial adsorption rate of lysozyme onto gold is linearly

dependent on the protein concentration, but about five times lower than the transport-limited flux of molecules to the surface. Electrostatic interactions do not play a role in the rate-determining step, since the initial adsorption rate is not affected by the electrolyte concentration. Furthermore, the pH of the electrolyte solution has only a small influence on the initial adsorption rate and this effect is not in line with what is expected on the basis of electrostatic interactions. The applied potential across the gold/electrolyte interface has no effect on the initial adsorption rate.

Under open circuit conditions, neutral pH and 1 mM KNO_3, the adsorbed amount, Γ, increases strongly with the concentration protein in solution up to 1 mg/l, which points to a high affinity of lysozyme for the gold surface. For all higher protein concentrations studied, the adsorbed amount increases slightly with increasing lysozyme concentration, indicating that the plateau level of the adsorption isotherm has not been reached yet. This is probably due to kinetic effects.

Varying the electrolyte concentration has little effect on the total adsorbed amount. Only at the highest electrolyte concentration measured (500 mM KNO_3) does the total adsorbed amount increase.

The pH of the solution has a pronounced effect on the total adsorbed amount: increases rather strongly with decreasing pH, i.e., with decreasing structural stability and increasing proton charge of the protein molecules.

The influence of the applied potential across the gold/electrolyte interface was investigated at two different pH values, pH 6.4 and pH 5. Both series of experiments show a minimum in the total adsorbed amount at an applied potential which is slightly positive from the potential of zero charge of the gold electrode.

When the total adsorbed amounts measured in the series of experiments performed at varying pH and at varying externally applied potential are plotted as a function of the double layer potential ψ^d of the gold (using the results of colloidal probe force measurements described in Chapter 2 for the conversion of pH and applied potential into the corresponding ψ^d value) a single master curve is obtained. Only the data points obtained at high and at low pH (pH 11 and pH 3, respectively) deviate from this curve. This is attributed to the deviating structural stabilities of lysozyme at these pH values: at pH 11, the i.e.p. of lysozyme, the protein is very stable, while at pH 3 it has lost quite a part of its stability. In the series in which the double layer potential of the gold surface was varied by the applied potential (at constant pH), the properties of the lysozyme remain the same. Consequently, the shape of the master curve (Γ versus ψ^d) must be due to the properties of the gold surface. Indeed, it has a remarkable resemblance with an electrocapillary curve, as described by Lippmann. The adsorption of lysozyme onto gold increases with decreasing interfacial tension between the gold surface and the solution, because the molecules occupy less area and pack more densely. These results show that the adsorption process of lysozyme onto gold is governed by surface-induced conformational changes depending on the solution pH and the polarity of the gold surface. Electrostatic interactions between protein and gold surface do play only a minor role.

6.5 References

1) Norde, W., Lyklema, J., *J. Biomater. Sci. Polymer Edn.*, **1991**, 2, 183.
2) Kleijn, J.M., Norde, W., *Heterogen. Chem. Rev.*, **1995**, 2, 157.
3) Bajpai, A.K., Dengre, R., *Indian J. Chem*, **1999**, 38A, 101.
4) Elwing, H., Welin, S., Askendahl, A., Nilsson, U.R., Lundström, K.I., *J. Colloid Interface Sci.*, **1987**, 119, 203.
5) Arai, T., Norde, W., *Colloids Surfaces*, **1990**, 51, 1.
6) Norde, W., Favier, J.P., *Colloids Surfaces*, **1992**, 64, 87.
7) Norde, W., Rouwendal, E., *J. Colloid Interface Sci.*, **1990**, 139, 169.
8) Buijs, J., Hlady, V., *J. Colloid Interface Sci.*, **1997**, 190, 171
9) Norde, W., Arai, T., Shirahama, H., *Biofouling*, **1991**, 4, 37
10) Bos, M.A., Shervani, Z., Anusiem, A.C.I., Giesbers, M., Norde, W., Kleijn, J.M., *Colloids Surf. B*, **1994**, 3, 91.
11) Hu, K., Fan, F.F., Bard, A.J., Hillier, A.C., *J. Phys. Chem. B*, **1997**, *101*, 8298.
12) Razumas, V., Kulys, J., Arnebrant, T., Nylander, T., Larsson, K., *Soviet Electrochem.*, **1988**, 24, 1399.
13) Morrissey, B.W., Smith, L.E., Strömberg, R.R., Fenstermaker, C.A., *J. Colloid Interface Sci.*, **1976**, 56, 557.
14) Beaglehole, D., Webster, B., Werner, S., *J. Colloid Interface Sci.*, **1998**, 202, 541.
15) Barten, D., Kleijn, J.M., Duval, J., van Leeuwen, H.P., Lyklema, J., Cohen Stuart, M.A., *Langmuir*, **2003**, 19, 1133; Chapter 2 of this thesis.
16) Blake, C.C.F., Koenig, D.F., Mair, G.A., North, A.C.T., Philips, D.C., Sarma, V.R., *Nature*, **1965**, 206, 757.
17) Wilson, K.P., Malcolm, B.A., Matthews, B.W., *J. Biol. Chem.*, **1992**, 267, 10842.
18) Privalov, P.L., Khechinashvili, N.N., *J. Mol. Biol.*, **1974**, 86, 665.
19) Haynes, C.A., Norde, W., *Colloids Surf. B* **1994**, *2*, 517.
20) Lee, B., Richards, F.M., J. Mol. Biol., **1971**, *55*, 379.
21) Wahlgren, M.C., Arnebrant, T., Paulsson, M.A., *J. Colloid Interface Sci.*, **1993**, 158, 46.
22) Haynes, C.A., Sliwinski, E., Norde, W., *J. Colloid Interface Sci.*, **1994**, 164, 394.
23) Ball, A., Jones, R.A.L., *Langmuir*, **1995**, 11, 3542.
24) Burns, N.L., Holmberg, K., Brink, C., *J. Colloid Interface Sci.*, **1996**, 178, 116.
25) Ball, V., Ramsden, J.J., *J. Phys. Chem. B.*, **1997**, 101, 5465.
26) Su, T.J., Lu, J.R., Thomas, R.K., Cui, Z.F., Penfold, J., *J. Colloid Interface Sci.*, **1998**, 203, 419.
27) Weast, R.C. (Ed.), Handbook of Chemistry and Physics 73rd edition, **1990**, CRC Press, West Palm Beach, Florida.
28) Dijt, J.C., Cohen Stuart, M.A., Hofman, J.E., Fleer, G.J., *Colloids Surf.* **1990**, 51, 141.
29) Giesbers, M., Kleijn, J.M., Cohen Stuart, M.A., *J. Colloid Interface Sci.*, **2002**, 2448, 88.
30) Lippmann, G., *Compt. Rend.*, 76,1407; **1873**, *Ann. Phys. Chem.*, 149, 546.
31) Lyklema, J., *Fundamentals of Interface and Colloid Science*, *Volume II: Solid-Liquid Interfaces*, **1995**, Academic Press Limited., London.

32) Bard, A.J., Faulkner, L.R., *Electrochemical Methods – Fundamentals and Applications*, **2001**, 2nd edition, John Wiley & Sons, New York etc.

7   Conclusions and Outlook

In this thesis the adsorption of various types of charged macromolecules from aqueous electrolyte solution onto gold as a function of the electric potential of the solid/liquid interface has been presented. Our aim was to elucidate the role of electrostatics in the adsorption process of these molecules and to evaluate the possibilities to control the process by applying an external potential across the interface. In this chapter we draw some general conclusions, lay our finger on remaining problems and give a number of suggestions for further research.

On the whole we can conclude that our approach to get more insight into the adsorption process of charged macromolecules onto a charged surface has been successful. Manipulating the potential of the sorbent surface in two different ways, i.e., by changing the properties of the solution (pH, electrolyte concentration) or by applying an external potential, has provided us with additional information concerning the different types of interactions that play a role in the adsorption. Unique in this study is our knowledge of the double layer potential of the gold surface under all experimental conditions. This is essential to compare the results of the different types of experiments and to draw conclusions on the role of electrostatic interactions and the importance of other factors in the adsorption process.

Our choice for gold as the substrate has proven to be a good one. Since the gold surface combines the features of a reversible and a polarizable surface, its potential can be manipulated by both the composition of the adjacent aqueous solution and an externally applied potential. Unfortunately, the range in which the double layer potential can be varied is limited: on the one hand by redox reactions occurring at the gold/electrolyte interface at high and at low applied potentials, and on the other hand by the (low) number of oxidic sites at the surface which can be (de-)protonated when the double layer potential of the gold is varied by the solution pH. Luckily enough, however, the range of double layer potentials that can be covered is approximately the same for both charging mechanisms. This facilitates the comparison of the adsorption experiments 'under pH control' and 'under external potential control'.

When performing adsorption studies on electrodes using optical detection techniques, like in our case reflectometry, one should always be aware of the possible interference of the electro-optic effect, which occurs when a potential is applied across an electrode/electrolyte interface. We investigated this electro-optic effect and found that, although it causes a relatively large shift in the reflectometer signal, it has little influence on the *sensitivity* of the reflectometer system. Therefore, accurate adsorption measurements under external potential control are well possible, provided that before each measurement a baseline is recorded at the same applied potential.

A disadvantage of gold as adsorbing surface is its high surface energy. Although the gold surface is hydrophilic, the interfacial tension between the gold and the aqueous solution is high. Molecules in the electrolyte solution, including any impurities, adsorb relatively easily onto the gold to lower this interfacial tension, and as a result the relative importance of electrostatic interactions is in any case somewhat limited. A possible way to avoid this problem is to cover the surface with, for example, a self-assembled thiol monolayer with functional end groups[1,2]. If these functional groups

have acid-base properties, the surface is still amphifunctional. Another possible advantage of surface modification is that the range in which the double layer potential can be varied becomes larger. One can make the proton binding site density at the surface much higher and possibly higher potentials can be applied to the gold surface before redox reactions occur at the interface. Of course, this needs verification by AFM force measurements.

The molecules chosen for the adsorption experiments cover a interesting range of different types of charged macromolecules, varying from the relatively simple PVP$^+$, which is a strong, linear polyelectrolyte, via the dendrimer DAB-64, which has a pH-dependent charge, but a relatively stable sphere-like shape, to the protein lysozyme, of which both the charge and the structure stability are dependent on the solution properties.

For PVP$^+$ the adsorbed amount is determined by electrostatic interactions between the molecule and the sorbent surface, enhanced by a non-electrostatic affinity. The adsorption experiments gave the same results for the two methods of controlling the surface potential. Since the charge and conformation of the polyelectrolyte are not dependent on the solution pH, this is what one would expect and indicates that our approach is an effective one.

The adsorption behaviour of DAB-64 is still not quite clear. In any case it is not determined by electrostatic interactions between the dendrimers and the gold surface, in spite of the high proton charge of the dendrimers. This is probably due to charge compensation within the dendrimer structure by counterions from solution, making the net charge of the molecule relatively low. Applying an external potential to the gold does have an effect on the adsorbed amount, whereas changing the pH of the solution does not. On the gold surface metallic as well as oxidic binding sites are present. On the basis of, among other things, the adsorption kinetics we suspect that binding to these metallic spots occurs less easily than binding to the oxidic sites. At more negative applied potentials, this difference appears to become smaller.

For both linear and dendritic polyelectrolytes model calculations (self-consistent field calculations) can be performed (see, e.g., Ref. 3) under constant surface potential, mimicking externally applied potentials. This would give more insight into their adsorption, since the effect of binding of counterions can be calculated and visualised. Moreover, in model calculations, there is no limitation to the potentials that are applied to the solid/liquid interface. Recently, in our laboratory a start in this direction has been made.

Like the adsorption of dendrimers, the adsorption of lysozyme is not determined by electrostatic interactions. Here, surface-induced conformational changes dominate the adsorption process. Under the experimental conditions chosen in the experiments, the adsorbed amount is determined by the area occupied by the adsorbed molecules. At the potential of zero charge of the gold electrode, the polarization of the surface is minimal, the interfacial tension is maximal and the adsorbed amount exhibits a minimum. This is attributed to surface-induced conformational changes in the adsorbed protein molecules, resulting into a larger occupied area per molecule. The more polarized the gold surface is, the less area is occupied by the protein molecules

and the larger is the total adsorbed amount until it corresponds to a full monolayer of protein molecules in their native conformation. The degree of polarization of the surface that can be reached is limited - again - by redox reactions occurring at the gold/electrolyte interface. It would be interesting to see, using a different substrate, whether the protein will start to desorb if the interfacial tension becomes even lower.

In this thesis the adsorption of only one particular protein was considered. Since the properties of proteins vary strongly from one protein to another, it is recommended to perform similar experiments with different types of proteins following the approach of this thesis, possibly using a less high-energetic surface (e.g., a gold surface modified with a functionalized thiol layer).

The possibilities for manipulating the adsorption process by applying an external potential seem to be limited, at any rate at metal electrodes and as long as one wants to avoid an electric current in the system[*]. In our experiments, desorption as a result from changing the applied potential was never observed. Probably, surface modification (for example, as mentioned above using thiol monolayers) will result in more reversible adsorption processes. The rate of adsorption on the gold electrode was also not affected by putting up an electrostatic barrier. In the case of the linear and dendritic polyelectrolytes, the reason for this is presumably the low effective charge of the adsorbing molecules due to charge compensation by counterions. The protein has only a few charges, spread over the outer side of the molecule. This result is at variance with the kinetic model for polyelectrolyte adsorption developed by Cohen Stuart et al[4], which is based on the assumption that a polyelectrolyte encounters a barrier in its motion towards a like-charged surface. The height of the barrier, which is of electrostatic origin, was calculated using self-consistent field theory. In these calculations the presence of countercharges in the polyelectrolyte coil was not taken into account. This can probably be further elaborated and tested using the results of this study.

The initial adsorption rate was either determined by the transport of molecules towards the surface (PVP^+) or by surface processes like attachment (which was probably the case for dendrimers) and structural rearrangements at the surface (lysozyme). More details on the adsorption kinetics of PVP^+ can in principle be obtained by increasing the transport of molecules toward the surface. Then, it is necessary to collect more data points of the adsorption curve per unit of time. In our experiments, this was not possible since our equipment could not measure at a high enough rate. For the dendrimer and the protein possibly more information about the adsorption kinetics can be obtained by using a less high-energetic surface for the adsorption experiments.

The work presented in this thesis shows a new approach to study complicated adsorption processes. However, the experiments described here are just a start. The approach opens doors to numerous other experiments, which can help to establish the relative importance of various interactions and other factors determining adsorption processes.

---

[*] It has been shown that biofilms and bacteria can be removed from indium tin oxide (ITO) electrodes by electrophoretic desorption, i.e., by applying an electric field through the bulk solution[5].

7.1 ***References***

1) Sondag-Huethorst, J.A.M., Fokkink, L.G.J., *Langmuir*, **1992**, 8, 2560.
2) Giesbers, M., Kleijn, J.M., Cohen Stuart, M.A., *J. Colloid Interface Sci.*, **2002**, 252, 138.
3) Klein Wolterink, J., Leermakers, F.A.M., Fleer, G.J., Koopal, L.K., Zhulina, E.B., Borisov, O.V., *Macromolecules*, **1999**, 32, 2365.
4) Cohen Stuart, M.A., Hoogendam, C.W., de Keizer, A., *J. Phys.: Condens. Matter*, **1997**, 9, 7767.
5) Poortinga, A.T., Bos, R., Busscher, H.J., *Langmuir*, **2001**, 17, 2851.

Summary

In this thesis we have examined the role of electrostatic interactions in the adsorption of charged macromolecules from aqueous solution to a solid surface and the possibilities for manipulating this process through the electric potential of the interface. Gold has been used as the adsorbent surface, and before studying the adsorption of several types of macromolecules onto this substrate we have determined the dependence of the double layer potential of the gold on the pH and on the externally applied potential across the gold/electrolyte solution interface.

Chapter 2 describes a colloidal probe atomic force microscopy study on the electric double layer of a gold electrode in aqueous solutions. The double layer potentials of the gold surface were obtained by fitting force-distance curves for the interaction with a spherical silica particle to the DLVO theory. It was found that the gold electrode combines the features of reversible and polarizable interfaces, i.e., its charge and potential are determined by both the solution pH and the external potential. The pH dependence is attributed to proton adsorption and desorption from oxidic groups at the gold surface. In the potential range studied, the double layer potential ψ^d varies linearly with the applied potential; at a background electrolyte concentration of 1 mM, the variation in ψ^d is roughly 10% of that in the applied potential. The potential of zero force (the external potential at which $\psi^d = 0$) varies with pH. The various features of the gold/electrolyte interface are described well by an amphifunctional double layer model, which takes into account the simultaneous effects of the external potential across the interface and the association/dissociation of functional surface groups. The results of this study form the basis of the interpretation of adsorption studies on gold as a function of pH and externally applied potential, described in chapters 4, 5 and 6.

Chapter 3 addresses the sensitivity of the reflectometer set-up for our adsorption studies as well as the electro-optic effect. The electro-optic effect involves a change in the optical properties of the gold electrode as a result of applying a potential. This leads to a change in the reflectometer signal. Furthermore, calculations and measurements concerning the sensitivity of reflectometer measurements in studying the adsorption of charged polymers from aqueous solution onto gold are presented. This provides a measure for the reproducibility of the adsorption data obtained with reflectometry. The gold substrate is in fact a thin gold film (15 nm) on a silicon wafer. Between the gold film and the wafer a 5 nm layer of titanium has been deposited for better attachment. The sensitivity-factor A_s was calculated by modelling the system as a stack of layers of uniform refractive index. The influence of several parameters, such as the layer thickness of the gold and the angle of incidence of the laser beam, on the sensitivity of the reflectometer set-up was examined. In the range of potentials applied (-0.2 to +0.6 V vs. Ag/AgCl reference electrode) it was found that the electro-optic effect is significant compared to the change in the reflectometer output signal resulting from adsorption. The sensitivity factor A_s, however, is much less affected by the electro-optic effect than by the effect of inaccuracies in the system parameters. Therefore, by recording a baseline at the same applied potential as at which adsorption is monitored, adsorption data can be obtained without interference of the electro-optic effect. The experimental error in the adsorption measurements is

generally between 2-7% and is dominated by the uncertainty in the thickness of the gold film.

In **chapters 4, 5 and 6** the adsorption of charged macromolecules onto gold as measured using reflectometry, is described. Generally, the adsorption kinetics and adsorbed amounts are determined as a function of the concentration of the macromolecule, the electrolyte concentration and the double layer potential of the gold. The double layer potential of the gold is varied through the pH as well as by applying an external potential. By comparing the results of adsorption measurements performed under pH control and under external potential control, effects of conformational changes and changes in the charge of the molecule in solution can be separated from effects of the variation electrostatic interactions between the molecule and the adsorbing surface.

In **chapter 4**, the adsorbing molecule is quaternized polyvinyl pyridine (PVP^+) of various molecular masses. This is a strong polyelectrolyte and the charge of this molecule is independent of the solution pH. It was found that the adsorption process can be characterised as electrosorption enhanced by a relatively high non-electrostatic affinity. The adsorbed amount decreases more or less linearly with the double layer potential of the gold, but approaches zero only at a relatively high value of this potential as a result of non-electrostatic interactions between surface and segments. It makes no difference whether the double layer potential of the gold/electrolyte interface is controlled by the solution pH or by an external potential. Surprisingly, the electrostatic barrier for adsorption is always low, even near the threshold potential for adsorption. This points to a relatively low effective charge of the polyelectrolyte coils in solution due to the presence of counterions in these structures.

Chapter 5 describes the adsorption of a fifth generation dendrimer, 1,4-diaminobutane poly(propylene imine). The charge of this molecule is determined by the solution pH. It is a spherical molecule and conformational changes are limited. The electrolyte concentration and the pH of the solution do not have any significant effect on the total adsorbed amount. Neither do the initial adsorption rates as a function of pH and as a function of applied potential follow the electrostatic interactions, on the contrary. From this, it was concluded that electrostatics is not the dominant factor in the adsorption process. However, the total adsorbed amount shows a linear decrease with increasing applied potential, similar to what was found for the adsorption of PVP^+ onto gold. We assume that the effect of the applied potential on the adsorbed amounts is an indirect one, e.g., stemming from an increase in binding strength between dendrimer and metallic surface sites with decreasing applied potential.

Protein adsorption onto gold was examined in **chapter 6**. Lysozyme was chosen as the adsorbate because the structure of this protein is relatively stable. For such a 'hard' protein electrostatic interactions in the adsorption process are believed to be more important than for proteins with low internal stability, especially when the sorbent surface is hydrophilic. The charge and structural stability of the protein varies with the solution pH. As for the dendrimers it was found that lysozyme adsorption from aqueous solution onto gold is not controlled by electrostatic interactions. The initial adsorption rate is neither dependent on the electrolyte concentration and pH,

nor on the externally applied potential. Quite unexpectedly, we found that the adsorbed amounts at constant pH exhibit a minimum around the potential of zero charge of the gold surface and increase more than linearly for decreasing as well as increasing potential. The curves of adsorbed amounts versus applied potential show a remarkable similarity with so-called electrocapillary curves for metallic electrodes. This is a strong indication that the interfacial tension of the gold/solution interface is an important factor in the adsorption process. At the positive and negative sides of the double layer potential window that could be studied, the adsorbed amount approaches the value corresponding to a full monolayer of undisturbed lysozyme molecules adsorbed 'side-on'. Therefore, it is concluded that at the high-energy gold surface the lysozyme molecules undergo conformational changes, but as the interface becomes more polarized and the interfacial tension decreases, the extent of the surface-induced conformational changes decreases. This conclusion is corroborated by the dependence of the adsorbed amount on the pH, which reflects the combined effects of the change in interfacial tension with double layer potential and the decrease in structural stability with decreasing pH.

Chapter 7 contains a number of general conclusions and suggestions for further research. It was concluded that our approach has been successful for determining the relative importance of electrostatic interactions in the adsorption process of charged macromolecules onto the gold substrate. The choice for gold as the sorbent surface has proven to be very suitable for our adsorption studies because of its amphifunctional character. A disadvantage is the high surface energy of gold, which makes that many kinds of molecules readily adsorb and that the role of electrostatics in adsorption processes is somewhat limited rather than dominant. This may be avoided by surface modification, for example attaching a thiol layer with proton binding functional groups to the gold surface. By doing so, the surface is still amphifunctional and the surface energy is lowered at the same time. Another possible advantage of surface modification is that the range in which the double layer potential can be varied is larger, because the density of proton binding sites can be made high and redox reactions are somewhat suppressed. In this thesis only one type of protein was investigated. Since the properties of proteins vary quite substantially from one protein to another, it is recommended to perform similar experiments with different types of proteins, possibly using a less high-energetic surface. The possibilities to control adsorption of macromolecules on metal electrodes seems to be limited. Desorption by changing the applied potential never occurred. Neither was it possible to affect the kinetics by raising an electrostatic barrier. For PVP$^+$ and dendrimer the latter is presumably resulting from charge compensation by the presence of counterions within the molecules. Self-consistent field model calculations may help to get more insight in these aspects.

Samenvatting

In dit proefschrift is de rol van elektrostatische wisselwerkingen in het adsorptie-proces van geladen macromoleculen op geladen oppervlakken onderzocht. Ook zijn de mogelijkheden nagegaan om dit proces te manipuleren via het aanleggen van elektrische potentialen op het oppervlak. Als adsorbensoppervlak hebben we goud gekozen. Voordat het adsorptiegedrag van verschillende geladen macromoleculen hierop is bestudeerd, is de dubbellaagpotentiaal van het goud bepaald als functie van de pH van de oplossing en als functie van de aangelegde potentiaal over het goud/ oplossing grensvlak.

In **hoofdstuk 2** wordt een studie beschreven naar de elektrische dubbellaag van een goudelektrode in waterige oplossingen. Hierbij is gebruik gemaakt van een AFM ('atomic force microscope') met een klein, rond silicadeeltje (diameter 6 μm) als sonde ('probe'). De dubbellaagpotentiaal van het goudoppervlak is bepaald door fitten van de gemeten interacties tussen dit oppervlak en het silicadeeltje (kracht-afstand curves) aan de DLVO-theory. Gevonden werd dat het goudoppervlak zich zowel reversibel als porariseerbaar gedraagt. Dat wil zeggen dat de lading en de potentiaal van het oppervlak worden bepaald door zowel de samenstelling van de oplossing (pH en zoutconcentratie) als de aangelegde potentiaal over het goud/oplossing grensvlak. De afhankelijkheid van de oplossingssamenstelling is het gevolg van de aanwezigheid van oxide-achtige groepen op het goudoppervlak waaraan protonadsorptie en -desorptie plaatsvindt. Gevonden is dat in het bestudeerde potentiaalgebied de dubbellaagpotentiaal van goud ongeveer lineair met de aangelegde potentiaal varieert. Bij een concentratie van 1 mM van het achtergrondelektrolyt (KNO_3) is de variatie in de dubbellaagpotentiaal ongeveer 10% van de variatie in de aangelegde potentiaal. De potentiaal waarbij de dubbellaagpotentiaal nul is (de "potential of zero force") is afhankelijk van de pH van de oplossing. De verschillende eigenschappen van het goud/oplossing grensvlak worden goed beschreven door een zogenaamd 'amfifunctioneel' dubbellaagmodel, dat het gecombineerde effect beschrijft van de aangelegde potentiaal en de associatie en dissociatie van functionele oppervlakte-groepen. De resultaten van dit deel van het onderzoek vormen de basis voor de interpretatie van de resultaten van de adsorptiestudies als functie van de pH van de oplossing en de aangelegde potentiaal, beschreven in de hoofdstukken 4, 5 en 6.

Hoofdstuk 3 beschrijft de gevoeligheid van de reflectometer-opstelling die gebruikt is in de adsorptiestudies en de invloed van het elektro-optisch effect op de reflectometriemetingen. (Het elektro-optisch effect wordt veroorzaakt door verande-ringen in de optische eigenschappen van de goudelektrode als gevolg van het aanleggen van een potentiaal.) Aan de hand van metingen en berekeningen, is de gevoeligheid van de reflectometer-opstelling voor het bestuderen van het adsorptieproces van geladen polymeren vanuit een waterige oplossing op goud bepaald. Factoren die deze gevoeligheid beïnvloeden worden bediscussieerd. Het substraat, de goudelektrode, bestaat in feite uit een dunne goudfilm (15 nm) op een silicium ondergrond. Tussen de goudfilm en het silicium bevindt zich een zeer dun laagje titanium (5 nm) dat zorgt voor een goede hechting. De gevoeligheid van het systeem voor adsorptie kan worden berekend door het te modelleren als een stapeling van verschillende lagen, waarbij elke laag een uniforme brekingsindex heeft. De invloed van verschillende parameters op de gevoeligheid, zoals de laagdikte van het

goud en de invalshoek van de laserstraal, is onderzocht. Vergeleken met de verandering in signaal als gevolg van adsorptie van macromoleculen is de signaalverandering ten gevolge van het elektro-optisch effect significant. De *gevoeligheid* van de reflectometer voor de geadsorbeerde hoeveelheid wordt er echter nauwelijks door beïnvloed. Bovendien hebben onnauwkeurigheden in de systeemparameters een beduidend grotere invloed op de gevoeligheid dan het elektro-optisch effect. Zodoende kunnen er adsorptiemetingen gedaan worden zonder hinder van het elektro-optisch effect mits een basislijn wordt opgenomen bij dezelfde potentiaal als waarbij adsorptie plaatsvindt. De experimentele fout in de adsorptiemetingen wordt geschat op 2 - 7% en deze wordt voornamelijk bepaald door de onzekerheid in de dikte van de goudlaag.

De **hoofdstukken 4, 5 en 6** beschrijven de adsorptie van geladen macromoleculen op goud, zoals gemeten met reflectometrie. Over het algemeen is de adsorptiekinetiek en de geadsorbeerde hoeveelheid bepaald als functie van de concentratie van het macromolecuul, de elektrolytconcentratie en de dubbellaagpotentiaal van het goudoppervlak. Deze dubbellaagpotentiaal is gevarieerd door de pH van de oplossing en de aangelegde potentiaal te variëren. Vergelijking van de resultaten van adsorptiemetingen onder variabele pH met die verkregen onder variabele aangelegde potentiaal geeft de mogelijkheid om effecten van conformatieveranderingen en ladingsveranderingen *in* het molecuul in oplossing te onderscheiden van effecten van veranderingen in de elektrostatische interacties *tussen* het molecuul en het adsorbens oppervlak.

In **hoofdstuk 4** is het adsorberende molecuul polyvinyl pyridinium (PVP^+); drie verschillende molecuulmassa's zijn gebruikt. Dit lineaire ketenmolecuul is een sterk polyelektrolyt en de lading op de keten is onafhankelijk van de pH en de zoutconcentratie van de oplossing. Het adsorptieproces kan worden gekarakteriseerd als elektrosorptie die wordt versterkt door een relatief hoge niet-elektrostatische affiniteit tussen het adsorberende molecuul en het goudoppervlak. De geadsorbeerde hoeveelheid neemt min of meer lineair af met de dubbellaagpotentiaal van het goudoppervlak, maar nadert pas naar nul bij een relatief hoge positieve potentiaal. Dit wordt veroorzaakt door de sterke niet-elektrostatische affiniteit tussen de segmenten van het molecuul en het goudoppervlak. Het maakt geen verschil of de dubbellaagpotentiaal wordt gevarieerd via de pH van de oplossing of via de aangelegde potentiaal. Verrassend genoeg is elektrostatische barrière voor adsorptie altijd laag, zelfs dicht bij het punt waar de geadsorbeerde hoeveelheid de nul nadert. Dit duidt op een relatief lage effectieve lading van de polyelektrolytketens, hoogst waarschijnlijk veroorzaakt door de aanwezigheid van tegenionen in de kluwens.

Hoofdstuk 5 beschrijft het adsorptiegedrag van het vijfde-generatie dendrimeer 1,4 diaminobutaan poly(propyleen imine). Dit is een bolvormig molecuul en veranderingen in de conformatie zijn maar beperkt mogelijk. De lading van dit molecuul wordt bepaald door de pH van de oplossing. Gevonden is echter dat de elektrolytconcentratie en de pH van de oplossing geen significant effect hebben op de geadsorbeerde hoeveelheid. Ook de initiële adsorptiesnelheid volgt niet de lijn der verwachting als de pH van de oplossing en de aangelegde potentiaal worden gevarieerd. Juist het tegenovergestelde wordt waargenomen: de adsorptiesnelheid neemt toe naarmate de elektrostatische repulsie tussen oppervlak en molecuul toeneemt. Onze conclusie is

dan ook dat het adsorptieproces niet wordt gedomineerd door elektrostatische wissel-werkingen tussen het molecuul en het goudoppervlak. Bij toenemende aangelegde potentiaal neemt de geadsorbeerde hoeveelheid dendrimeer echter wel af, ongeveer lineair, vergelijkbaar met wat wordt gevonden voor PVP^+ op goud. Aangenomen wordt dat dit effect indirect van aard is en wordt veroorzaakt door een afnemende bindingssterkte tussen het dendrimeer en de bindingsplaatsen op het metaal.

In **hoofdstuk 6** wordt de adsorptie van een eiwit op goud beschreven. Als adsorberend molecuul is lysozym gekozen vanwege zijn relatief hoge structuur-stabiliteit. Algemeen wordt aangenomen dat voor zulke zogenaamde "harde" eiwitten de elektrostatische interacties tussen het molecuul en het oppervlak een grotere rol spelen in het adsorptieproces dan bij eiwitten met een lage structuurstabiliteit, vooral als het oppervlak hydrofiel is. De lading en de stabiliteit van het eiwit variëren met de pH van de oplossing. Evenals bij de adsorptie van dendrimeren, is ook hier gevonden dat het adsorptieproces niet wordt bepaald door elektrostatische interacties. De initiële adsorptiesnelheid wordt niet bepaald door de elektrolytconcentratie, de pH van de oplossing of de aangelegde potentiaal. Verrassend genoeg vonden we dat de geadsor-beerde hoeveelheid lysozym bij constante pH een minimum vertoont rond de potentiaal waar de oppervlakteladng van het goudoppervlak nul is, en dat deze meer dan lineair toeneemt bij zowel afnemende als toenemende potentiaal. Als de geadsorbeerde hoeveelheid wordt uitgezet tegen de aangelegde potentiaal is een opvallende gelijkenis met de zogenaamde elektrocapillair curves voor metaal-elektrodes te zien. Dit is een sterke aanwijzing dat de geadsorbeerde hoeveelheid voornamelijk bepaald wordt door de grensvlakspanning van het goud/oplossing grensvlak. Aan de positieve en negatieve kanten van het bereikbare dubbellaag-potentiaalinterval nadert de geadsorbeerde hoeveelheid de waarde van een volledige monolaag van lysozymmoleculen in hun natieve conformatie, waarbij de moleculen "side-on" zijn geadsorbeerd. Hieruit leiden we af dat de lysozymmoleculen op het hoog-energetische goudoppervlak conformatieveranderingen ondergaan waardoor ze meer ruimte op het oppervlak innemen. Naarmate het goudoppervlak meer gepola-riseerd wordt, neemt de grensvlakspanning af en worden de conformatie-veranderingen steeds minder drastisch, zodat er meer moleculen op het oppervlak passen. Deze verklaring wordt ondersteund door de wijze waarop de geadsorbeerde hoeveelheid van de pH afhangt. Deze laat de gecombineerde effecten zien van de veranderingen in de grensvlakspanning van het goud/oplossing grensvlak en de afname in de structuurstabiliteit van het eiwit met dalende pH.

In **hoofdstuk 7** wordt een aantal algemene conclusies weergegeven, evenals aanbevelingen voor verder onderzoek. De in dit onderzoek gevolgde aanpak om de rol van de elektrostatische interacties in het adsorptieproces van geladen macromoleculen op geladen goudoppervlakken op te helderen is geslaagd. Vanwege zijn amfifunc-tionele karakter is goud hiervoor een heel bruikbaar substraat gebleken. Een nadeel van goud is zijn hoge oppervlakte-energie die ervoor zorgt dat veel moleculen snel en gemakkelijk adsorberen. Daardoor is de rol van elektrostatische wisselwerkingen in het algemeen beperkt en niet doorslaggevend voor het adsorptieproces. Dit probleem kan worden omzeild door het goudoppervlak te modificeren, bijvoorbeeld met een monolaag van thiolen met functionele groepen waaraan protonen kunnen binden. Hierdoor blijft het oppervlak amfifunctioneel, terwijl de oppervlakte-energie aanzien-lijk verlaagd wordt. Mogelijk wordt hiermee ook het potentiaalgebied waarin kan

worden gemeten groter, doordat redoxreacties minder snel plaats kunnen vinden. In dit proefschrift wordt slechts één type eiwit onderzocht. Omdat de eigenschappen van eiwitten nogal variëren, wordt aangeraden om dezelfde soort experimenten te herhalen met andere typen eiwitten, eventueel met een minder hoog-energetisch oppervlak dan het kale goudoppervlak. De mogelijkheden om het adsorptieproces van macromoleculen op metaalelektrodes te beïnvloeden lijken erg gelimiteerd. Desorptie door het veranderen van de aangelegde potentiaal is in geen van de experimenten waargenomen. Het is ook niet mogelijk gebleken om de kinetiek van het adsorptie-proces te beïnvloeden door middel van het aanleggen van een elektrostatische barrière. Voor PVP$^+$ en het dendrimeer wordt dit waarschijnlijk veroorzaakt door ladingscompensatie door de aanwezigheid van tegenionen in de moleculen. Computerberekeningen gebaseerd op een zelf-consistent veld roostermodel kunnen een bruikbaar hulpmiddel zijn bij het verkrijgen van meer inzicht in deze aspecten.

Curriculum Vitae

Desiree Barten is geboren op 27 mei 1974 te Rotterdam. In 1992 behaalde zij het VWO-diploma aan de 'Blaise Pascal' te Spijkenisse. Daarna studeerde zij Chemische Technologie aan de Technische Universiteit Delft. Hier studeerde zij in 1997 af in de richting *microbiologie en enzymologie*. In mei 1998 begon zij aan een promotieonderzoek bij de leerstoelgroep Fysische Chemie en Kolloïdkunde aan de Landbouwuniversiteit Wageningen. Het onderzoek heeft geleid tot dit proefschrift. Vanaf 1 januari 2003 is zij werkzaam bij het Ingenieursbureau van Gemeentewerken Rotterdam bij de afdeling bodem.

Dankwoord

Ik wil graag een woord van dank uitspreken aan allen die direct of indirect een bijdrage hebben geleverd aan de totstandkoming van dit proefschrift.
Allereerst mijn promotor Martien Cohen Stuart en mijn co-promotor Mieke Kleijn voor de begeleiding van het onderzoek. Ik heb met veel plezier met jullie samengewerkt. Speciale dank aan Mieke voor de grote hulp bij het schrijven van verschillende artikelen en dit proefschrift.

Vanwege bijzondere hulp en vriendschappelijke ondersteuning wil ik enkele vakgroepsleden hier bij name noemen. Ben Spee, Remco Fokkink, Wim Threels, Ab van der Linde en Rob Vullings worden bedankt voor hun niet in een woord te vangen, maar zeer veelzijdige hulp. In dit verband wil ik ook enkele mede-aio's noemen: Martijn Oversteegen, Marijn van der Veen, Maarten van der Wielen, Wim Wijting en Stefan Jansen.

Bij de totstandkoming van hoofdstuk 2 heb ik bijzonder prettig samengewerkt met Jérôme Duval en Herman van Leeuwen. Voor zijn speciale adviezen gaat mijn dank uit naar Hans Lyklema. Ook de andere leden van de EPD-groep, zowel bij Fysko als bij Philips, worden bij deze bedankt voor hun medewerking.

Mijn kamergenote, Monique Bremer, wil ik in dit dankwoord ook noemen omdat zij zo'n geduldige en onvermoeibare feed-back heeft gegeven, ook bij onderwerpen die niet zoveel met het werk te maken hebben.

Last but not least de steunpilaren van de vakgroep, Josie Zeevat en Wil Kleijne. Zij worden bedankt voor de ondersteunende en gezellige bijdrage aan dit onderzoek.